WYOMING STATE GEOLOGICAL SURVEY
Lance Cook, State Geologist

GEOLOGY OF THE IRON MOUNTAIN KIMBERLITE DISTRICT AND NEARBY KIMBERLITIC INDICATOR MINERAL ANOMALIES IN SOUTHEASTERN WYOMING

by

W. Dan Hausel, Robert W. Gregory,
Roger H. Motten, and Wayne M. Sutherland

Report of Investigations No. 54
2003

Laramie, Wyoming

This and other publications available from:
Wyoming State Geological Survey
P.O. Box 3008
Laramie, WY 82071-3008
Phone: (307) 766-2286
Fax: (307) 766-2605
Email: sales@wsgs.uwyo.edu
Web Page: http://wsgsweb.uwyo.edu

People with disabilities who require an alternative form of communication in order to use this publication should contact the Editor, Wyoming State Geological Survey at (307) 766-2286. TTY Relay operator 1(800) 877-9975.

First printing (March, 2003) of 750 copies by Pioneer Printing and Stationery Company, Cheyenne, Wyoming.

Geology of the Iron Mountain kimberlite district and nearby kimberlitic indicator mineral anomalies in southeastern Wyoming, by W. Dan Hausel, Robert W. Gregory, Roger H. Motten, and Wayne M. Sutherland
ISBN 1-884589-33-2

Front Cover: Paleozoic and Mesozoic rocks exposed on the southern flank of the Iron Mountain kimberlite district. View is to west-northwest from county road west of Farthing. Dipslopes on horizon are developed on top of the Casper Formation (Permian-Pennsylvanian); red beds in distant foreground are part of the Permian Goose Egg Formation (or Satanka Shale and Forelle Limestone) and Triassic Chugwater Formation. The Iron Mountain kimberlite district is located to the north in Precambrian terrain behind the rocks exposed on the right half of the horizon.

WYOMING STATE GEOLOGICAL SURVEY
Lance Cook, State Geologist

Report of Investigations No. 54

GEOLOGY OF THE IRON MOUNTAIN KIMBERLITE DISTRICT AND NEARBY KIMBERLITIC INDICATOR MINERAL ANOMALIES IN SOUTHEASTERN WYOMING

by

W. Dan Hausel, Robert W. Gregory,
Roger H. Motten , and Wayne M. Sutherland

Laramie, Wyoming
2003


STATE OF WYOMING
1933
GEOLOGICAL SURVEY

Table of contents

Illustrations

Figures

Tables

Plates (back pocket)

Abstract

Based on geology and abundance of kimberlitic indicator mineral anomalies, the Wyoming craton (in Colorado, Montana, and Wyoming) may have the highest potential for discovery of significant diamond deposits in the United States. There are dozens of kimberlites (some diamondiferous), dozens of lamproites and ultramafic lamprophyres, and hundreds of kimberlitic indicator mineral anomalies in the Wyoming craton. However, only a very small part of Wyoming and the cratonized margin has been examined for diamonds to date.

One major kimberlite district within this craton was the subject of mapping and geophysical studies by the Wyoming State Geological Survey (WSGS). Studies in the Iron Mountain kimberlite district, central Laramie Mountains of southeastern Wyoming, resulted in the discovery of several kimberlites along with several geomorphic and geophysical anomalies. This district is now known as one of the two largest kimberlite districts in the United States. The other district is the Colorado-Wyoming State Line district located to the south of Iron Mountain.

Geochemical analyses of samples from the Iron Mountain kimberlites suggest that a large part of the kimberlites originated within the diamond-stability field in the upper mantle. Even so, only a very small part of the district has ever been tested for diamond.

Kimberlitic indicator mineral anomalies have been found at several other localities south, west, and north of the Iron Mountain district within the Laramie Mountains. Collection of stream sediment samples, augmented with limited geochemical testing of indicator minerals and reconnaissance geophysics in some areas, has revealed a number of localities that should contain hidden kimberlite intrusives originating from the diamond-stability field. Further research in these areas is warranted.

Introduction

The Iron Mountain district lies in southeastern Wyoming, immediately south of the Wyoming province. The southeastern boundary of the province lies in contact with a cratonized belt of Proterozoic gneisses and schists that were accreted to the Wyoming province about 1770 Ma (Mega-annum or millions of years before present) (Loucks and others, 1988). The northern edge of this cratonized belt, known as the Green Mountain terrain, is marked by a relatively wide suture zone known as the as the Cheyenne belt (Karlstrom and Houston, 1984), or in earlier terminology, the Mullen Creek-Nash Fork shear zone. We interpret this region (Wyoming province + Green Mountain terrain) to have high potential for discovery of diamond deposits.

About 30 to 40 diamondiferous kimberlites have been identified in the Green Mountain terrain along the Colorado-Wyoming border; a diamondiferous(?) breccia pipe (with associated dikes and blows) has been found in the Greater Green River Basin (Hausel and others, 1999); and one diamondiferous kimberlite is reported in eastern Montana (Pete Ellsworth, written communication, 2000). Several detrital diamond occurrences have also been described in Montana and Wyoming. Geological, geochemical, and geophysical evidence gathered over the last two decades has provided evidence for dozens of undiscovered kimberlites in the Archean and Proterozoic terrains in southeastern Wyoming. The Wyoming province also hosts one of the largest lamproite fields in the world, the Leucite Hills area of southwestern Wyoming. Other lamproites and lamprophyres are found in the northern part of the Wyoming province in Montana (Mitchell and Bergman, 1996; Hausel, 1998). Vast regions of the Wyoming craton have only been partially explored for diamonds while other regions in the craton remain unexplored.

Kimberlite was first reported in the Iron Mountain district in 1971. Six years later Smith (1977) described these and other kimberlites in the district as a small group of dikes and blows. In the early 1980s, some diamond interest in the district was generated following the discovery of several diamondiferous kimberlites 45 miles to the south in the Colorado-Wyoming State Line district. Interest in the Iron Mountain district was limited and short-lived due to the lack of diamond discoveries in the area and the apparent small volume of kimberlite. A restricted diamond-testing program involved the recovery of kimberlite from three sample sites; much of the complex remained untested.

In 1997, the authors initiated investigations in the district to search for additional kimberlite. During this study, several new kimberlites were discovered and mapped, and several vegetation anomalies and depressions suggestive of hidden kimberlite were identified. Many of the proven kimberlites yielded kimberlitic indicator minerals with geochemical similarities to diamond-stability minerals. Further investigation of the Iron Mountain kimberlites may be warranted because of the geochemical similarities with kimberlites at the

Kelsey Lake diamond mine in the Colorado-Wyoming State Line district.

Following a two-year research project by the WSGS, it became clear that the Iron Mountain district includes one of the two largest kimberlite districts in the country. The district is also one of the better exposed root zone complexes in North America. There is potential for the discovery of additional kimberlites in the district, as well as in the surrounding region; potential also exists for the discovery of diamonds within the district.

The Wyoming craton

The Green Mountain terrain, the basement complex underlying both the Iron Mountain and State Line districts, consists of 1.6- to 1.9-Ga (Giga-annum or billions of years before present) cratonized Proterozoic volcanogenic gneiss and schist intruded by 1.4-Ga Sherman Granite. This complex lies south of the Wyoming (Archean) province. The Cheyenne belt, exposed in the Richeau Hills about 4 miles north of the Iron Mountain district, forms part of an east-west-trending cataclastic suture zone that separates the Proterozoic Green Mountain terrain from the Wyoming Archean province to the north (Houston and others, 1979).

Much of Wyoming is underlain by the Wyoming province, which forms the core of an ancient craton. However, only slices of this terrain are exposed at the surface in the cores of several of Wyoming's mountain ranges. The remainder of the terrain underlies a thick sequence of Phanerozoic sedimentary rocks that fill the Wyoming basins. According to Eggler and others (1988), the Wyoming craton was established by 2.7 Ga and affected by a regional metamorphic event at 1.9 to 1.7 Ga.

During the Laramide orogeny, parts of the craton were tectonically reactivated and subjected to brittle deformation that produced the present-day structure of the mountains and basins. This event was essentially non-thermal. The potential for discovery of Laramide and pre-Laramide kimberlite and lamproite is considered good, as the Wyoming craton had stabilized following a cratonization event during the Precambrian.

The Wyoming craton (including the Wyoming province and the cratonized Green Mountain terrain) hosts the largest swarm of kimberlites and lamproites in the U.S. (Hausel, 1998). This fact, coupled with a few hundred kimberlitic indicator mineral anomalies identified in stream sediment samples collected over widespread regions (Hausel and others, 1988), provides evidence of an extensive kimberlite province. To date, the cratonized Green Mountain terrain has been the most productive region in the U.S. for diamonds. More than 130,000 diamonds have been recovered from this terrain, yet much of the region remains unexplored for diamonds.

Acknowledgements

In 1998, the WSGS received supplemental funding from the Wyoming State Legislature to search for kimberlite in the Iron Mountain district and to test for favorable geochemistry with the philosophy of eventually developing a new industry in Wyoming. The project was designed as a six-year study, but unfortunately, funding ended after two years of research. Even so, the project was very successful, for which we are grateful to the Wyoming Legislature for funding. Without this funding, the many new discoveries described in this publication would not have been possible.

We would like to thank Tom Evans and the late Max Evans with the American Diamond Company, as well as Paul J. Graff, Gordon Marlatt, and Vic Norris for unrestricted access to their mining claims and leased properties at Iron Mountain. We are also grateful for access to private lands. In particular, we would like to thank John Dilts, John McGuire, Mark Mills, David L. True, Randall Perry, Bonnie Reider, Genevieve Wagner, and Duer Wagner. We want to thank Dr. Susan Swapp of the Department of Geology and Geophysics at the University of Wyoming. Dr. Swapp helped ensure access to the department's microprobe and scanning electron microscope and provided a great deal of technical assistance. We also appreciate the editorial work and efforts of Richard W. Jones and Jaime R. Moulton. Richard Jones also provided the stratigraphic information for the cover photograph and Figure 2.

Location and history of exploration

The Iron Mountain district of Laramie, Albany, and Platte counties, Wyoming lies on the eastern flank of the Laramie Mountains. The district is 35 miles north-northwest of Cheyenne and 45 miles north-northeast of the State Line diamond district (**Figure 1**). The district has an average elevation of 7000 feet, and is characterized by rolling hills with sparse scattered sagebrush and local stands of coniferous trees. Rock exposures are good, although large grassy fields covered with soil and regolith are prevalent in many areas, providing excellent cover for hidden kimberlite.

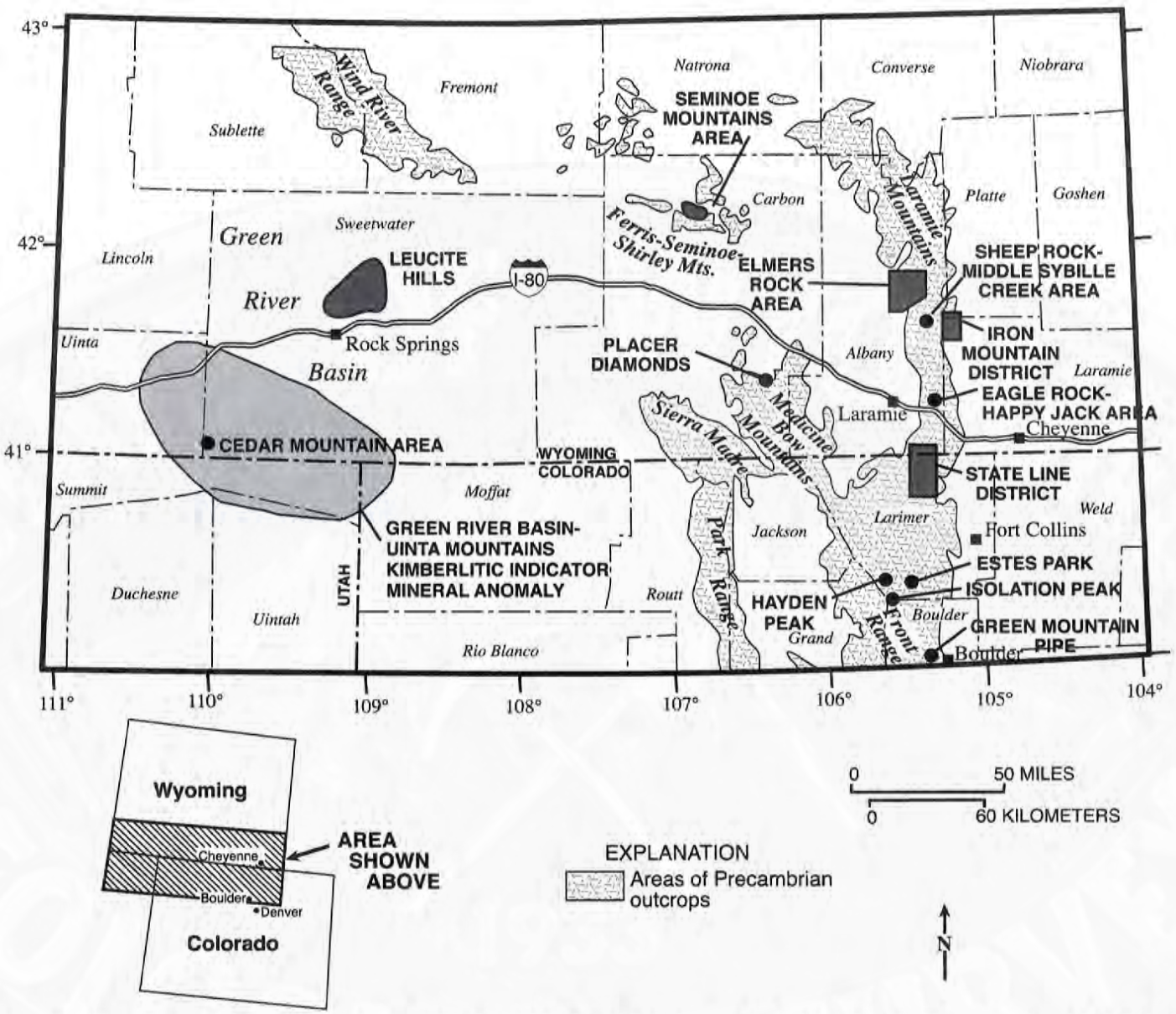

Figure 1. General map of southern Wyoming, northern Colorado, and northeastern Utah showing the location of the Iron Mountain district and its relationship to the State Line district and other areas in the Colorado-Wyoming kimberlite province, the Leucite Hills, and adjacent anomalous areas (modified from Hausel, 1998).

The Iron Mountain district was named after several massive and disseminated titaniferous magnetite deposits found in the 1.5-Ga Laramie anorthosite batholith immediately west of the kimberlite field. Some of the titaniferous magnetite deposits were mined in the 1950s for ballast.

According to Smith (1977), kimberlite was first reported in the district by W.A. Braddock and D. Nordstrom in 1971. Smith (1977) mapped the district and expanded the known extent of kimberlite, describing the ultrabasic intrusives as a complex of small, discrete, discontinuous dikes and blows; these were identified by 57 different sample sites. Mapping by the WSGS beginning in 1997 further expanded the known extent of the district. Based on geologic and petrographic studies (Smith, 1977; Hausel and others, 2000), the Iron Mountain kimberlites form a well-exposed, deeply eroded, root zone complex. An estimated 3000 to 5000 feet of rock has been eroded, including much of the original pipe structures that emanated from the dike complex.

Age of emplacement

Diamond provinces typically exhibit multiple intrusive episodes of mantle-derived rock. This is also the case for the Wyoming craton, where a group of kimberlitic, lamproitic, and lamprophyric intrusive events have been recognized, including those in the Late Precambrian (Proterozoic), Early Devonian, Tertiary, and Quaternary (Hausel, 1996). Other unrecognized events are possible.

Kimberlites in the State Line and Iron Mountain districts, which intrude the cratonized Green Mountain terrain, were dated as Early Devonian based on the presence of Paleozoic xenoliths; fission track dating of sphene (Larson and Amini, 1981) and zircon (Naeser and McCallum, 1977); and Rb-Sr dating of phlogopite (Smith, 1977; 1983). More recently, a Late Proterozoic (600 to 700 Ma) episode was also recognized in some State Line kimberlites (Alan P. Lester, personal communication, 1996). This age is essentially equivalent to the emplacement age determined for the Green Mountain kimberlite located near Boulder, Colorado in the southern part of the Colorado-Wyoming kimberlite province (**Figure 1**). In eastern Montana, the Williams kimberlites are dated at middle Tertiary (Hearn and McGee, 1983); the age of the recently discovered diamond-bearing Homestead kimberlite near Yellow Water Butte is unknown, but assumed to be Tertiary (Pete Ellsworth, personal communication, 2000). Lamproites and related lamprophyres in eastern Montana are also Tertiary in age (Mitchell and Bergman, 1996). The Leucite Hills lamproites in southwestern Wyoming are very young, with age dates from very late Tertiary to Quaternary (3.1 to 1.1 Ma) (Bradley, 1964; McDowell, 1971).

A kimberlite in the southwestern part of the Iron Mountain district (SW section 17, T19N, R70W) contains sedimentary xenoliths of probable Ordovician and Silurian age (Smith, 1977). The sedimentary xenoliths indicate that the intrusive penetrated the former Silurian surface and assimilated fragments of the once extensive or preserved sedimentary cover. The xenoliths establish the oldest possible emplacement age for their primary episode of eruption.

Sedimentary xenoliths in the State Line and Iron Mountain districts are accompanied by crustal and mantle xenoliths. Upper crustal xenoliths found in the kimberlites include quartz monzonite, anorthosite, syenite, hypersthene syenite, amphibolite, biotite schist, and fragments of mafic igneous rock. Lower crustal xenoliths include pyroxenite and garnet granulite. Mantle xenoliths include garnet and spinel peridotite, websterite, eclogite, and diopside-ilmenite intergrowths. Metacrysts include clinopyroxene, orthopyroxene, garnet, ilmenite, and rare olivine (Smith, 1977).

Geology

The Iron Mountain district lies in a salient along the eastern flank of the Laramie Mountains, southwest of the town of Chugwater. The salient was uplifted and thrust eastward during the Laramide orogeny. Iron Mountain is currently surrounded on the east, south, and west by Phanerozoic sedimentary rocks, which were distorted by crustal shortening into several broad folds, anticlines, domes (**Figure 2**), synclines, low angle thrusts, and associated tear faults. Within the Precambrian terrain at Iron Mountain, a northeast-trending zone of cataclasis unrelated to Laramide tectonism is recognized in the northwestern part of the district (Smith, 1977).

Kimberlites in the district lie immediately south of a major suture zone known as the Cheyenne belt, which marks the division between the southern edge of the Wyoming province, and the northern edge of the Proterozoic basement. This structure is exposed in the Richeau Hills 6 miles to the north (Paul Graff, personal communication, 1995), and in the central Medicine Bow Mountains and Sierra Madre to the west (Houston and others, 1979). The Iron Mountain kimberlites parallel the trend of the Cheyenne belt, suggesting that the emplacement of the kimberlites may have been influenced by this structure. If this conjecture is valid, then the probability of finding kimberlite along or near the Cheyenne belt in the Medicine Bow Mountains and Sierra Madre to the west would be considered likely.

Kimberlites mapped at Iron Mountain form a deeply dissected feeder dike complex with periodic blows and sills that intrude 1.4-Ga Sherman Granite (**Figure 3**). The granite and kimberlites are exposed in the core of an eroded, south-plunging anticlinorium. It is very likely that the kimberlite complex continues to the east and west under the Phanerozoic cover. The possibility of exposed kimberlites farther north and west in the Precambrian terrain is considered likely, and needs to be examined. In particular, a group of circular depressions were identified on aerial photography 5 miles west of the district along trend. Precambrian rocks immediately north of the district remain unmapped and unexplored for kimberlites, and parts of this area to

Figure 2. A nearly perfect dome (center) developed in Paleozoic rocks occurs south of the Iron Mountain district. The Iron Mountain district is in the background behind the dome. Dip slopes on the dome are Casper Formation; redbeds to right and left of dome are Satanka Shale and Chugwater Formation. View is to the northwest.

the north include rocks affected by deformation related to the Cheyenne belt. The belt could provide numerous deep access fractures for kimberlite intrusives.

Anorthosite crops out in the northwestern part of the district and also occurs as detrital material in Tertiary conglomerate, xenoliths in some kimberlites, and in a poorly exposed north-trending string of xenoliths in the Sherman Granite (Smith, 1977). The anorthosite was intruded by Sherman Granite (Peterman and others, 1968).

A variety of granitic rocks found in the district are interpreted as different facies of the Sherman Granite, which are distinguished by grain size. One facies is fine-grained granite in the northeastern, northwestern, west-central, and southeastern parts of the district. Coarse-grained porphyritic quartz monzonite facies is found elsewhere in the district. Discontinuous simple pegmatite and aplite dikes are scattered throughout the district.

North- to northwest-trending Precambrian mafic dikes intrude the Sherman Granite (**Figure 3**). These are from 6 to 10 feet wide, nearly vertical, and form sharp contacts with the granite. A few dikes are cut by kimberlite.

Mississippian(?) and younger sedimentary rocks unconformably overlie the Sherman Granite and kimberlite, and dip off the core of the Iron Mountain anticlinorium to the east, south, and west. Immediately west of the district, sedimentary rocks are exposed in the asymmetrical, southward-plunging Hay Canyon syncline. Precambrian rocks of the Laramie anorthosite-syenite batholith and titaniferous magnetite deposits crop out west of the syncline (west of the mapped area in **Figure 3**).

The oldest *in situ* sedimentary rocks in the area consist of thin, calcareous, arkosic sandstone beds with underlying dolomitic limestone. These may be a southern extension of the Mississippian Madison Formation, which unconformably overlies the Precambrian surface. The Madison is overlain by the Casper Formation (Permian-Pennsylvanian), the Satanka Shale and Forelle Limestone (Permian), and the Chugwater Formation (Triassic).

A large area in the western part of the district is covered by Tertiary(?) conglomerate (paleoplacer), which lies directly on the erosional surface developed on the Sherman Granite (**Figure 3**). The conglomerate is unsorted and poorly consolidated, with rounded to angular boulders, pebbles, and cobbles of Precambrian igneous and metamorphic rocks interspersed with Paleozoic and Mesozoic fragments and occasional kimberlitic indicator minerals. The conglomerate is younger than the kimberlite. Kimberlite was mapped along the east and west edges of the conglomerate, and presumably continues under the conglomerate. The extent of hidden kimberlite beneath the conglomerate is unknown and considerable clay in the conglomerate masks electrical responses (in an electromagnetic survey) from any buried kimberlite.

Kimberlite

Kimberlite, a serpentinized, peridotitic, potassic, ultramafic rock, is only one of two rock types presently mined for diamonds in the world. Because of their potential commercial value, all kimberlites (as well as lamproites and some lamprophyres) are typically examined for diamond.

In the Iron Mountain district, kimberlite forms an extensive, continuous, feeder-dike complex (**Figure 4**). The dike complex contains several enlargements, some of which are interpreted as *blows*, or the eroded remnants of former pipes. A few possible pipes were recognized in the western part of the district but their geologic and petrologic characteristics have not been assessed. The central part of the complex contains numerous branching kimberlite dikes. One sill was mapped in the east near the center of section 10 (T19N, R70W). The dikes range from a few feet to 400 feet wide, dip steeply to vertically, and exhibit several branches and offshoots which are the result of strong joint influence.

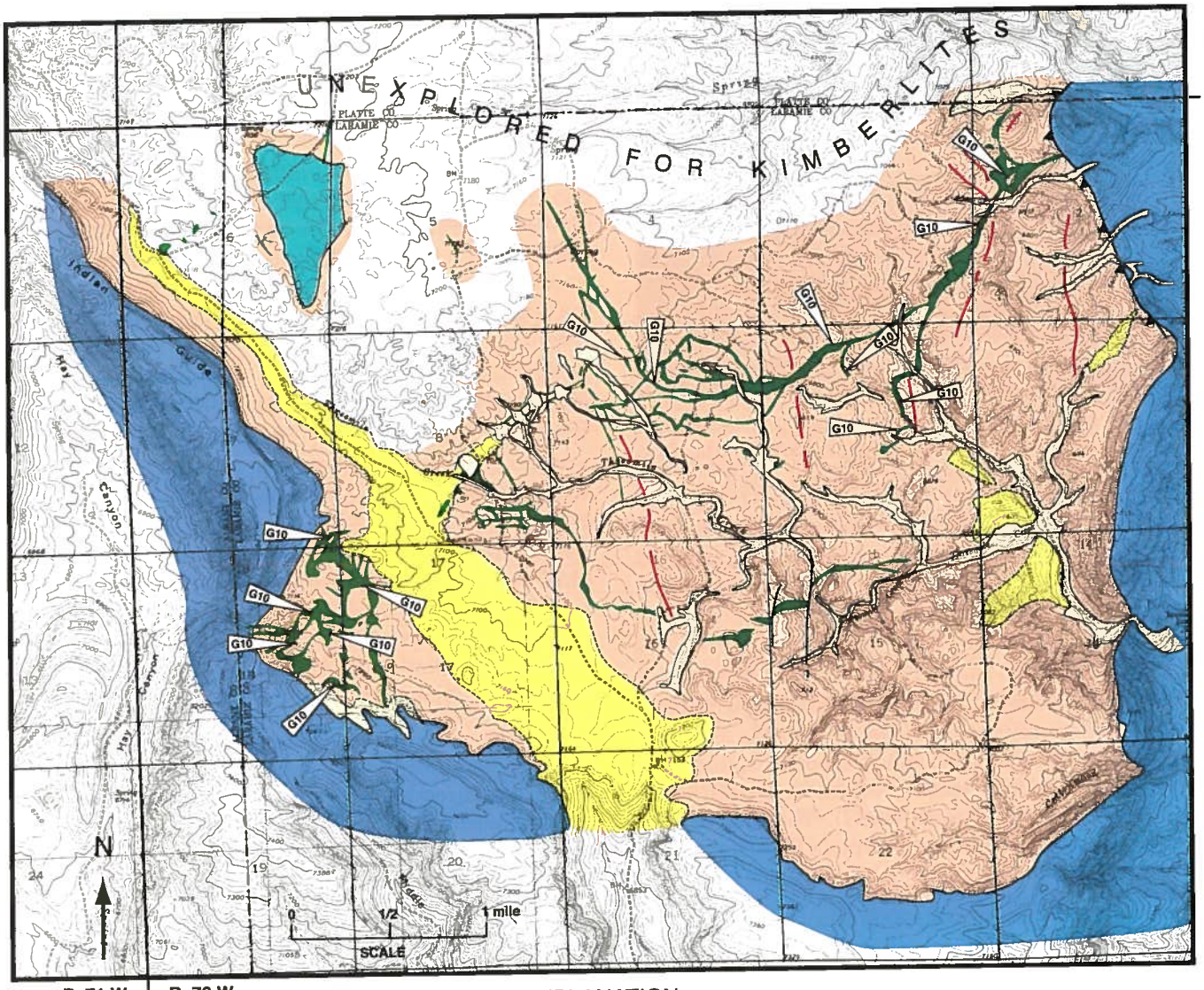

Figure 3. Geologic map of the Iron Mountain kimberlite district, Laramie Mountains, Wyoming. Base map from topographic maps of the Delano Ranch, Indian Guide, Farthing, and Goat Mountain 7 1/2-minute quadrangles, Wyoming.

The kimberlite dike complex was traced over a strike-length of 5 miles within an area of 12 mi² (**Figure 3**), and intrudes the Sherman Granite. Along the eastern and western extent of this trend, both the Precambrian rocks and the kimberlite are overlain by steeply dipping Paleozoic rocks. Presumably, kimberlite continues under the younger Paleozoic cover.

Some enlargements of the kimberlite occur in the area. In SE section 3, T19N, R70W (**Figure 3**) and in the NW section 2 of the same township, distinct swells are present along the dike trend. However, the kimberlite occupying these swells is massive kimberlite porphyry, and thus, the swells are probably not true blows, which are defined as root zones of former diatremes. They are interpreted as dike swells instead.

A few blows were identified within the dike complex. These are thought to exist where enlargement of the dike complex coexists with some brecciation and

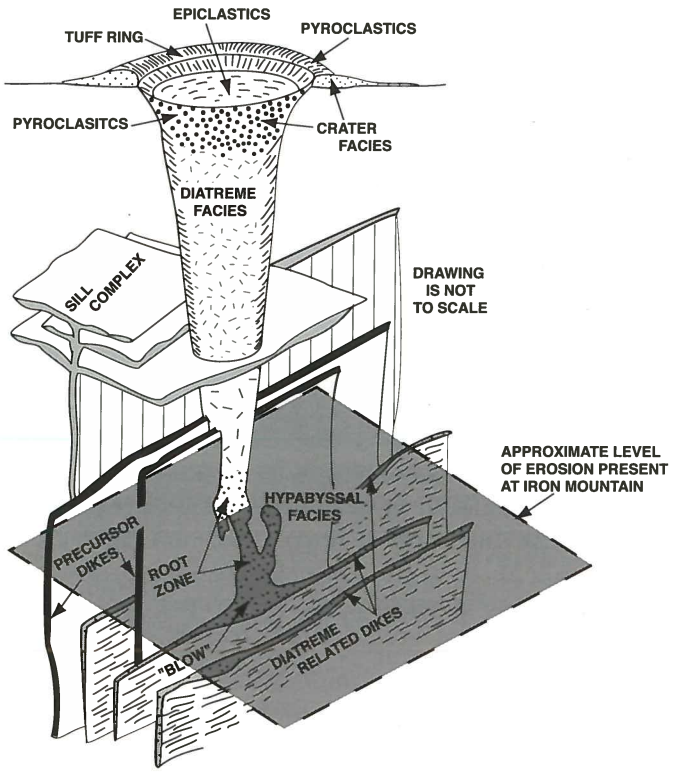

Figure 4. Model (not to scale) of a kimberlite pipe showing different kimberlite facies and kimberlite-related features originating from a root zone at depth (modified from Mitchell, 1986). Shaded area represents a horizontal plane at the approximate level to which the kimberlites at Iron Mountain have been eroded.

carbonatization of the kimberlite (**Figure 4**). Dike enlargements were also mapped in sections 17 and 18, T19N, R70W, along the western margin of the district. Some of these are interpreted as blows, particularly those that contain mantle and crustal xenoliths. One of these blows, located in the W/2 section 17, T19N, R70W, also contains Lower Paleozoic xenoliths, indicating that it penetrated the Silurian and possibly the Devonian surface. The presence of the xenoliths confirms that this enlargement is a true blow (Smith, 1977).

A dike of carbonatized breccia was mapped in sections 15 and 16, T19N, R70W. The breccia contains abundant fragmented breccia clasts of Sherman Granite, and according to Smith (1977), contains some xenoliths of massive kimberlite porphyry. The presence of these clasts and the lack of Paleozoic xenoliths indicate a degassing event of the kimberlitic magma. These breccia pipes are interpreted as the root zones of blind diatremes (which did not penetrate the Earth's surface when emplaced).

For the most part, the dikes are mapped as scattered serpentinized porphyritic kimberlite outcrops (**Figure 3**) connected by grus-covered kimberlitic soil (weathered kimberlite or *blue ground*). In places, the kimberlitic soils are distinct, particularly where the grus is thin. These soils contain intermixed rock fragments of kimberlite and granite in blue ground with variable amounts of kimberlitic indicator minerals (notably picroilmenite, less commonly pyrope garnet, and rarely chromian diopside). The kimberlitic soils are typically outlined by distinct vegetation anomalies (**Figure 5**). Because kimberlite is eroded faster than the surrounding granite, many kimberlites are expressed by slight topographic depressions or flat areas (**Figure 6**).

Blue ground consists of gray montmorillonite clay and carbonated soils that are the result of weathering and decomposition of kimberlite. This blue ground was mapped over wide areas in the State Line diamond district (Hausel and others, 1979; 1981). Vegetation anomalies within the blue ground include dense, lush grasses and areas devoid of trees. These vegetation anomalies are visually prominent at certain times of the growing season—the kimberlites can literally be mapped by these anomalies after a few weeks of rain in late May and early June. The kimberlitic soils are also attractive for burrowing animals, and those that reside in them, including rattlesnakes (e.g., Billman, 1998).

Mapping by the WSGS during the summers of 1997 and 1998 resulted in numerous discoveries, including a group of depressions in the western part of the district within the E/2 of section 8, T19N, R70W, that continue into the extreme NW section 9 of the same township. These depressions, however, remain an enigma. The depressions contain distinct vegetation anomalies as well as apparent blue ground. In addition, some narrow kimberlite dikes were traced into a few of the depressions, and electromagnetic (EM) responses over the depressions yielded excellent conductors as would be expected from weathered kimberlite (see ***Geophysics***, p. 15).

Figure 5. Distinct grass anomaly over kimberlite at Iron Mountain. The thick, lush, grass on the right side of the photograph covers kimberlitic (blue ground) soil, whereas the thinner, shorter grass on the left side of the photograph overlies granitic soils. Also note that no trees grow within the kimberlitic soils.

Figure 6. Depressions outlined by grassy anomalies are suspected kimberlites. This depression in the Iron Mountain district is one of several found that line up along a northeasterly trend.

Following discovery of the depressions, Eagle-Hawk Mining from Colorado collected small backhoe samples from two of the depressions. The WSGS received a portion of the samples, which consisted of common granite fragments with some organic material and quartz cemented by massive clay. A small portion of the material was processed on a Wilfley Table® in an attempt to extract kimberlitic indicator minerals; however, none were found in the clay.

Additional soil samples collected during field investigations were tested with dilute hydrochloric acid, which demonstrated the presence of carbonate. X-ray diffraction (XRD) analysis of the clay showed a good match for montmorillonite, as would be expected in kimberlitic blue ground, but the absence of kimberlitic indicator minerals is an enigma. Future studies are recommended on the chemistry, mineralogy, and genesis of these depressions.

From these depressions, kimberlite continues to the southwest under Tertiary(?) conglomerate in sections 8 and 17, T19N, R70W (**Figure 3**). This conglomerate undoubtedly conceals additional kimberlite. Material collected from the conglomerate included some picroilmenite megacrysts. Some garnet peridotite and eclogite xenoliths were collected from kimberlite in section 9, near Smith's (1977) locality 26, just east of the conglomerate.

Petrography

Smith (1977) described three petrographic varieties of kimberlite in the district: (1) porphyritic to massive kimberlite (Type I), (2) carbonatized kimberlite (Type II), and (3) carbonatized to silicified kimberlite breccia (Type III). All stages of gradation from one variety to another have been recognized. Much of the following petrographic, mineralogic, and geochemical data are summarized from Smith's (1977) thesis, and supplemented with petrographic and geochemical work by the WSGS.

Type I. Porphyritic to massive kimberlite

Type I kimberlite is a highly serpentinized hypabyssal facies kimberlite that is essentially restricted to dikes and sills (**Figure 7**). This rock consists of large, rounded, <1- to 3-cm diameter olivine megacrysts in a green massive aphanitic serpentinized groundmass. The groundmass consists of abundant small rounded serpentinized olivine grains set in a mesh of serpentine and minor interstitial to poikilitic carbonate. Very little primary olivine remains, and the megacrysts are pervasively replaced by gray-black magnetite (**Figure 8a**), reddish hematite (**Figure 8b**), and light-green serpentine. Much of the groundmass olivine occurs as serpentine pseudomorphs after olivine. Locally, the kimberlite exhibits irregular flow texture consisting of a rough alignment of the long axes of the megacrysts and xenocrysts.

Only minor amounts of xenocrysts and xenoliths are found in this kimberlite. Uncommon, mantle-derived xenocrysts include pyrope garnet, chromian diopside, chromian enstatite, and enstatite. Ilmenite megacrysts may form as much as 2 to 3% of the rock locally. The most common xenolith in the kimberlite is granite with rare eclogite and peridotite nodules. The porphyritic kimberlite represents a magmatic dike facies, and is the least differentiated kimberlite magma in the district.

Figure 7. Massive kimberlite porphyry exposed at the surface in one of the dikes at the Iron Mountain kimberlite district.

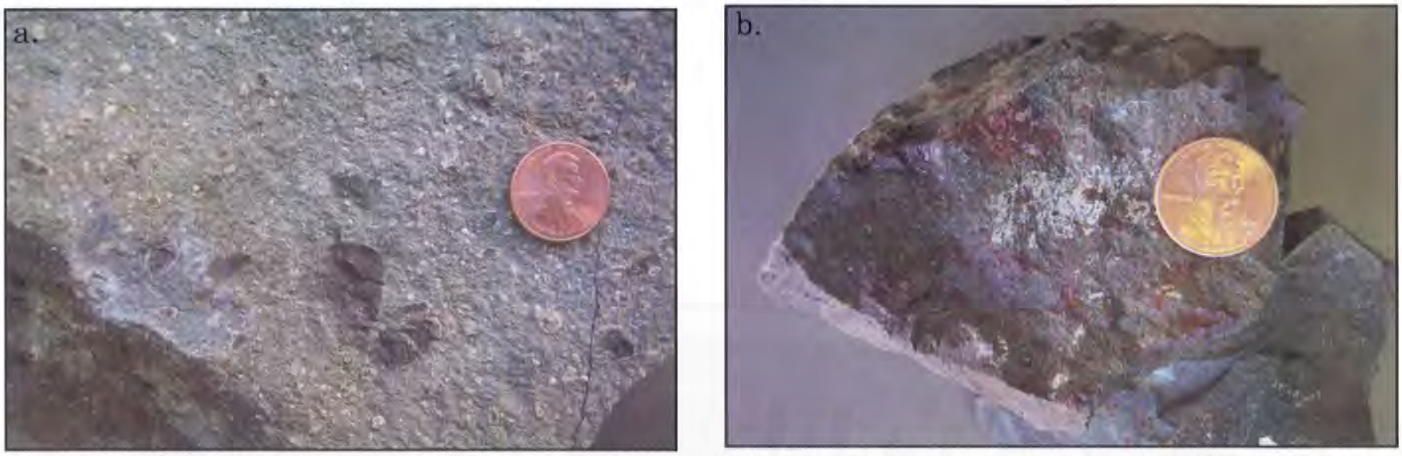

Figure 8. Hand specimens of (a) massive kimberlite porphyry (Type I) with magnetite pseudomorphs (black minerals) after olivine set in an aphanitic serpentinized groundmass and (b) massive hypabyssal facies (Type I) kimberlite porphyry with pseudomorphs of hematite (red minerals) after olivine set in an aphanitic serpentinized groundmass.

In thin section, the rock shows abundant subrounded serpentinized olivine grains set in a fine-grained matrix dominated by serpentine, with lesser calcite, magnetite, perovskite, phlogopite, and trace apatite. The presence of relatively common magnetite, both in the groundmass and as replacements of olivine grains, suggests that these kimberlites should be susceptible to exploration by airborne magnetic surveys.

Type II. Carbonatized kimberlite

Type II kimberlite is dark gray to grayish-green rock with porphyritic to massive texture (**Figure 9**) similar to the porphyritic kimberlite. This kimberlite is spatially associated with blow features, and shows weak to strong carbonatization, which is also expressed in the geochemistry. The rock is primarily hypabyssal facies with local diatreme facies.

The carbonatized kimberlite may contain minor to 80% carbonate as replacements of olivine megacrysts in a serpentine-carbonate groundmass. Carbonatized rounded megacryst ghosts are commonly found in the massive carbonate-rich rock. Hematite mantles some of the megacrysts. Groundmass minerals include hematite, magnetite, minor chromian-spinel and a variety of iron-titanium oxides. Serpentine is usually present in small amounts dispersed throughout the matrix and is intimately intermixed with carbonate. Small amounts of secondary phlogopite may be present.

The heterogeneous nature of this kimberlite is accented by a varied group of xenoliths. In general, a greater amount of mantle xenoliths and xenocrysts are found in this kimberlite compared to other kimberlite varieties found at Iron Mountain. In the southwestern part of the district, this kimberlite contains angular, elongate granitic fragments that locally exhibit flow alignment.

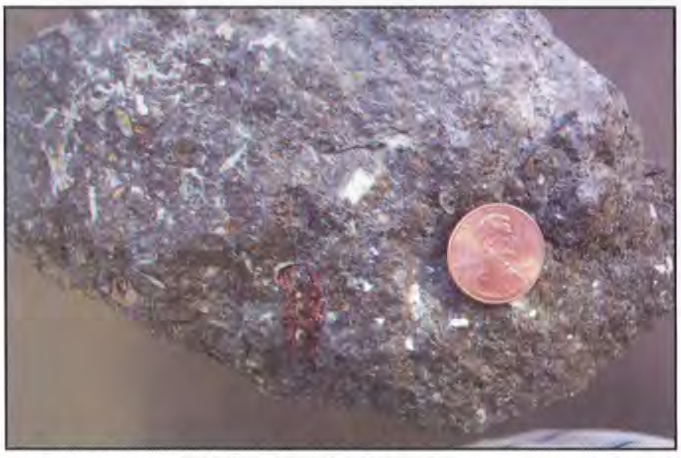

Figure 9. Petrographic Type II kimberlite is a hypabyssal to diatreme facies kimberlite with red pyrope megacrysts in a fine-grained serpentinized matrix with small rounded yellow-brown olivine grains and some white carbonate grains.

Type III. Carbonatized to silicified kimberlitic breccia

Type III kimberlite is exposed in a group of blows interpreted to represent the eroded roots of blind diatremes and feeder dikes. This rock type is gradational to the carbonatized kimberlite, and based on the rock geochemistry, does not appear to be a true kimberlite, although whole-rock geochemistry of this hybrid is difficult to assess due to the abundant granitic xenoliths. The breccias are serpentine-deficient relative to normal intrusive kimberlite breccia. In hand specimen, the rock is gray to black and may contain as much as 70% granitic fragments in a carbonate-rich matrix (**Figure 10**). The breccia shows varying degrees of silicification, and exposures commonly stand out. The granitic wall rock adjacent to kimberlite exposures may be weakly silicified (**Figure 11**) (Smith, 1977).

In thin section, granitic rock fragments are set in a finely crystalline matrix of carbonate, pulverized

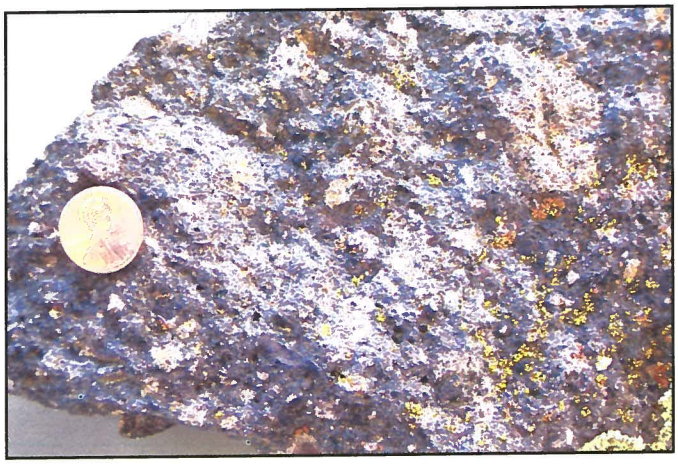

Figure 10. Type III kimberlite at Iron Mountain is a carbonatized breccia containing abundant granite xenoliths in a carbonate-rich matrix.

Figure 11. Distinct saddle produced by resistant outcrops of granite enclosing less resistant kimberlite within the saddle. Note distinct vegetation anomaly, including the lighter shade of grass and very little sagebrush in the saddle.

granitic material, cryptocrystalline to microcrystalline quartz, hematite, magnetite, and rounded carbonatized grains. Hematite commonly rims altered xenocrysts, most of which were probably olivine. Smith (1977) reported finding an altered kimberlite xenolith in the breccia, and used this information to support his interpretation that the magma was originally kimberlite.

Whole-rock geochemistry

Overall, the mineralogy as well as the whole-rock geochemistry shows that kimberlite in the district ranges from serpentine-dominant to carbonate-dominant. Even though some kimberlites are essentially carbonatites based on geochemistry, this may be due to replacement textures. Based on the mineralogy and geochemistry of all three kimberlite rock types, it is apparent that kimberlite grades from distinct serpentinized kimberlite porphyry with little carbonate to carbonatized kimberlite with little serpentine (Smith, 1977).

The Iron Mountain kimberlites bear little resemblance to their initial mantle melt due to fractionation, differentiation, and incorporation of abundant xenolithic material (Smith, 1977). Representative whole-rock analyses are difficult to assess, as the kimberlites are hybrids contaminated with appreciable foreign material incorporated into peridotitic magma as it rose from the mantle through Earth's crust. Samples of Type I and II kimberlites were selected for analysis because of their lower amount of visible contaminates, but it is essentially impossible to find samples that are not contaminated. All samples of the Type III kimberlite were pervasively contaminated by granitic xenoliths; thus, significant contribution of the granitic material to the whole-rock chemistry is unavoidable.

Major oxide, minor element, and trace element concentrations of many of the Iron Mountain kimberlites are compatible with worldwide kimberlite averages. Many of the Iron Mountain intrusives are also similar to the State Line diamondiferous kimberlites.

The Type I kimberlite, or massive kimberlite porphyry, is characteristic of a primitive peridotitic magma containing considerable groundmass and megacrystal olivine with minor pyroxene and picroilmenite, accessory minerals, and contaminates. The olivine throughout the samples is pervasively serpentinized, with little preserved primary olivine. Where preserved, the olivine is found in the cores of some megacrysts and groundmass grains that are enclosed in a reaction rim of serpentine. But for the most part, the grains occur as serpentine pseudomorphs after olivine. The mineralogy emphasizes the magnesium-rich chemistry of the rock.

The average chemistry of the Type I kimberlite is comparable to the average basaltic kimberlite (sample A, **Table 1**). Samples of the Type I kimberlite have higher average magnesium (28.6% MgO) and higher average potassium (1.04% K_2O) than the average basaltic kimberlite (compare with 27.9% MgO and 0.98% K_2O). For the Type I kimberlite, the magnesium content is higher, and the potassium content lower, than the average micaceous kimberlite (compare with 23.9% MgO and 2.1% K_2O)(sample B, **Table 1**). Samples of the kimberlite porphyry from the Iron Mountain district range from a low of 23.1% MgO to a high of 33.31% MgO, and from 0.18% K_2O to 1.8% K_2O.

The carbonatized kimberlite (Type II) shows a wide range in major oxide chemistry, in part due to contamination and differentiation. However, carbonatization appears to have had the greatest influence on the chemistry variance. These kimberlites show a wide range of carbonatization from weakly carbonated rock where the serpentinized olivine megacrysts contain

reaction rims of carbonate with some interstitial carbonate in the groundmass, to extreme carbonatization showing pervasive alteration of the rock. In the pervasively altered rocks, the megacrysts and groundmass appear to be completely replaced by carbonate, and the chemistry is typical of carbonatite.

Samples IM7-98 and IM18-98 (**Table 2**) are weakly carbonatized kimberlites. These contain common serpentinized olivine as megacrysts and groundmass grains. Whole rock chemistry shows 28.91 and 32.92% MgO, respectively, and 7.11 and 2.64% CaO, respectively. Loss on ignition (LOI) totals 12.29 and 13.38%, respectively, much of which probably occurs as water with some CO_2. The other Type II samples listed on **Table 2** are pervasively carbonatitized. In particular, sample IM4-98, which contains 5.56% MgO, 39.27% CaO, and 34.9% LOI, is dramatically depleted in silica (9.85% SiO_2) and potassium (0.34% K_2O). Based on the chemistry, either this sample represents extreme carbonatization with depletion of MgO, or the original magma was a carbonatite.

Other samples from this group also show intense carbonatization. For example, samples IM15-98 and IM30-98 contain serpentinized olivine megacrysts with a groundmass pervasively replaced by carbonate. These yielded 8.95 and 11.7% MgO, respectively, and 21.05 and 19.13% CaO, respectively.

The carbonatized breccias (Type III) have been contaminated by abundant granite breccia clasts; thus, it is impossible to eliminate the effects of the xenoliths on the whole-rock chemistry. Typically, these rocks look more like a fault breccia than kimberlite. Samples with the least amount of granitic xenoliths were selected for whole rock analysis; however, these exhibit enrichment in SiO_2, Al_2O_3, and K_2O (**Table 3**), some of which was contributed by the granite. These samples also show extreme depletion of MgO and enrichment of CaO. Only sample IM14-97 contained appreciable magnesium (4.92% MgO). The other three samples ranged from 0.54 to 1.44% MgO. CaO in the samples ranged from 7.55 to 15.87%, much of which occurs in the form of calcite.

Thus, the whole-rock chemistry of the Type III kimberlites is suggestive of a magnesian-poor, carbonatitic magma, or a pervasively carbonatized kimberlite breccia. Thin section examination of these samples showed considerable granitic material in a matrix of fine-grained granitic material and carbonate. No magnesium-silicate minerals were identified in thin section. It is likely that the breccia represents a degassing phase in a blind diatreme, where CO_2 gas exolved from the magma as the lithostatic pressure decreased near the surface.

Trace rare earth element contents of the kimberlites from Iron Mountain (**Tables 1, 2,** and **3**) show chondrite normalized distribution patterns to be highly fractionated toward light rare earths. La/Yb ratios range from 25 to 238, and the kimberlites from Iron Mountain (as well as the State Line district) display negative europium (Eu) anomalies. Similar patterns have been recognized in some South African and Siberian diamondiferous kimberlites (Smith, 1977).

The geology, mineralogy, and geochemistry all support an interpretation that the Iron Mountain kimberlites represent a deeply dissected kimberlite dike-sill-pipe complex. As much as 3000 to 5000 feet of overlying rock was probably removed by erosion since the kimberlites were emplaced in the Devonian (see **Figure 4**).

The carbonatized kimberlite appears to be closely associated with blows or former pipe structures, indicating that diatreme formation occurred in the parts of the dike system where carbonate-rich fluids concentrated. The presence of rare Type I and Type II kimberlite xenoliths in the Type III carbonatized breccia implies that diatreme formation began after solidification of parts of the dike system (Smith, 1977).

Carbonatized kimberlites (Type II and III) are located within close proximity to the roots of diatremes. These rocks are associated with the most intense wall rock alteration, carry the highest xenolith concentrations, and were the most violently emplaced (Smith, 1977).

Because only one blow in the district (located in SW section 17, T19N, R70W) contains sedimentary xenoliths, most (if not all) of the remaining pipes were probably blind diatremes that never penetrated the overlying Lower Paleozoic sedimentary cover. Based on geological and mineralogical evidence, diatreme formation probably was initiated when the internal gas pressures exceeded the lithostatic load pressure, a process possibly augmented by migration and concentration of fluid phases following the solidification of parts of the dike complex. A rapid increase in the volume of the fluid phases promoted sudden oversaturation within the magma, resulting in explosive brecciation. The eruption of a diatreme which penetrated the Devonian or younger surface may have triggered a pressure drop throughout much of the remaining complex (Smith, 1977).

Mineral geochemistry

Kimberlitic indicator minerals were extracted from kimberlite and tested using geochemistry to determine the probability of finding diamonds at Iron Mountain. In particular, pyrope garnet, chromian diopside, chromian enstatite, chromite, and picroilmenite are many orders of magnitude more common than diamond in kimberlite, and can be used to assess the diamond

Table 1. Major and trace element analyses of Type I (massive kimberlite porphyry) kimberlite samples from Iron Mountain compared to worldwide average kimberlite. Samples IM16-5 and IM21-1 are from Smith (1977). Sample A is an average basaltic kimberlite and Sample B is an average micaceous kimberlite. All other samples are from this study. Dashes indicate not analyzed.

		World wide average									
		A	B	IM8-98	IM16-98	IM21A-98	IM21B-98	IM21C-98	IM28-98	IM60-97	IM16-5
SiO_2	(%)	35.2	31.1	31.67	30.86	30.2	30.93	30.44	30.08	31.76	33.8
TiO_2	(%)	2.3	2	2.83	3.11	2.62	2.89	2.77	2.76	2.6	3
Al_2O_3	(%)	4.4	4.9	3.9	3.81	2.49	2.94	2.71	2.69	2.62	2.8
Fe_2O_3	(%)	-	-	11.88	12.83	11.75	12.41	12.06	12.06	11.97	7.8
FeO	(%)	9.8	10.5	-	-	-	-	-	-	-	3.8
Cr_2O_3	(%)	-	-	-	-	-	-	-	-	-	-
MnO	(%)	0.11	0.1	0.28	0.24	0.18	0.21	0.18	0.19	0.19	0.18
MgO	(%)	27.9	23.9	33.31	27.62	29.26	28.91	28.95	29.11	28.42	28.6
CaO	(%)	7.6	10.6	2.37	6.82	8.76	8.28	8.04	8.62	6.46	5.1
Na_2O	(%)	0.32	0.31	0.12	0.06	0.15	0.11	0.12	0.1	<0.01	0.05
K_2O	(%)	0.98	2.1	0.18	0.65	0.91	1.33	1.23	1.24	0.58	1.4
P_2O_5	(%)	0.72	0.66	0.54	0.75	0.16	0.14	0.22	0.2	0.33	0.35
CO_2	(%)	3.3	7.1	-	-	-	-	-	-	-	1.7
LOI	(%)	7.4	5.9	13.4	13.08	13.68	12.22	12.86	13.44	15.57	11.3
Total		**100.03**	**99.17**	**100.64**	**100.04**	**100.37**	**100.57**	**99.79**	**100.7**	**100.69**	**99.88**
Cr	ppm	660	610	787	951	912	934	1005	985	210	970
Ce	ppm	290	660	290	414	334	362	377	346	-	220
Eu	ppm	2	4.1	2.5	4.2	3.4	3.5	3.7	3.6	-	2
La	ppm	120	380	169	238	195	212	218	203	-	98
Lu	ppm	-	-	<0.2	<0.2	<0.2	<0.2	<0.2	<0.2	-	-
Nd	ppm	150	190	81	120	100	110	120	100	-	80
Sc	ppm	-	-	14.4	20.7	17.4	19.6	19	17.7	-	-
Sm	ppm	-	-	11.4	17.3	13.8	15.1	15.5	14.3	-	-
Tb	ppm	-	-	<1	1	1	2	1	1	-	-
Th	ppm	22	56	28	32	25	27	29	26	-	22
U	ppm	-	-	6	5	5	6	5	5	-	-
Yb	ppm	1.3	2.2	1	1	<1	1	1	1	-	1.3
Hf	ppm	-	-	3.6	5.1	5.2	5.1	4.8	4.7	-	-
Cu	ppm	21	22	13	10	47	18	66	47	-	85
Pb	ppm	23	72	32	41	19	19	27	20	-	13
Zn	ppm	140	190	87	100	93	87	96	96	-	75
Mo	ppm	4.2	7.6	1	2	1	1	2	2	-	2.6
Ni	ppm	530	500	635	549	756	692	714	719	-	820
Co	ppm	37	28	96	88	94	97	94	93	-	69
As	ppm	-	-	5	6	<5	<5	<5	<5	-	-
Ba	ppm	650	1900	1643	>2000	797	144	439	514	-	720
V	ppm	60	120	115	142	57	57	66	67	-	62
Sr	ppm	330	1300	398	658	325	332	339	311	-	320
Y	ppm	13	26	14	17	13	15	15	14	-	9.7
Ga	ppm	5.5	8.5	<10	<10	<10	<10	<10	<10	-	8.4
Li	ppm	-	35	9	40	4	8	3	3	-	-
Nb	ppm	110	310	223	245	215	240	231	227	-	100
Ta	ppm	-	-	9	11	6	7	7	9	-	-
Zr	ppm	68	280	123	160	178	173	163	161	-	81

potential of the intrusives. These indicator minerals were collected from sample concentrates processed in the WSGS heavy mineral laboratory, and tested on an EPMA (electron probe micro analyses = microprobe) at the University of Wyoming's Department of Geology and Geophysics. Solid geochemistry analyses were completed on a large number of garnets. Many pyroxenes and ilmenites were also collected for testing, but were not analyzed prior to loss of funding for this project.

When diamonds are found in kimberlite, they are primarily derived from mantle xenoliths trapped within the kimberlitic magma. These xenoliths disaggregate during transportation to Earth's surface, resulting in the dissemination of diamonds and indicator minerals throughout the kimberlite magma. The principal diamondiferous xenoliths include pyrope harzburgite, eclogite, chromite harzburgite, and less commonly pyrope lherzolite.

Some minerals derived from diamondiferous xenoliths will exhibit unique chemistries and show similar geochemical trends to diamond-inclusion minerals. Kimberlitic indicator minerals that have similar chemistry to diamond inclusions are interpreted to originate within the diamond-stability field. When present, these minerals can be used to predict the presence of diamond, and very generally, can be used to predict the relative grade of ore. They cannot, however, be used to predict the clarity or value of the diamonds. Diamonds must be extracted for this assessment.

Table 1, continued. Major and trace element analyses of Type I (massive kimberlite porphyry) kimberlite samples from Iron Mountain compared to worldwide average kimberlite. Samples IM16-5 and IM21-1 are from Smith (1977). Sample A is an average basaltic kimberlite and Sample B is an average micaceous kimberlite. All other samples are from this study. Dashes indicate not analyzed.

		IM21-1	IM15-97	IM16-97	IM21-98	IM24-98	IM27-98	IM47-98	IM51-98
SiO_2	(%)	29.9	30.2	33.48	31.93	33.01	33.2	32.36	33.29
TiO_2	(%)	4	2.36	2.56	2.56	2.64	2.64	2.4	2.57
Al_2O_3	(%)	4	2.34	3.08	2.54	2.91	3.18	2.85	3.8
Fe_2O_3	(%)	10.4	11.26	11.56	11.82	11.9	12.52	12.27	12.4
FeO	(%)	1.8	-	-	-	-	-	-	-
Cr_2O_3	(%)	-	0.2	0.2	0.2	0.21	0.23	0.2	0.18
MnO	(%)	0.19	0.23	0.22	0.18	0.29	0.21	0.2	0.21
MgO	(%)	23.1	25.92	29.12	28.82	29.28	28.54	27.89	27.59
CaO	(%)	13.2	10.11	5.28	7.72	5.32	5.2	5.72	8.88
Na_2O	(%)	0.07	<0.01	<0.01	<0.01	<0.01	<0.01	<0.01	<0.01
K_2O	(%)	1.8	1.21	0.4	1.04	0.52	0.91	1.48	0.45
P_2O_5	(%)	0.3	0.78	0.41	0.21	0.58	0.36	0.63	0.32
CO_2	(%)	1.3	-	-	-	-	-	-	-
LOI	(%)	9.9	16.01	12.74	13.29	13.67	12.1	14.39	10.73
Total		**99.96**	**100.62**	**100.06**	**100.31**	**100.35**	**99.08**	**100.4**	**100.43**
Cr	ppm	930	-	-	-	-	-	-	-
Ce	ppm	390	-	-	-	-	-	-	-
Eu	ppm	2.8	-	-	-	-	-	-	-
La	ppm	220	-	-	-	-	-	-	-
Lu	ppm	-	-	-	-	-	-	-	-
Nd	ppm	61	-	-	-	-	-	-	-
Sc	ppm	-	-	-	-	-	-	-	-
Sm	ppm	-	-	-	-	-	-	-	-
Tb	ppm	-	-	-	-	-	-	-	-
Th	ppm	36	-	-	-	-	-	-	-
U	ppm	-	-	-	-	-	-	-	-
Yb	ppm	2.2	-	-	-	-	-	-	-
Hf	ppm	-	-	-	-	-	-	-	-
Cu	ppm	97	-	-	-	-	-	-	-
Pb	ppm	21	-	-	-	-	-	-	-
Zn	ppm	130	-	-	-	-	-	-	-
Mo	ppm	6.8	-	-	-	-	-	-	-
Ni	ppm	1100	-	-	-	-	-	-	-
Co	ppm	80	-	-	-	-	-	-	-
As	ppm	-	-	-	-	-	-	-	-
Ba	ppm	1400	-	-	-	-	-	-	-
V	ppm	130	-	-	-	-	-	-	-
Sr	ppm	910	-	-	-	-	-	-	-
Y	ppm	23	-	-	-	-	-	-	-
Ga	ppm	12	-	-	-	-	-	-	-
Li	ppm	15	-	-	-	-	-	-	-
Nb	ppm	220	-	-	-	-	-	-	-
Ta	ppm	-	-	-	-	-	-	-	-
Zr	ppm	250	-	-	-	-	-	-	-

Magnesian pyrope garnets derived from pyrope harzburgite and pyrope lherzolite are tested for MgO, Cr_2O_3, and CaO. The purple-red- to lilac-colored magnesian garnets are separated into chromian (>2wt% Cr_2O_3) calcic garnets and chromian sub-calcic garnets. Sub-calcic, chromian, high-magnesian pyrope garnets have a high probability of originating within the diamond-stability field and are thought to be derived from the disaggregation of diamondiferous pyrope harzburgite. Calcic, chromian, magnesian pyrope garnets are interpreted to have been derived from pyrope lherzolite (McCallum and Waldman, 1991). Although most pyrope lherzolites are considered to have formed within the graphite stability field, a few lherzolites are diamondiferous (McCallum and Mabarak, 1976). Overall, the contribution of diamonds from lherzolite is generally considered to be minor.

The sub-calcic chromian magnesian pyrope garnets from Iron Mountain that plot to the left of the inclined line on **Figure 12** are designated as G10 and most are assumed to have originated from the diamond-stability field. The garnets that plot to the right of the inclined line are calcic chromian magnesian pyropes (designated G9) and are of probable pyrope lherzolite paragenesis. For the most part, these are interpreted to have originated within the graphite stability field. The geologic map of the Iron Mountain district (**Figure 3**) shows the location of some of the samples sites that produced G10 pyropes. It should be noted that only a small part of the kimberlite complex was tested for pyrope geochemis-

Table 2. Major and trace element analyses of Type II, transitional (carbonatized) kimberlite samples from Iron Mountain compared to worldwide average kimberlite. Samples IM1-8 and IM53-1 are from Smith (1977). Sample A is an average basaltic kimberlite and Sample B is an average micaceous kimberlite. All other samples are from this study. Dashes indicate not analyzed.

		World wide average										
		A	B	IM7-98	IM18-98	IM15-98	IM1-8	IM53-1	IM4-98	IM30-98	IM16-98A	IM54-98
SiO_2	(%)	35.2	31.1	34.04	31.68	25.69	26	27.8	9.85	25.34	30.62	19.57
TiO_2	(%)	2.3	2	1.9	2.96	1.84	2.6	2.5	1.81	1.55	1.52	1.56
Al_2O_3	(%)	4.4	4.9	3.44	3.26	5.44	2.1	2.8	1.97	3.25	3.68	2.04
Fe_2O_3	(%)	-	-	9.84	11.96	6.72	8.8	7.5	4.74	8.12	8.64	7.84
FeO	(%)	9.8	10.5	-	-	-	0.89	2.8	-	-	-	-
Cr_2O_3	(%)	-	-	-	-	-	-	-	-	-	-	-
MnO	(%)	0.11	0.1	0.18	0.27	0.21	0.16	0.21	0.78	0.16	0.19	0.17
MgO	(%)	27.9	23.9	28.91	32.92	8.95	12.7	12.3	5.56	11.7	8.93	13.75
CaO	(%)	7.6	10.6	7.11	2.64	21.05	20.1	11.8	39.27	19.13	18.79	23.23
Na_2O	(%)	0.32	0.31	0.12	0.1	0.08	0.05	0.07	<0.01	<0.01	<0.01	<0.01
K_2O	(%)	0.98	2.1	1.79	0.15	4.59	1	1.7	0.34	2.87	2.83	0.66
P_2O_5	(%)	0.72	0.66	0.67	0.53	1.79	0.35	0.55	0.44	0.19	1.95	0.7
CO_2	(%)	3.3	7.1	-	-	-	20.2	21.5	-	-	-	-
LOI	(%)	7.4	5.9	12.29	13.38	24.27	5.1	8.5	34.9	28.26	23.01	30.82
Total		**100.03**	**99.17**	**100.47**	**100**	**100.73**	**100.05**	**100.03**	**99.77**	**100.7**	**100.29**	**100.48**
Cr	ppm	660	610	915	711	467	850	1000	1300	1200	1200	1300
Ce	ppm	290	660	358	285	150	480	390	-	-	-	-
Eu	ppm	2	4.1	2.9	2.3	1.7	3.5	2.5	-	-	-	-
La	ppm	120	380	212	169	121	270	190	-	-	-	-
Lu	ppm	-	-	0.2	<0.2	0.9	-	-	-	-	-	-
Nd	ppm	150	190	100	85	55	120	180	-	-	-	-
Sc	ppm	-	-	13.4	14.5	13	-	-	-	-	-	-
Sm	ppm	-	-	14	11.2	8.5	-	-	-	-	-	-
Tb	ppm	-	-	1	<1	1	-	-	-	-	-	-
Th	ppm	22	56	29	24	24	42	22	-	-	-	-
U	ppm	-	-	6	6	8	-	-	-	-	-	-
Yb	ppm	1.3	2.2	1	1	3	3	1.9	-	-	-	-
Hf	ppm	-	-	4.1	4	4	-	-	-	-	-	-
Cu	ppm	21	22	52	66	75	71	54	-	-	-	-
Pb	ppm	23	72	30	27	37	32	13	-	-	-	-
Zn	ppm	140	190	76	94	208	120	110	-	-	-	-
Mo	ppm	4.2	7.6	1	<1	4	7.5	<2.2	-	-	-	-
Ni	ppm	530	500	740	676	245	940	500	-	-	-	-
Co	ppm	37	28	75	106	34	79	56	-	-	-	-
As	ppm	-	-	<5	<5	9	-	-	-	-	-	-
Ba	ppm	650	1900	>2000	1395	1946	1000	580	-	-	-	-
V	ppm	60	120	108	151	219	120	70	-	-	-	-
Sr	ppm	330	1300	1037	590	1279	800	600	-	-	-	-
Y	ppm	13	26	16	14	21	31	15	-	-	-	-
Ga	ppm	5.5	8.5	<10	<10	<10	11	11	-	-	-	-
Li	ppm	-	35	10	7	65	10	-	-	-	-	-
Nb	ppm	110	310	228	224	182	290	150	-	-	-	-
Ta	ppm	-	-	6	9	<5	-	-	-	-	-	-
Zr	ppm	68	280	132	124	85	290	110	-	-	-	-

try, and the geochemistry supports our interpretation that many of the Iron Mountain kimberlites originated within the diamond-stability field.

Eclogites provide another significant source for diamonds in kimberlite, although most diamonds from kimberlite appear to be derived from peridotite. Pyrope garnets of eclogitic paragenesis are yellow-orange, low chromian (<2% Cr_2O_3), magnesian garnets. These typically plot below the 2% Cr_2O_3 line on **Figure 12**. Eclogitic garnets from Iron Mountain with elevated Na_2O and TiO_2 similar to diamond-inclusion garnets fall within the diamond-inclusion field (McCallum and Waldman, 1991) as shown on **Figure 13**. A significant concentration of garnets tested from the Iron Mountain district fall along the edge of the diamond-inclusion field. Based on the microprobe data, some contribution of diamonds from diamondiferous eclogite is anticipated.

Another source for diamonds in kimberlite may be chromite harzburgite. High-Cr, high-Mg chromites have chemistries comparable to diamond-inclusion chromites (McCallum and Waldman, 1991). A plot of MgO and Cr_2O_3 chromites from Iron Mountain kimberlites (**Figure 14**) shows no apparent diamond contribution from this source, as all the samples were outside the diamond stability field. Unfortunately, only a few chromites were collected before funding ended.

Based on the geochemistry of indicator minerals, one can make a tentative appraisal of the diamond grade of the Iron Mountain kimberlites. The above data show a moderate contribution of indicator miner-

Table 3. Major and trace element analyses of Type III, carbonatized breccia samples from Iron Mountain compared to worldwide average kimberlite. Sample A is an average basaltic kimberlite and Sample B is an average micaceous kimberlite. Dashes indicate not analyzed.

		World wide average					
		A	B	IM14-97	IM13-98	IM14-98	IMK1-97
SiO_2	(%)	35.2	31.1	52.18	46.13	58.72	49.03
TiO_2	(%)	2.3	2	0.82	0.86	1.14	1.08
Al_2O_3	(%)	4.4	4.9	9.26	9.26	9.66	7.59
Fe_2O_3	(%)	-	-	5.54	5.81	6.98	6.37
FeO	(%)	9.8	10.5	-	-	-	-
Cr_2O_3	(%)	-	-	-	-	-	-
MnO	(%)	0.11	0.1	0.09	0.11	0.12	0.12
MgO	(%)	27.9	23.9	4.92	0.86	0.54	1.44
CaO	(%)	7.6	10.6	7.55	15.87	7.82	15.03
Na_2O	(%)	0.32	0.31	0.11	0.15	0.22	0.02
K_2O	(%)	0.98	2.1	7.35	7.72	7.92	6.35
P_2O_5	(%)	0.72	0.66	0.27	0.24	0.42	0.34
CO_2	(%)	3.3	7.1	-	-	-	-
LOI	(%)	7.4	5.9	11.92	13.52	6.75	13.36
Total		**100.03**	**99.17**	**100.07**	**100.58**	**100.36**	**100.82**
Cr	ppm	660	610	600	232	344	700
Ce	ppm	290	660	-	300	251	-
Eu	ppm	2	4.1	-	2.1	2.2	-
La	ppm	120	380	-	160	150	-
Lu	ppm	-	-	-	0.8	0.9	-
Nd	ppm	150	190	-	110	94	-
Sc	ppm	-	-	-	8.5	8.4	-
Sm	ppm	-	-	-	18.9	18.7	-
Tb	ppm	-	-	-	2	3	-
Th	ppm	22	56	-	26	29	-
U	ppm	-	-	-	5	6	-
Yb	ppm	1.3	2.2	-	6	6	-
Hf	ppm	-	-	-	9.4	9.5	-
Cu	ppm	21	22	-	11	17	-
Pb	ppm	23	72	-	38	49	-
Zn	ppm	140	190	-	129	113	-
Mo	ppm	4.2	7.6	-	3	4	-
Ni	ppm	530	500	-	128	118	-
Co	ppm	37	28	-	25	26	-
As	ppm	-	-	-	15	18	-
Ba	ppm	650	1900	-	839	1370	-
V	ppm	60	120	-	43	47	-
Sr	ppm	330	1300	-	273	279	-
Y	ppm	13	26	-	45	54	-
Ga	ppm	5.5	8.5	-	13	13	-
Li	ppm	-	35	-	9	12	-
Nb	ppm	110	310	-	141	174	-
Ta	ppm	-	-	-	<5	<5	-
Zr	ppm	68	280	-	128	159	-

als from both pyrope harzburgite and eclogite, and no contribution from chromite harzburgite. The contribution from lherzolite is unknown.

Geophysics

Several vegetation anomalies and depressions were identified in the district during this project: some may be an expression of hidden kimberlite. Where accessible, many of the anomalies were tested by preliminary profile geophysical surveys, which included a Geometrics® Proton Precession magnetometer and a Geonics® EM 31 portable electromagnetic unit. For the most part, no distinct magnetic anomalies were detected over the depressions, but several strong conductors were identified. Some grassy vegetation anomalies with sporadic carbonate-rich soils and clay (that are suggestive of the presence of blue ground) are recommended for future detailed grid geophysical surveys, sampling, and trenching to determine the source of the anomalies. More prominent anomalies should be tested for the presence of hidden kimberlite.

The features that were investigated included a group of northeasterly-trending depressions found in sections 8 and 9, T19N, R70W, in the western part of the Iron Mountain district during geologic mapping. These depressions are overlain by distinct grassy vegetation anomalies. The southernmost depression also exhibited a small exposure of blue ground(?) along its southeastern edge, suggesting that some of the depressions may overlie kimberlites. EM surveys over the depressions (**Figure 15** and **Appendix A**) yielded distinct conductors, further supporting the possibility of hidden kimberlite pipes.

Samples collected from two of these depressions were inconclusive. For example, a backhoe sample collected by Eagle-Hawk Mining from Lyons, Colorado, was clay-rich with minor carbonate, typical of blue ground. The clay matrix supported common granitic fragments. When processed for kimberlitic heavy minerals, the clay yielded none. Samples tested by XRD to assess the clay mineralogy showed a strong affinity for montmorillonite, as would be expected in blue ground. With these conflicting data, the origin of the sampled depressions remains unknown. More detailed sampling is needed, especially to determine the source of the montmorillonite.

EM lines were run in SW section 8, T19N, R70W, to search for hidden kimberlite in the Tertiary paleoplacer west of the depressions. South-north line 5 (**Figure 15** and **Appendix A**) was run across the paleoplacer near the projected southwesterly trend of the belt of kimberlites. The line detected conductive material that averaged about 55 mmhos/meter along its entire length. A strong EM conductor was detected along the northern edge of the line, which peaked at 123 mmhos/meter, possibly indicating the presence of hidden kimberlite.

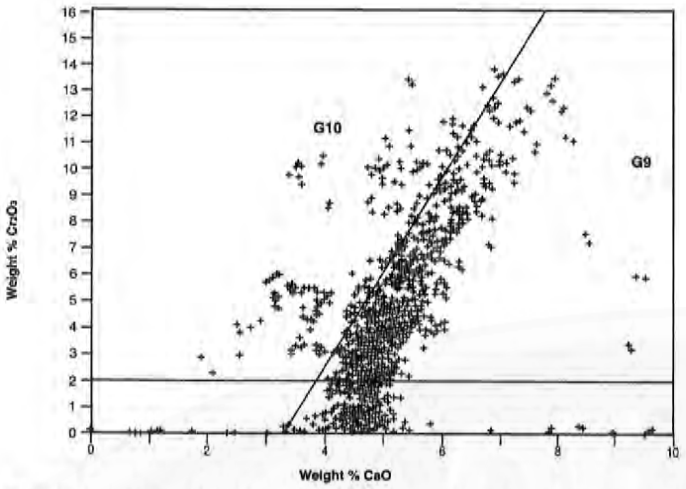

Figure 12. Plots of CaO and Cr_2O_3 from microprobe analyses of pyrope garnets collected from Iron Mountain kimberlites. Those with compositions lying to the left of the inclined line have compositions equivalent to G10 garnets and have high probability of originating from the diamond-stability field.

In all probability, this paleoplacer covers one or more kimberlites, as blue ground was mapped along its western and eastern edges. The paleoplacer apparently contains carbonate derived from the adjacent Paleozoic limestones as well as clay from an unknown source, and tends to mimic the geophysical signatures typical of kimberlitic blue ground, making it difficult to prospect by electrical surveys.

Near the eastern edge of the district, kimberlite was traced to the easternmost extent of the Sherman granite, where they both project under steeply dipping Paleozoic sedimentary rocks. Geophysical lines were run over some depressions in this area, and a few of the lines yielded conductivity anomalies.

Line 17 (**Figure 15** and **Appendix A**) was run in the valley adjacent to the Precambrian-Paleozoic contact and detected an EM anomaly which ranged from 4 to 25.8 mmhos/meter over 450 feet. Although

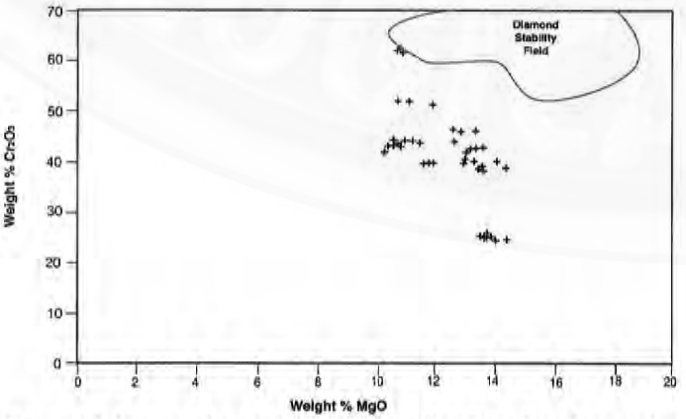

Figure 14. Microprobe analyses of chromites from Iron Mountain. None of the chromites plot within the diamond stability field, although a few plot along the edge of the field.

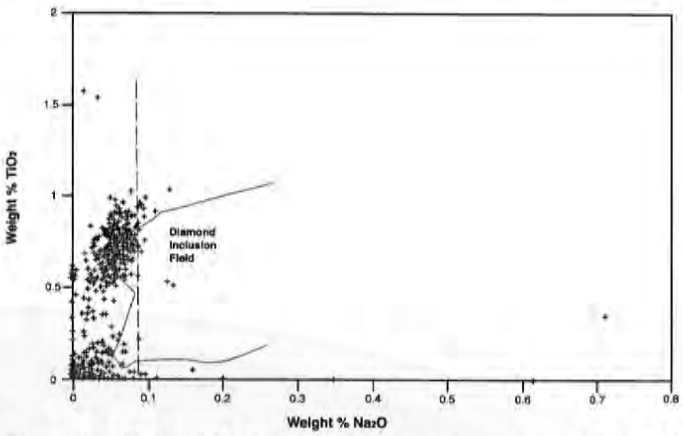

Figure 13. Plots of Na_2O and TiO_2 from microprobe analyses of eclogitic garnets from Iron Mountain show a significant number of garnets with compositions similar to diamond-inclusion garnets.

the anomaly is relatively low, the symmetry of the anomaly deserves further investigation. Farther west, the kimberlite dike trends under an intermittent stream valley near the western edge of section 2, T19N, R70W. Geophysical lines 2, 3, and 4 (**Figure 15** and **Appendix A**) were run in the drainage to search for the continuation of the kimberlite dike. The distinct EM anomalies that were detected in the drainage along trend with the kimberlite are interpreted as a reflection of a buried kimberlite.

In SE section 3, T19N, R70W, geophysical lines 18, 20, and 21 were run across the mapped kimberlite dike (**Figure 15** and **Appendix A**). At this point, the dike is exposed as periodic outcrops of massive, serpentinized, hypabyssal facies kimberlite, with some blue ground containing calcium carbonate and periodic grains of picroilmenite, pyrope garnet, and rare chromian diopside in the soils. The dike also has a well-developed grassy vegetation anomaly. Grus-covered soils and outcrops of granite occur adjacent to the kimberlite. The outcrops of kimberlite and granite along with a presumably thin soil profile suggest that geophysical lines across this dike would yield only very weak conductors, as the weathered kimberlite profile should be relatively thin. As predicted, all three lines detected weak conductivity anomalies. The anomalies ranged from only 2 to 7.5 mmhos/meter. However, the host granite averaged only 1 mmho/meter. Based on geologic mapping and the geophysical profiles, the dike is about 180 feet wide at this point, and covered by a very thin soil profile.

About 0.75 mile west of the above three lines, in N/2 section 10, T19N, R70W, geophysical line 22 (**Figure 15** and **Appendix A**) was run along a dirt road crossing two kimberlite dikes. The clay and soil profile over these two intrusives was assumed to be poorly developed and relatively thin. The westernmost kimberlite

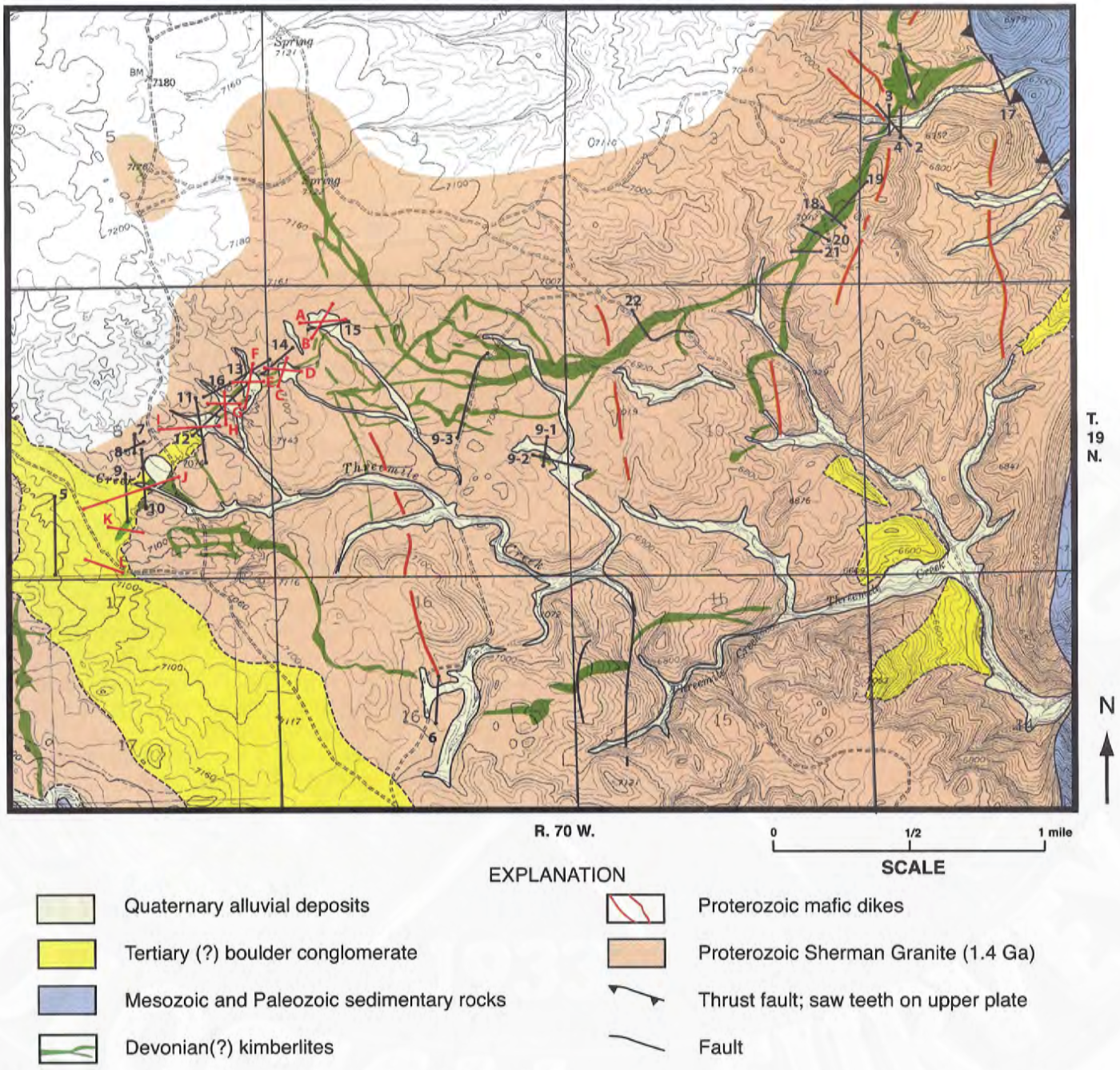

Figure 15. Geologic map of the Iron Mountain kimberlite district showing locations of geophysical lines. Numbered lines in black, lettered lines in dark red. See **Appendix A** for descriptions of lines and the electromagnetic (EM) and/or magnetic profiles.

yielded a 240-foot wide anomaly ranging from only 4 to 8 mmhos/meter. The second dike yielded a 4- to 19-mmhos/meter anomaly over a 330-foot width.

Farther west of geophysical line 22, in NE section 9, T19N, R70W, the dike complex separates into a maze of dikes. Some of these were identified based on the presence of distinct grassy vegetation anomalies associated with carbonated soil. Geophysical line 9-3 was run across five of the dikes (**Figure 15** and **Appendix A**). The line detected five prominent conductivity peaks associated with the mapped dikes.

An alluvial-filled depression with minor blue ground along its western and eastern margin was found near the eastern edge of section 9, T19N, R70W. The depression continued into the western edge of adjoining section 10. Both EM and magnetics were run along a northwesterly trend over the depression (geophysical line 9-2, **Figure 15** and **Appendix A**).

The magnetic survey was inconclusive. The EM survey showed a conductivity high ranging from 7.5 to 23.1 mmhos/meter over 300 feet. Line 9-1, perpendicular to 9-2, showed a background of about 1 mmho/meter over its length with a conductivity peak of about 4.5 mmhos/meter over 100 to 120 feet. The data suggests the presence of a clay-rich zone within the depression.

In section 16, T19N, R70W, another depression was identified that yielded a 45-foot-wide conductor with a high conductivity of 35 mmhos/meter along geophysical line 6 (**Figure 15** and **Appendix A**). The conductor may also be a reflection of a hidden kimberlite.

Economic geology

For a few decades, the Iron Mountain kimberlites have been interpreted as poor exploration targets based on size and geochemistry. Early mapping by Smith (1977) indicated little tonnage was available for mining even if diamonds could be found. Geochemical data published by McCallum and Waldman (1991) also suggested that these kimberlites were unfavorable targets for diamond, as diamond preservation was considered improbable based on geochemistry.

Recent mapping by the WSGS has greatly increased the amount of known kimberlite within the district, very little of which has been tested for diamond. Reconnaissance by the WSGS also indicates that the potential for discovering additional kimberlite is considered high within and adjacent to the district. Thus, sufficient tonnage may be available for mining. Additionally, the indicator-mineral geochemistry supports an interpretation that much of the complex originated within the diamond-stability field, and systematic testing of the kimberlites should be considered.

Samples collected from Iron Mountain show a presence of sub-calcic, high chromian garnets with chemistry similar to G10 (diamond-stability) pyrope garnets (see ***Geochemistry***, above). This data suggests that the Iron Mountain magmas may have originally contained a low to moderate diamond ore grade from a garnet harzburgite mantle. The contribution of diamond from Group I eclogites (eclogites containing pyrope garnets with Na_2O contents of ≥0.09 wt.% and low Cr_2O_3 contents, typically <0.05 wt. %) is predicted to be similar—low to moderate. Little data is available on the geochemistry of chromites, thus any diamond contribution from chromite harzburgite is inconclusive. The available geochemical data supports the interpretation that the Iron Mountain magmas originally contained low to moderate diamond contents from peridotitic and eclogitic sources at depth within the mantle. Thus, the question that remains is whether diamonds have been preserved in the Iron Mountain kimberlite complex, or were they resorbed or burned during transport and emplacement.

The texture and geochemistry of picroilmenite found in kimberlite is used to provide an indication of diamond preservation, as discussed in **Appendix B**. Picroilmenites with exsolution textures and unfavorable geochemistry are often used to predict destruction of the original diamond budget in the kimberlite during emplacement. The geochemistry of the Iron Mountain ilmenites at first analysis indicates poor diamond preservation.

However, the ilmenite geochemistry of Iron Mountain and Kelsey Lake kimberlites is almost identical. Ilmenites from the Kelsey Lake diamond mine in the State Line district have as much as 38% hematite component, nearly identical to the 39% hematite component in the Iron Mountain ilmenites (Schulze and others, 1995; Coopersmith and Schulze, 1996). Based on the ilmenite geochemistry, poor diamond preservation would also be predicted at Kelsey Lake; however, diamond production at the mine includes a large percentage of high-quality gemstones with octahedral habit, providing little evidence of resorption. The chrome/magnesian ratios and chrome depletion in ilmenites detailed in **Appendix B** provide inconsistent information on diamond preservation (Coopersmith and Schulze, 1996) and may also provide inconclusive information in predicting diamond preservation at Iron Mountain.

To date, only a small amount of material has been collected from Iron Mountain for diamond testing. Microdiamond testing has recovered only a small number of stones from a few kimberlites (Coopersmith and others, in press). Since a large volume of the kimberlite at Iron Mountain has been removed by erosion, a study of paleo-drainages should be considered for future research, especially if the eroded kimberlites originally contained diamonds.

During the early 1980s, Cominco American Incorporated collected small bulk samples from Smith's (1977) IM7 and IM46 sample sites in W/2 section 17, T19N, R70W, and from the IG3 kimberlite in SW section 6, T19N, R70W. These sites were chosen based upon their size, pipe-like nature, and mineral chemistry. Between 40 and 60 metric tons (tonnes) were sampled from each kimberlite and processed at Cominco's mill in Fort Collins, Colorado. Some microdiamonds and one macro-diamond (>2mm) were

recovered–a 0.3-carat white octahedral stone from IG3. No further bulk sampling was performed by Cominco (Howard Coopersmith, personal communication, 1998, 2002).

Pure Gold Exploration subsequently collected a group of eleven 18- to 22-pound (8- to 10-kg) samples for diamonds, and reported that the samples were barren (Gordon Marlatt, written communication, 1998). Samples collected by Waldman Consulting for Kennecott Exploration Company in 1998 produced six diamonds, however three were synthetic. The synthetic diamonds were contamination from a rock crusher normally used to crush core samples (which sometimes contain synthetic diamonds from drill bits). However, no explanation was provided for the presence of three natural diamonds (Gordon Marlatt and Paul Graff, personal communication, 1998).

The present WSGS project was originally outlined as a six-year effort with testing of small bulk samples from several kimberlites planned during the last two years. Unfortunately, since the project terminated after two years, diamond testing was not done. However, based on the chemistry of the Iron Mountain kimberlites, we would expect recovery of some diamonds from some of the kimberlites. The value of diamonds cannot be predicted without diamond recovery. At the Kelsey Lake diamond mine, for instance, ore grades are low, but the average value of the diamonds is high offsetting the low ore grades.

The potential for finding other diamond deposits in Wyoming is considered by the authors to be moderate to high. Currently, 30 to 40 diamondiferous kimberlites have been identified in the Colorado-Wyoming State Line district within the same cratonized Proterozoic basement into which the Iron Mountain kimberlites were emplaced. Grades of bulk samples collected from the State Line district have ranged from 0.5 to 135 carats per 100 tonnes. About 50% of the diamonds are gem quality, ranging from microdiamonds up to a 28.3-carat stone, with some evidence for stones weighing 80 or more carats (Howard Coopersmith, personal communication, 2002). Ore grades for commercial diamond mines around the world have ranged from 1 to 680 carats per 100 tonnes (Hausel, 1995a; 1995b).

Samples collected in the Iron Mountain district for diamond to date have been discouraging, but the amount of material collected for diamond testing has been very minor. It should be noted that even in the richest diamond deposits, diamond occurs in amounts much less than 1 part per million, so it requires considerable material to sufficiently test for diamond (Lampietti and Sutherland, 1978).

Other anomalous areas

Research was conducted in some nearby areas as well as in the Iron Mountain district. The results, combined with earlier data collected by the WSGS, show that Wyoming is highly anomalous and in all probability, is host to numerous other kimberlite intrusives, several of which may be diamondiferous. Stream sediment samples collected during this and previous studies were used to search for other anomalous regions that might host kimberlite.

Worldwide, stream sediment sampling in the search for specific tracer minerals associated with kimberlites commonly referred to as *kimberlitic indicator minerals*, has been one of the most successful means of exploration for diamond pipes. Tracer minerals eroded from kimberlite intrusives, or related rocks, are dispersed into the soils and adjacent stream drainages. Transportation distances, before complete disaggregation due to stream abrasion, will vary from mineral to mineral and geomorphic environment. A general rule of thumb is that kimberlitic indicator minerals found in stream sediment samples in the Wyoming craton suggest that their source intrusive(s) may lie 2 to 2.5 miles upstream of the anomaly (which is defined by the presence of indicator minerals). Transportation distances of indicator minerals in other regions, such as subarctic terrains, are much greater than those reported for Wyoming and Colorado. When abundant (>10) indicator minerals are found in a sample in the Wyoming craton, the source kimberlite may be proximal (±2 miles).

Approximately 1600 stream sediment samples were collected in southeastern Wyoming by the WSGS in the mid-1980s for the purpose of searching for kimberlite (Hausel and others, 1988). Of these samples, nearly 20% (approximately 300) contained kimberlitic indicator minerals, providing evidence that the Wyoming craton has been intruded by a major kimberlite swarm. Additional samples were collected in 1998 and 1999 for this project, but only a small percentage was examined. A similar percentage (~20%) of anomalous samples (those with kimberlitic indicator minerals) were identified from those examined.

During the earlier stream sediment sampling surveys, solid geochemical tests were not budgeted, and research was limited to mineralogical studies. Geochemical testing of kimberlitic indicator minerals is a relatively new procedure, developed in the last two to three decades of the 20th century in South Africa, to search for diamondiferous kimberlite in cratonic

environments. It is currently used to identify potential diamond targets (Fipke and others, 1995; Gurney, 1984; Gurney and others, 1993).

Diamond-stability pyrope garnets were identified in stream sediment samples DR9, DR29, and DR30 from the Dodge Ranch region in the Elmers Rock greenstone belt; SR1, SR10, and SR14 in the Middle Sybille Creek district; H890110-3 east of Baggs; NSW-2 from Mule Creek north of Iron Mountain; and IM80b, IM32, and IM35 from the Iron Mountain district. Most other indicator minerals collected by the WSGS have not been geochemically tested, and many of these could also contain diamond-stability minerals. Reports of diamond-stability kimberlitic indicator minerals found by exploration groups in the Big Horn and Owl Creek Mountains and in the Hartville Uplift have expanded the anomalous area (John Churchill, personal communication, 1998).

Results of the stream sediment sampling programs are summarized in the sections below. The areas sampled are arranged by 1:100,000-scale topographic quadrangle maps.

Shirley Basin 1:100,000-scale Quadrangle

Samples collected several years ago from a Tertiary paleoplacer along the banks of the North Platte River north of the Seminoe Mountains yielded gold and pyrope garnets. Duplicate samples were collected during this study from the west and east sides of the river (NW section 18 and W/2 section 14, T26N, R84W). The original pyropes collected exhibited a distinct purple coloration and were thought to have a high probability of being sub-calcic. Microprobe analyses of additional pyropes confirmed this and showed G10 (diamond-stability) signatures. Mapping in this region by Hausel (1994) suggested that the source region of the paleoplacer might have been in the vicinity of Bradley Peak on the western edge of the Seminoe Mountains. No kimberlites are known in this region, but the area has yet to be explored for kimberlite or diamond.

Rock River 1:100,000-scale Quadrangle

Several dozen samples were collected within the Rock River Quadrangle (**Plate 1**). The Laramie Mountains within this quadrangle are formed of Proterozoic-age Sherman Granite (1.4 Ga) and Laramie anorthosite-syenite (1.5 Ga). Much of the terrain lies north of Eagle Rock and south of Elmers Rock. The Cheyenne belt suture zone (1.9 to 1.7 Ga) approximately parallels Highway 34 in Sybille Canyon, and is exposed in the Richeau Hills (Robert Houston, personal communication, 1998) which are east of Sybille Canyon and north of the Iron Mountain kimberlite district. To the west, the Cheyenne belt is masked by the intrusion of the anorthosite-syenite batholith. Numerous kimberlitic indicator mineral anomalies were detected on this quadrangle and some of the more prominent are discussed below. For the most part, only a small percentage of the indicator minerals were tested for geochemistry.

Widespread kimberlitic indicator mineral anomalies shown on **Plate 1** are suggestive of a widespread kimberlite swarm. Several areas stand out as highly anomalous and are suggestive of proximal sources: Grant Creek, Middle Sybille Creek, and the Dodge Ranch within the Elmers Rock greenstone belt. Other notable anomalies include Plumbago Canyon, Rawhide Park, Mule Creek, and a tributary of South Sybille Creek.

Iron Mountain anomaly

Samples collected several years ago along the western edge of the Iron Mountain district provided direct evidence of kimberlite (Hausel and others, 1988). A group of samples collected in Spring Creek (Hay Canyon) were highly anomalous (**Plate 1**). One sample collected in a tributary draining the Iron Mountain district (W/2 section 18, T19N, R70W) yielded more than 100 pyrope garnets, 10 chromian diopsides, and some picroilmenite. This sample was collected within 0.5 mile of the mapped kimberlites.

A short distance downstream from the above sample, a second sample showed a dramatic decline in indicator minerals. This sample yielded 18 pyrope garnets, no chromian diopside, and some picroilmenite. The dramatic decrease in indicator minerals may have been due to selection of a poor sample site, as well as the influx of sediment from Spring Creek.

A third sample collected in Spring Creek was located about 0.5 mile farther downstream from the previous sample. Concentrates from this sample yielded 23 pyrope garnets. The fourth sample collected 0.8 mile downstream from this site yielded only 5 pyrope garnets. A fifth sample 0.5 mile farther downstream contained no indicator minerals.

All these samples provide a general guide in the search of kimberlite in similar Wyoming terrains. For example, they indicate that:

- Chromian diopside is greatly restricted in stream transport distance. Maximum transportation distances of only 0.6 to 0.8 mile from a source kimberlite are assumed. Where chromian diopside is found, it suggests a proximal source.

- Pyrope garnet may be transported at least 2.25 miles from the source kimberlite.

- When recovered in stream sediment samples, the indicator minerals suggest that a kimberlite source lies within a few miles upstream.
- Abundant indicator minerals (>10) suggest a proximal source.

Grant Creek anomaly

Grant Creek lies north of the Iron Mountain district near the projected trend of the Cheyenne belt, just south of Sybille Canyon. This is a promising anomaly that is very localized. At this location, Grant Creek is relatively wide and flat. Along the western edge of the creek is a small outcrop of carbonate rock of unknown origin that should be investigated in greater detail.

Eleven sediment samples were collected over a distance of about one mile in the vicinity of section 36, T21N, R71W. Five of the samples yielded from 1 to 5 kimberlitic indicator minerals to >100 kimberlitic indicator minerals with traces of visible gold (see figure 23, Hausel, 1998). Chromian diopside was recovered from four samples, and three contained 50 or more kimberlitic indicator minerals, producing a similar distribution to the Iron Mountain anomaly described above. Samples collected a few hundred feet upstream from the anomaly were devoid of kimberlitic indicator minerals, providing very good evidence for the presence of a nearby buried kimberlite or kimberlites.

Reconnaissance geophysical lines were run over the anomalous area in section 36, in an attempt to find a distinct buried conductor that might be related to a hidden kimberlite. Lines were also run over the carbonate outcrop along the edge of Grant Creek in the same general area. However, the geophysical data was inconclusive and is not presented here.

It is highly recommended that this anomaly be further investigated as follows: (1) kimberlitic indicator minerals need to be geochemically tested to determine the probability of diamonds; (2) a detailed grid magnetic and electromagnetic geophysical survey needs to be completed over the entire area in order to isolate the source of the indicator minerals and to determine the configuration of any conductors; and (3) if the source of the anomaly can be found, the source should be explored by drilling and trenching.

Middle Sybille Creek anomaly

Middle Sybille Creek, which lies along the Cheyenne belt, was initially investigated by the WSGS in 1980. A previously unreported kimberlite was first described by the WSGS along the northern bank of Middle Sybille Creek, and named in honor of Mr. and Mrs. Jack Radichal, the land owners (Hausel and others, 1981). A few years later, WSGS field crews conducted a district-wide stream sediment sample survey to search for additional kimberlites (Hausel and others, 1988).

The distribution of kimberlitic indicator mineral anomalies in the drainage basin supports the presence of several hidden kimberlites. Kimberlitic indicator minerals were recovered from 42 separate sample sites in the main drainage and tributaries over a distance of 10 miles (**Plate 1**). Seven of the samples contained chromian diopside along with pyrope and picroilmenite, indicating a proximal source(s). A few garnets that were still available from the earlier study were geochemically tested during this project, and some yielded G10 (diamond-stability) geochemistry. The presence of the G10 garnets makes this area high priority as the geochemistry supports an interpretation that some undiscovered kimberlites in the area originated from the diamond-stability field.

The Radichal kimberlite, which lies near the center of the indicator mineral anomaly (**Figure 16**), is a small blow consisting of hypabyssal facies kimberlite similar to many of the Iron Mountain kimberlites. Many of the indicator mineral anomalies found downstream from this kimberlite could have been derived from this intrusive. However, at least two sample sites (and probably more) are interpreted to have had different sources, as these were taken in closed basins in tributaries draining into Middle Sybille Creek. Additionally, more than a dozen anomalous sample sites lie upstream from the kimberlite. This evidence indicates that several undiscovered kimberlites occur within this region.

During the 2000 field season, geophysical lines were run in Middle Sybille Creek near the Radichal kimberlite (**Figure 16** and **Appendix C**). This drainage contains a large hay meadow that could potentially hide several kimberlites; a few geophysical lines were run there.

As noted in **Appendix C**, the geophysical lines detected several buried conductors, some of which could be hidden kimberlite. These anomalies, along with the presence of several kimberlitic indicator mineral anomalies (including some G10 garnets) and one verified kimberlite in the district (**Figure 16**), are strong reasons that this district should be given priority for future research.

Any future research in this area should run grid geophysical surveys over some of the more distinct EM anomalies in the drainage basin. Additional stream sediment sampling may also assist in isolating anomalies. Some of the better conductivity anomalies should also be drilled to determine their source.

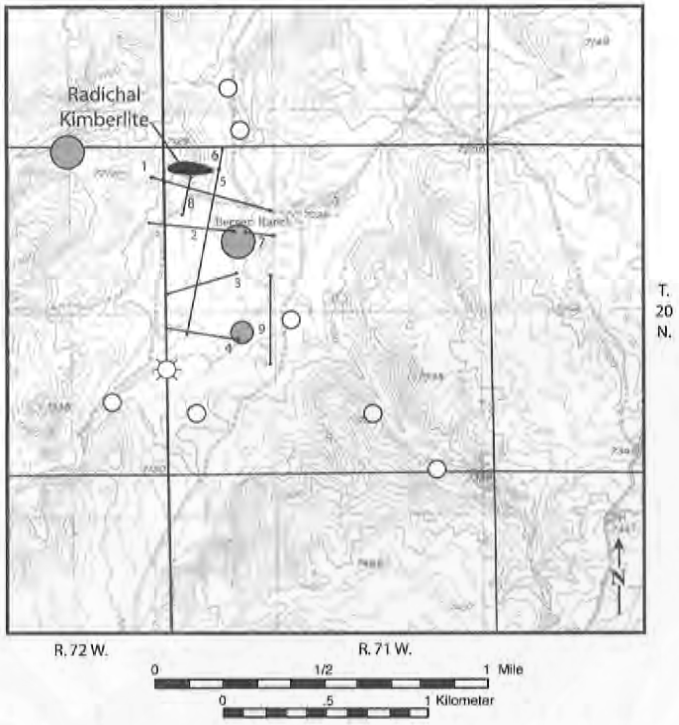

Figure 16. Location map of geophysical lines and stream sediment samples in the Middle Sybille Creek area, Laramie Mountains, Wyoming. Base map taken from 1:24,000-scale topographic map of the Sheep Rock Quadrangle, Wyoming. See **Appendix C** for descriptions and profiles of geophysical lines and **Plate 1** for explanation of symbols.

Dodge Ranch

Dodge Ranch lies within the Elmers Rock greenstone belt, an Archean metasedimentary-metavolcanic synform along the edge of the Wyoming craton north of Sybille Canyon. This greenstone belt hosts one of the most impressive, widespread, kimberlitic indicator mineral anomalies in the U.S., suggesting the presence of many hidden kimberlites. The presence of some G10 diamond-stability garnets in this region indicates that some of the undiscovered intrusives originated from the diamond-stability field. Many of the anomalies are impressive, but only a few will be discussed below.

Bull Camp Peak (located in section 5, T22N, R72W), located along the western flank of the Laramie Mountains, and east of the Dodge Ranch headquarters, lies in the center of a group of anomalous samples (**Plate 1**). Streams draining in nearly every direction from Bull Camp Peak contain pyrope garnet, chromian diopside, and picroilmenite as well as some sapphires and visible gold. A few of the samples also yielded more than 50 kimberlitic indicator minerals, and one sample yielded 128 pyrope garnets. The anomalies and distribution suggest a proximal source for the indicator minerals. Most samples were not geochemically tested, but a few garnets still available from Hausel and others (1988) were tested and a few had sub-calcic, chrome (G10) geochemistry.

Additional stream sediment sampling needs to be completed in the headwaters of all drainages surrounding Bull Camp Peak to locate the source of the indicator minerals. Geochemical analyses of the indicator minerals should follow to identify the better diamond targets, followed by detailed geological mapping and geophysical grid surveys, where necessary. A few depressions with vegetation anomalies were examined with EM profiles, and a few buried conductors were detected.

Another very prominent anomaly in the greenstone belt was identified near Wheatland tunnel on the Laramie River in section 36, T23N, R72W. A large group of samples in the vicinity contained indicator minerals; however, samples within section 36 show a dramatic increase in the number of indicator minerals. One sample yielded 73 indicator minerals (including some chromian diopside), indicating a proximal source. Three samples in this section also contained sapphire. [Authors' note: gem-quality corundum (sapphire) and cordierite (iolite) were identified by the WSGS in the Palmer Canyon area to the northeast in 1995 (see Hausel, 2002). The presence of sapphire in these samples suggests similar nearby corundum occurrences that are unrelated to kimberlite.] It is highly recommended that additional samples be taken, and a detailed geologic map be completed in this area in order to isolate the source of the indicator minerals and sapphires.

South Cooney Hills anomaly

Near the eastern edge of the Laramie Mountains, four samples were collected along the edge of South Cooney Hills (**Plate 1**). Two samples collected in the headwaters of restricted drainages in section 29, T23N, R69W, yielded pyropes with G10 chemistry. To the south in Mule Creek (NE section 34, T22N, R70W), another sample collected adjacent to Highway 34 yielded some pyrope garnets including some with G10 geochemistry. Detailed sampling and mapping throughout the region is recommended to help find the source of the anomalies.

Indian Guide district

Stream sediment samples in the Indian Guide area (west of the Iron Mountain kimberlite district) show few anomalies (**Plate 1**). Even so, a group of intriguing depressions was identified by the WSGS during airphoto reconnaissance of this area. These depressions are structurally controlled, circular to elliptical in outline, and lie within the Laramie anorthosite complex (**Figure 17**). Furthermore, the depressions lie along trend with the Iron Mountain kimberlites 4 miles to the east. The depressions occur in sections 8, 9, 16, and 17, T19N, R71W.

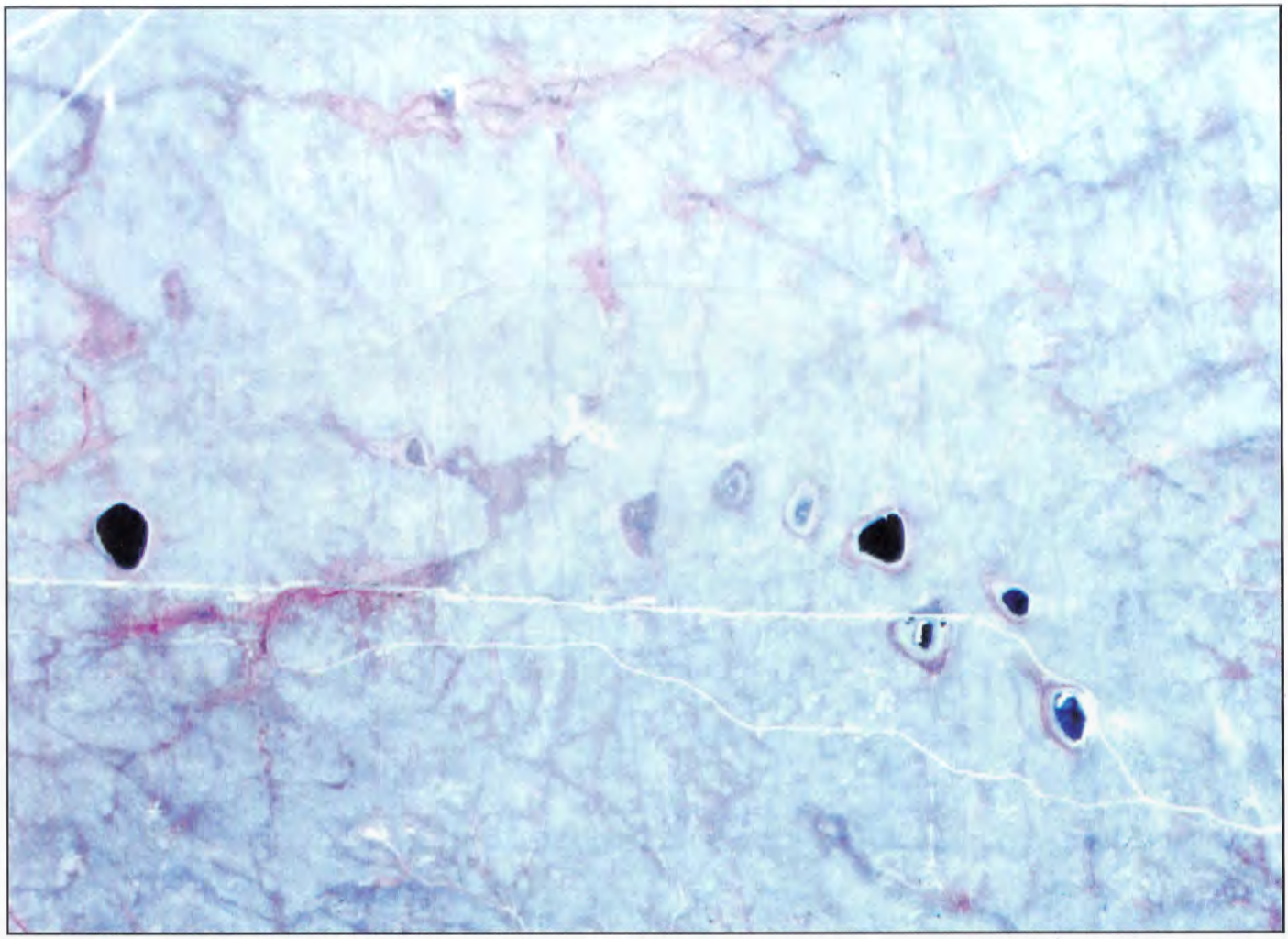

Figure 17. BLM Color InfraRed, RWIR 2-15-14 air photograph over the Indian Guide area west of the Iron Mountain kimberlite district. Note the very distinct, structurally controlled depressions near the haulage road. Geophysical lines over some of the anomalous areas are shown on **Figure 18** and described in **Appendix D.**

Several of the depressions support shallow intermittent lakes, and lie on distinct north-trending fractures. Northwesterly-trending fractures also are evident, and many of the depressions lie at the intersections of the fracture sets.

The circular depressions mimic several known kimberlite localities in the world. In particular, some recent discoveries of diamondiferous kimberlite in the Lac de Gras region of the Northwest Territories, Canada, were made on similar water-filled depressions (Kjarsgaard and Levinson, 2002). However, the lack of kimberlitic indicator mineral anomalies in the Indian Guide area is disconcerting: samples collected along the margins of two of these depressions yielded no indicator minerals.

Electrical conductors were detected along most of the geophysical lines (**Figure 18** and **Appendix D**) that were run over the depressions. The source of the conductors was not determined, and it is suggested that the lakes may contain zones of clay. With the lack of any kimberlitic indicator minerals in the area, it is unlikely that any of the depressions are related to kimberlite. However, the presence of the depressions along the projected trend of the Iron Mountain kimberlites seems more than coincidence, and the presence of controlling fractures make it unlikely that any of these are impact features. We recommend drilling one or more of the depressions in order to assist in an interpretation of their genesis.

Laramie 1:100,000-scale Quadrangle

Several dozen stream sediment samples were collected from the area shown on the Laramie Quadrangle (**Plate 2**). The Precambrian core of the Laramie Mountains consists of vast outcrops of Sherman Granite over much of the quadrangle, and anorthosite-syenite outcrops in the northern part of the quadrangle. These 1.4- to 1.5-Ga batholithic complexes intruded the Proterozoic basement located south of the Cheyenne belt. This quadrangle also encloses the northern part of the Colorado-Wyoming State Line diamond district,

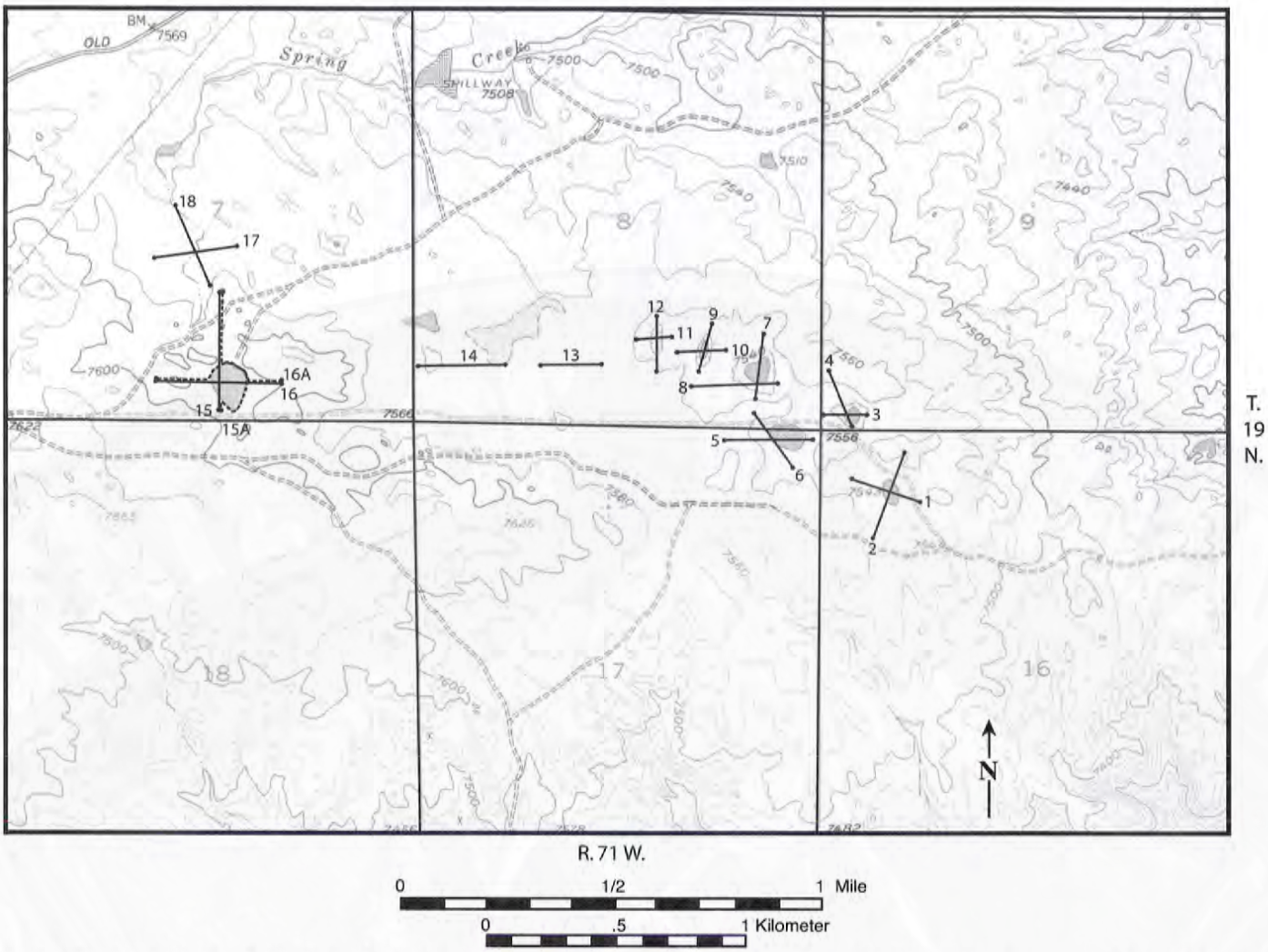

Figure 18. Location map of geophysical lines in the Indian Guide area, Laramie Mountains, Wyoming. Base map taken from 1:24,000-scale topographic maps of the Sheep Rock, Indian Guide, Goat Mountain, and Baldy Mountain quadrangles, Wyoming. See **Appendix D** for descriptions and profiles of geophysical lines and **Plate 1** for locations of nearby stream sediment samples.

which includes at least 20 known Devonian diamond-bearing kimberlites in Wyoming.

Eagle Rock anomaly

North of the State Line district, a highly anomalous area known as Eagle Rock encloses an impressive dispersion of kimberlitic indicator mineral anomalies over an area of 50 to 60 mi² (**Plate 2**). The anomalous samples were collected on North, Middle, and South branches of Lodgepole Creek near Eagle Rock (Ts15 and 16N, Rs70 through 72W), several miles north and east of Interstate 80.

Several samples yielded pyrope garnet, with a few scattered chromian diopsides and picroilmenites in a distinct anomaly on North Lodgepole Creek east of Pilot Hill (sections 5 and 6, T15N, R71W). These samples were collected in areas dammed by beavers, and represent poor sample sites due to the lack of heavy mineral concentrates. Even so, several indicator mineral anomalies were identified. The area is heavily timbered, and difficult to prospect. It is recommended that additional samples be taken for geochemical testing to determine the probability of finding diamonds in this region.

This area also hosts a regional fluorite anomaly covering 150 mi² and outlined by samples collected between North Lodgepole Creek and Interstate 80. Most samples collected within the area contained fluorite from unknown sources. In all probability, the fluorite is related to the Sherman Granite. The fluorite has no relationship to kimberlite, but represents a separate mineral resource.

Boulder Ridge anomalies

Samples collected in the Boulder Ridge area west of Tie Siding (Ts12 and 13N, R73W) yielded some sparse and weak kimberlitic indicator mineral anomalies. Most of the anomalies were defined by only one or two

picroilmenite grains, with a few containing pyrope. This area is anomalous, but considered low priority due to the limited number of indicator minerals.

Laramie Peak 1:100,000-scale Quadrangle

Several dozen stream sediment samples were panned and collected north of the Dodge Ranch on the Laramie Peak Quadrangle (**Plate 3**) during this project. These were panned and examined microscopically by Roger Motten, contract geologist, and a few were reported to contain pyrope garnet. However, examination of all the sample concentrates to verify the pyropes or their geochemistry has not been completed. Other samples collected by Hausel and others (1988) showed a group of anomalous stream sediment samples in Duck Creek south of Davidson Flats (near the south edge of the quadrangle) that contained pyrope garnet and a few with chromian diopside (**Plate 3**). The data suggests that some undiscovered kimberlite intrusives may exist in this area.

A kimberlitic anomaly was reported east of Laramie Peak in section 31, T28N, R70W. Property in this section was leased to Cominco American in the early 1980s for diamond testing (Lee Peterson, personal communication, 2001). Stream sediment samples collected from the area by Cominco contained hundreds of kimberlitic indicator minerals (Howard Coopersmith, personal communication, 2001).

Saratoga 1:100,000-scale Quadrangle

Only a few stream sediment samples were collected in the vicinity of Centennial Ridge in the Medicine Bow Mountains. Samples collected along the Middle Fork of the Little Laramie River and on Libby Creek yielded pyrope garnets (**Figure 19**). Additional samples taken above Sand Lake in Deep Creek (center E/2 section 17, T17N, R79W) and in a tributary of the East Fork of the Medicine Bow River (NE section 1, T17N, R80W) contained no kimberlitic indicator minerals.

Two octahedral diamonds were recovered on Cortez Creek (section 35, T17N, R81W), on the west flank of the Medicine Bow Mountains by prospector Paul Boden in 1977 along with some gold. The source of the diamonds and gold is unknown. The region is underlain by a variety of Proterozoic and Late Archean metasedimentary rocks, including some conglomeratic facies, which could be the source of the diamonds and gold. Stream sediment samples collected in Cortez Creek yielded no pyrope garnets.

Another area of interest is Iron Creek, a tributary of French Creek to the south. Superior Minerals Company reported finding pyrope garnets in this area in the early 1980s. The source of the garnets was not found (T.E. McCandless, personal communication, 1998).

Pyrope garnets have been recovered from Douglas Creek by a gold prospector (Paul Allred, personal communication, date unknown). Dredged gold samples collected immediately south of the Bobbie Thompson campground contained some pyrope garnets. A few of the garnets were tested by the WSGS and exhibited an index of refraction consistent for pyrope garnet.

Other pyrope garnets were collected by individuals who attended a public field trip sponsored by the WSGS in 1999. During a gold-panning session on the Middle Fork of the Little Laramie River, some attendees panned several pyrope garnets in section 1, T15N, R79W.

Figure 19. Stream sediment sample location map showing kimberlite indicator mineral anomalies in the Medicine Bow Mountains, Wyoming. Base map from part of the Saratoga 1:100,000-scale Quadrangle, Wyoming.

Conclusions

Data collected by the WSGS and others indicates that the Wyoming craton encloses a major kimberlite-lamproite-lamprophyre province (Hausel, 1998). The presence of diamonds and a large number kimberlitic indicator minerals supports the fact that this craton and cratonized margin is highly anomalous.

This report provides evidence that a major kimberlite district exists at Iron Mountain. The limits of the district have not yet been determined, as it is unexplored and unmapped for kimberlites to the north and west, and kimberlites probably continue eastward and westward under the sedimentary cover. Several geophysical anomalies and associated depressions within the district deserve further investigation, as some of these contain montmorillonite clay, a product that is often produced in blue ground over kimberlite. The lack of kimberlitic indicator minerals associated with these depressions is enigmatic. These are possibly related to the kimberlitic indicator mineral-poor carbonatized kimberlite breccias (Type III) found elsewhere in the district. It is recommended that one or more of these depressions be drilled to determine their origin.

Geophysical and topographic anomalies in the Indian Guide area may suggest a possible westward extension of the Iron Mountain district. However, the lack of kimberlitic indicator mineral anomalies in this area is disconcerting.

Kimberlites also continue north of the Iron Mountain district. For example, a group of hidden kimberlites (IG1, IG2, IG3, and IG17) was discovered by Cominco American in the 1980s following stream sediment sampling and follow-up geophysical surveys (Howard Coopersmith, personal communication, 2002). One of the kimberlites was buried under about 60 to 90 feet of alluvium and colluvium. Kimberlite dikes trending to the north were discovered during mapping of the area by the WSGS. In all probability, these dikes continue farther to the north. Even farther north, kimberlitic indicator mineral anomalies (including G10 pyrope garnets) surrounding the Radichal kimberlite, as well as anomalies in the Grant Creek and Mule Creek areas, suggest that a sizable district may occur in this region.

Based on the geochemistry of both the kimberlites and kimberlitic indicator minerals, there is potential for finding additional diamonds in the Iron Mountain district and in areas to the north. The data in this report suggests that some Iron Mountain kimberlites may contain diamonds. We recommend collecting bulk samples from the kimberlites that have yielded G10 pyropes and testing these samples for diamond. Additional detailed geologic mapping, stream sediment sampling, and the initiation of airborne INPUT® and remote sensing surveys would provide much needed information on the extent of the district and the kimberlite province.

Additional research, and more detailed surveys and sampling programs that lead to discovery of commercial diamond deposits could ultimately reap tremendous benefits to the economy of Wyoming, as some diamonds are the most valuable gemstones on earth.

In summary, the data from Iron Mountain and the surrounding area supports an interpretation that Wyoming is underlain by a significant kimberlite province. Only the southeastern part of Wyoming has been prospected for kimberlites in much detail, and many large gaps between data sets remain. The rest of Wyoming is considered to have even greater potential for diamondiferous kimberlite due to the presence of favorable Archean basement complexes north of the Cheyenne belt.

References cited

Billman, J., 1998, Tiffany's? Hardly. We picked ours up in Laramie: Outside Magazine, v. 23, no. 10, p. 41-50.

Bradley, W.H., 1964, Lazurite, talc and chlorite from the Green River Formation: American Mineralogist, v. 49, p. 778-781.

Coopersmith, H.G., 1991, Geology and exploration of the Kelsey Lake diamondiferous kimberlites, Colorado: Society of Mining Engineers Preprint 91-174, 18 p.

Coopersmith, H.G., Mitchell, R.H., and Hausel, W.D., in press, Kimberlites and lamproites of Colorado and Wyoming, USA: 8th International Kimberlite Conference, Field Trip Guidebook.

Coopersmith, H.G., and Schulze, D.J., 1996, Development and geology of the Kelsey Lake diamond mine, Colorado, *in* Thompson, T.B., editor, Diamonds to gold - I. State Line Kimberlite district, Colorado, II. Cresson mine, Cripple Creek district, Colorado: Society of Economic Geologists Guidebook Series, p. 5-19.

Eggler, D.H., Meen, J.K., Welt, F., Dudas, F.O., Furlong, K.P., McCallum, M.E., and Carlson, R.W., 1988, Tectonomagmatism of the Wyoming Province: Colorado School of Mines Quarterly, p. 25-40.

Fipke, C.E., Gurney, J.J., and Moore, R.O., 1995, Diamond exploration techniques emphasizing indicator mineral geochemistry and Canadian examples: Canada Geological Survey Bulletin 423, 86 p.

Griffin, W.L., Moore, R.O., Ryan, C.G., Gurney, J.J., and Win, T.T., 1997, Geochemistry of magnesian ilmenite megacrysts from southern African kimberlites, *in* Russian Geology and Geophysics, v. 38, no. 2. p. 421-443.

Gurney, J.J., 1984, A correlation between garnets and diamonds in kimberlite, *in* Clover, J.E., and Harris, P.G., editors, Kimberlite occurrences and origin: a basis for conceptual models in exploration: Geology Department and University Extension, University of Western Australia, Publication No. 8, p. 143-166.

Gurney, J.J., 1989, Diamonds, *in* Ross, J., and others, editors, Kimberlites and related rocks, Volume 2, Their mantle/crust setting, diamonds, and diamond exploration, Proceedings of the 4th International Kimberlite Conference, Perth, Australia: Geological Society of Australia Special Publication 14, p. 935-965.

Gurney, J.J., Helmstaedt, H.H., and Moore, R.O., 1993, A review of the use and application of mantle mineral geochemistry in diamond exploration: Pure and Applied Chemistry, v. 65, p. 2423-2442.

Hausel, W.D., 1994, Economic geology of the Seminoe Mountains greenstone belt, Carbon County, Wyoming: Wyoming State Geological Survey Report of Investigations 50, 31 p.

Hausel, W.D., 1995a, Diamond, kimberlite, lamproite, and related rocks in the United States: Exploration and Mining Geology, v. 4, no. 3, p. 243-270.

Hausel, W.D., 1995b, Diamonds and their host rocks in the United States: Mining Engineering, v. 47, no. 8, p. 723-732.

Hausel, W.D., 1996, Recurring kimberlite and lamproite magmatism in the Wyoming craton–an overview (abstract): Geological Society of America Abstracts with Programs, 48th Annual Rocky Mountain Section, v. 28, no. 4, p. 10.

Hausel, W.D., 1998, Diamonds and mantle source rocks in the Wyoming Craton, with a discussion of other U.S. occurrences: Wyoming State Geological Survey Report of Investigations 53, 93 p.

Hausel, W.D., 2002, A new source of gem-quality cordierite and corundum in the Laramie Range of southeastern Wyoming: Rocks & Minerals, v. 76, no. 5, p. 334-339.

Hausel, W.D., Glahn, P.R., and Woodzick, T.L., 1981, Geological and geophysical investigations of kimberlites in the Laramie Mountains of southeastern Wyoming: Wyoming State Geological Survey Preliminary Report 18, 13 p., 2 plates (scale 1:24,000).

Hausel, W.D., Gregory, R.W., Motten, R.H., and Sutherland, W.M., 2000, Economic geology of the Iron Mountain kimberlite district, Wyoming: Wyoming Geological Association Field Conference Guidebook, p. 151-164.

Hausel, W.D., Kucera, R.E., McCandless, T.E., and Gregory, R.W., 1999, Mantle-derived breccia pipes in the southern Green River Basin of Wyoming (USA): Proceedings of the 7th International Kimberlite Conference, University of Cape Town, South Africa, p. 348-352.

Hausel, W.D., McCallum, M.E., and Woodzick, T.L., 1979, Exploration for diamond-bearing kimberlite in Colorado and Wyoming: an evaluation of exploration techniques: Wyoming State Geological Survey Report of Investigations 19, 29 p.

Hausel, W.D., Sutherland, W.M., and Gregory, E.B., 1988, Stream-sediment sample results in search of kimberlite intrusives in southeastern Wyoming: Wyoming State Geological Survey Open-File Report 88-11, 11 p. (5 plates) (revised 1993).

Hearn, B.C., Jr., and McGee, E.S., 1983, Garnets in Montana diatremes: a key to prospecting for kimberlites: U.S. Geological Survey Bulletin 1604, 33 p.

Houston, R.S., Karlstrom, K.E., Hills, F.A., and Smithson, S.B., 1979, The Cheyenne Belt: the major Precambrian crustal boundary in the western United States (abstract): Geological Society of America Abstracts with Programs, v. 11, p. 446.

Karlstrom K.E., and Houston, R.S., 1984, The Cheyenne Belt: analysis of a Proterozoic suture in southern Wyoming: Precambrian Research, v. 25, p. 415-446.

Kjarsgaard, B.A., and Levinson, A.A., 2002, Diamonds in Canada: Gems and Gemology, v. 38, no. 3, p. 208-238.

Lampietti, F.M.J., and Sutherland, D., 1978, Prospecting for diamonds—some current aspects: Mining Magazine, August, p. 117-123.

Larson, E.E., and Amini, M.H., 1981, Fission-track dating of the Green Mountain kimberlite diatreme near Boulder, Colorado: The Mountain Geologist, v. 18, no. 1, p. 18-22.

Loucks, R.R., Premo, W.R., and Snyder, G.L., 1988, Petrology, structure and age of the Mullen Creek complex and age of arc accretion, Medicine Bow Mountains, Wyoming (abstract): Geological Society of America Abstracts with Programs, v. 20, p. A73.

McCallum, M.E., and Mabarak, C.D., 1976, Diamond in State Line kimberlite diatremes, Albany County, Wyoming and Larimer County, Colorado: Wyoming State Geological Survey Report of Investigations 12, 36 p.

McCallum, M.E., and Waldman, M.A., 1991, The diamond resources of the Colorado-Wyoming State Line district: kimberlite indicator mineral chemistry as a guide to economic potential: Wyoming Geological Association 42nd Field Conference Guidebook, p. 77-90.

McDowell, F.W., 1971, K-Ar ages of igneous rocks from the western U.S.: Isochron/West, no. 2, p. 1-16.

Mitchell, R.H., 1986, Kimberlites: mineralogy, geochemistry, and petrology: Plenum Press, New York, New York, 442 p.

Mitchell, R.H., and Bergman, S.C., 1996, Petrology of lamproites: Plenum Press, New York, New York, 447 p.

Naeser, C.W., and McCallum, M.E., 1977, Fission-track dating of kimberlitic zircons: Extended Abstracts, Second International Kimberlite Conference, Santa Fe, New Mexico, p. 242-243.

Peterman, Z.E., Hedge, C.E., and Braddock, W.A., 1968, Age of Precambrian events in the northeast Front Range, Colorado: Journal of Geophysical Research, v. 73, p. 2277-2296.

Schulze, D.J., Anderson, P.F.N., Hearn, B.C., Jr., and Hetman, C.M., 1995, Origin and significance of ilmenite megacrysts and macrocrysts from kimberlite: International Geology Review, v. 37, p. 780-812.

Smith, C.B., 1977, Kimberlite and mantle derived xenoliths at Iron Mountain, Wyoming: M.S. thesis, Colorado State University, Fort Collins, 218 p.

Smith, C.B., 1983, Rb-Sr, U-Pb, Sm-Nd isotopic studies of kimberlite and selected mantle-derived xenoliths: Ph.D. dissertation, University of Witwatersrand, Johannesburg, South Africa, 436 p.

Appendix A – Geophysical lines, electromagnetic profiles, and magnetic profiles, Iron Mountain district

This contains descriptions of geophysical lines, electromagnetic (EM) profiles, and magnetic profiles in the Iron Mountain district, Laramie Mountains, Wyoming. Stations for geophysical lines 9-1, 9-2, 9-3, and 13 through 22 are 30 feet apart; stations for all other geophysical lines are 15 feet apart. See **Figure 15** for locations of geophysical lines.

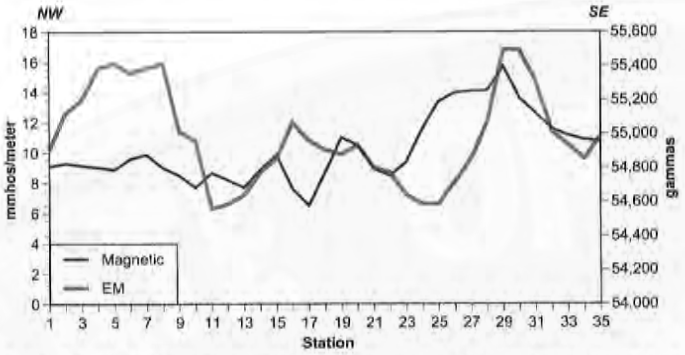

Line 1 trends north-northwest and was located in kimberlite along the eastern margin of the district in section 2, T19N, R70W. Both the EM and magnetic profiles show a complex pattern in the kimberlite, which may be either the influence of large granitic xenoliths trapped in the kimberlite or differential weathering. The kimberlite in this part of the district appears to be quite homogeneous; the complex pattern is probably not due to different kimberlite facies.

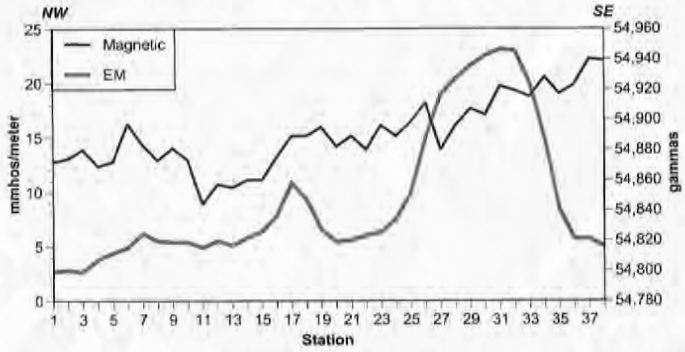

Line 2, a northwest-trending line which crossed the projected trend of the kimberlite dike, detected a 45-foot-wide conductor with a maximum conductivity of 24 mmhos/meter. The magnetic survey showed no obvious anomalies.

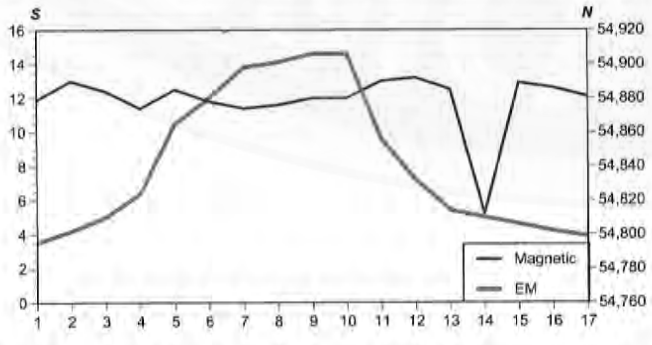

Line 3, a south to north profile across a bog, detected a 90-foot-wide conductor. This conductor is interpreted to be a reflection of a dike beneath the heavily vegetated depression. The magnetic survey only showed an anomaly at station 14.

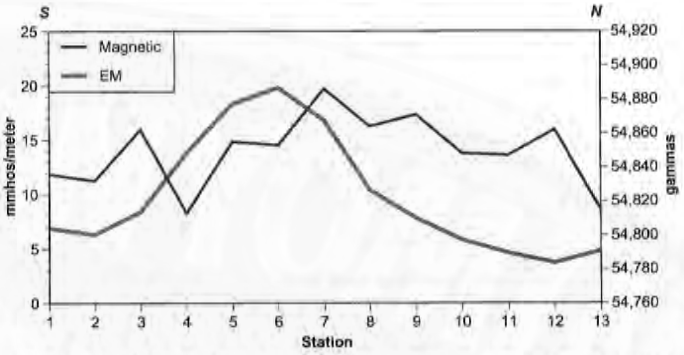

Line 4, a south to north line east of the northeasterly trending kimberlite dike, detected a 60-foot-wide conductor with a maximum conductivity of 20 mmhos/meter.

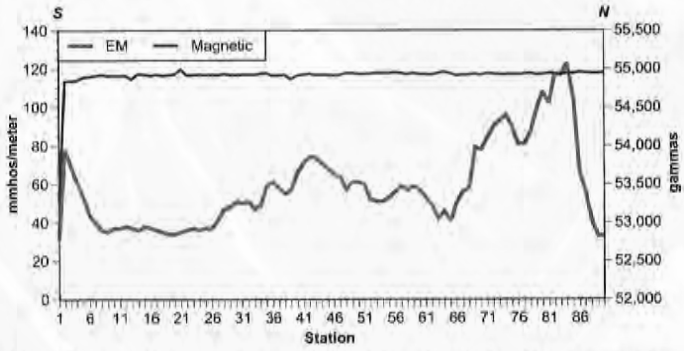

Line 5, a south to north geophysical line located within the Tertiary paleoplacer along the western edge of the district, was set up to search for hidden kimberlite beneath the paleoplacer. EM anomalies were detected near station 3, surrounding station 43, station 73, and station 83. It is not known if these anomalies represent hidden kimberlite, but further investigations are warranted. The magnetic survey was not distinctive.

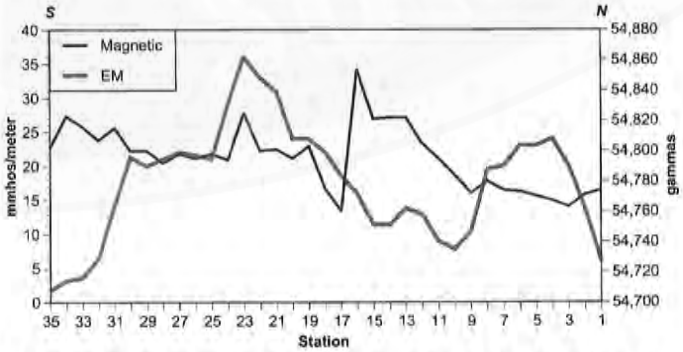

Line 6, a north to south line, was run over a linear depression in section 16, T19N, R70W. The response showed a sinuous conductor with a maximum conductivity of 36 mmhos/meter and a magnetic profile with several peaks.

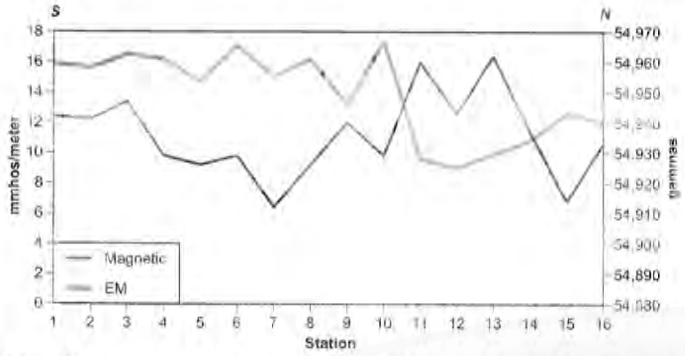

Line 7 was run over apparent blue ground along the edge of the Tertiary paleoplacer. This line is the northward continuation of Line 10, below. The EM data shows strong conductivity as soon as the blue ground is reached, with the strong conductivity continuing into the paleoplacer. The magnetic profile was not definitive.

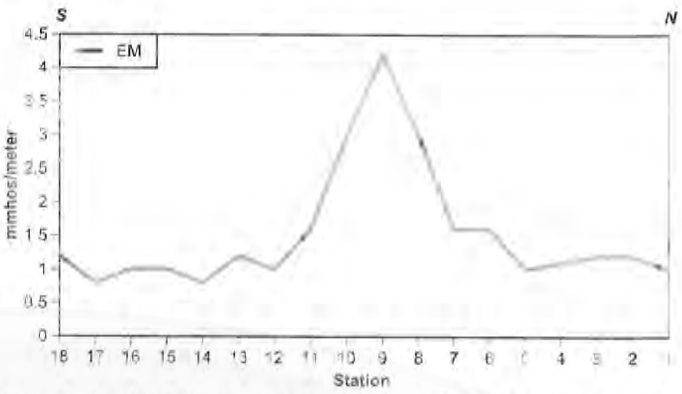

Lines 9-1 and 9-2 were run to test a depression in the E/2 section 9, T19N, R70W, which included a small exposure of blue ground along the western edge of the depression. Although distinct, the anomaly detected in north-south **Line 9-1** had a maximum conductivity of only 6.5 mmhos/meter compared to a background of about 1 mmho/meter.

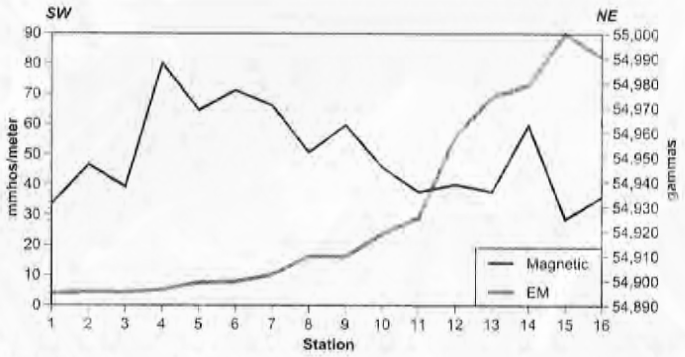

Line 8 was a southwest to northeast line that crossed the south end of line 7 at an acute angle. A very high conductivity peak at station 15 was encountered near the northeast end of the profile. The magnetic profile was not definitive over the conductivity high or the rest of the profile.

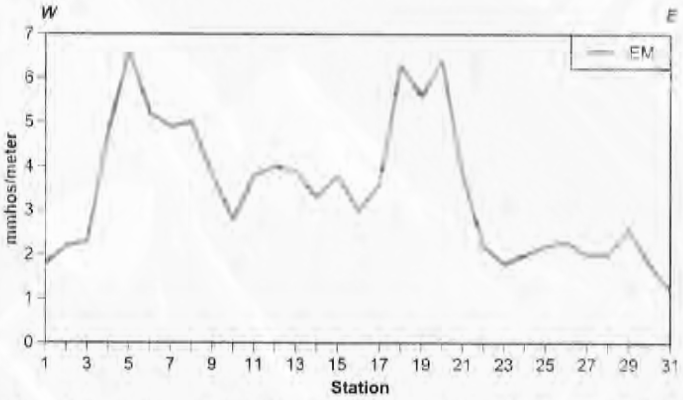

Line 9-2, a west to east line, detected the same 6.5-mmhos/meter anomaly found in line 9-1 as well as another similar anomaly farther to the east.

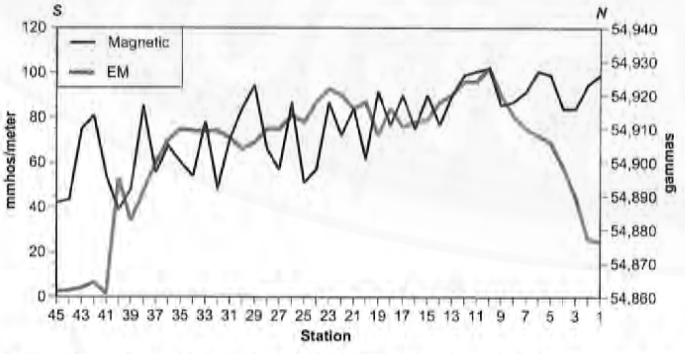

North to south **Line 9** was run perpendicular to line J (below) over a depression found in section 8, T19N, R70W. This line was north of the kimberlite profiled in line K (below) and west of line 10. A strong conductor was apparent in the Tertiary paleoplacer across much of the line. A conductivity peak of 100 mmhos/meter was detected. The magnetic profile showed a saw-toothed pattern over the anomaly.

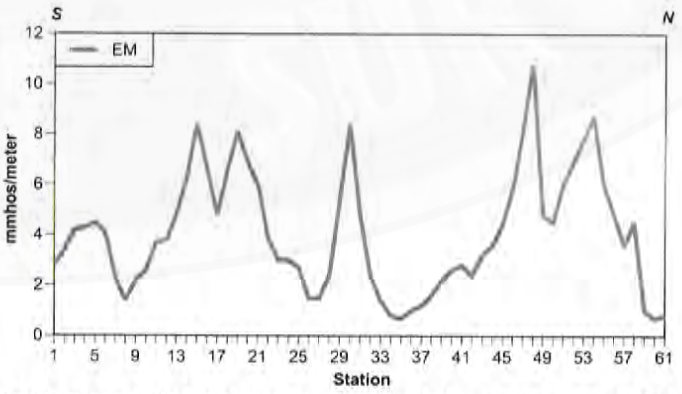

South to north **Line 9-3** was run to investigate a group of vegetation anomalies that were interpreted as hidden kimberlite dikes in the NE section 9, T19N, R70W. Conductors were detected over at least five anomalies, suggesting that these may be extensions of the mapped kimberlite dikes.

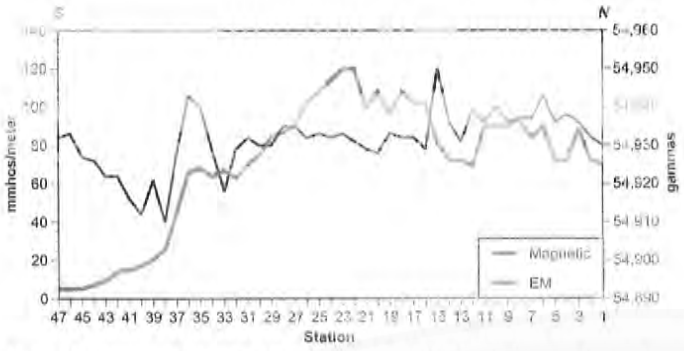

Line 10 was located west of and ran parallel to line 9. It is the southward extension of line 7 (above). The north to south profile showed a high conductivity anomaly over the northern three fourths of the line, with a peak conductivity of 120 mmhos/meter. The magnetic profile was not distinctive over the anomaly.

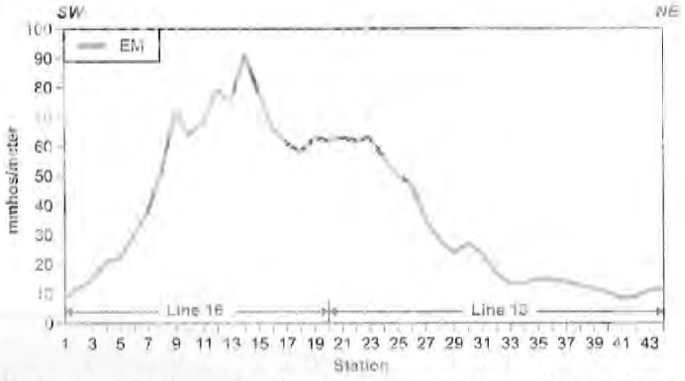

Line 13, a southwest to northeast line, and **Line 16**, the southwestward continuation of line 13, were run northwest of and parallel to lines 12 and 14 (below). A conductivity anomaly greater than 30 mmhos/meter over 600 feet was detected, with a maximum conductivity of 91 mmhos/meter.

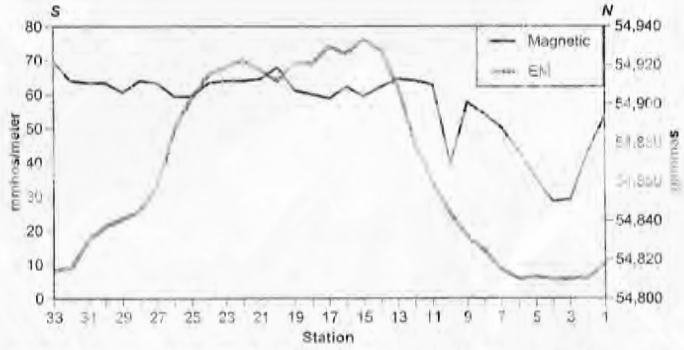

Line 11 was run perpendicular to line I (below) over a distinct depression in section 8, T19N, R70W. This north to south line detected a distinct 230-foot wide conductor. The magnetic profile was not distinctive over the anomaly.

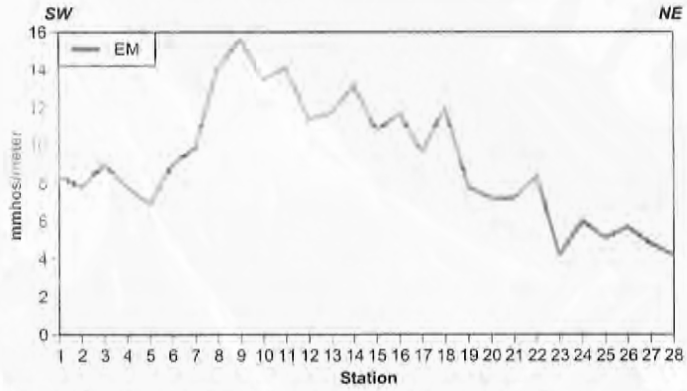

Line 14 was a southwest to northeast line located northwest of lines C and D (below). It extended line 12 to the northeast. A conductivity anomaly of 15.6 mmhos/meter was detected on the southwestern end of the profile.

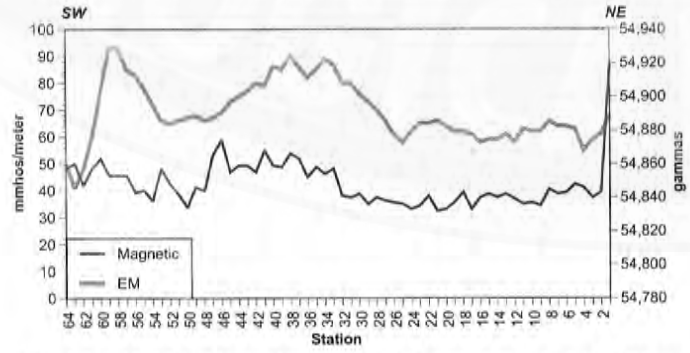

Line 12, a northeast to southwest line, was run at an angle to lines 11, G, H, and I. The conductivity was relatively high over the entire profile (background conductivity of about 65 mmhos/meter) with two obvious anomalies on the southwestern end of the profile.

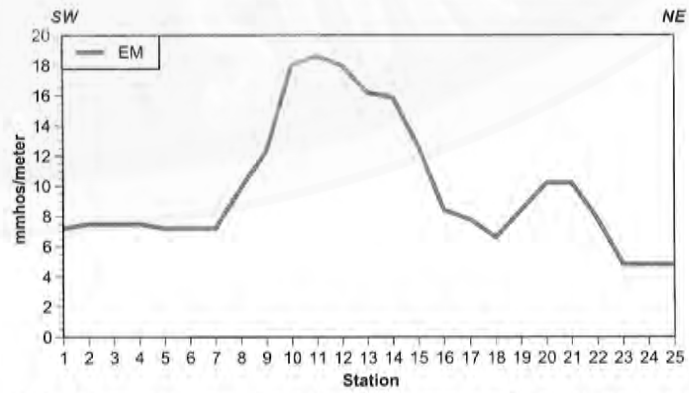

Line 15 was run almost along the same traverse as line A (below) and detected the two easternmost EM anomalies found on line A.

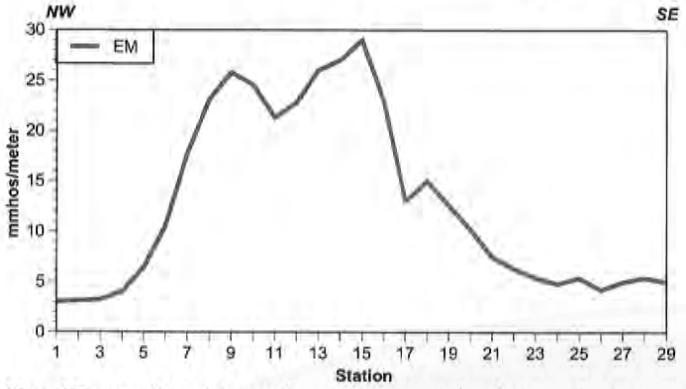

Line 17, a northwest to southeast line, crossed a drainage basin near the Precambrian-Paleozoic contact in C section 2, T19N, R70W, in the eastern Iron Mountain district. The EM response was a relatively symmetrical conductor with a maximum conductivity of 28 mmhos/meter.

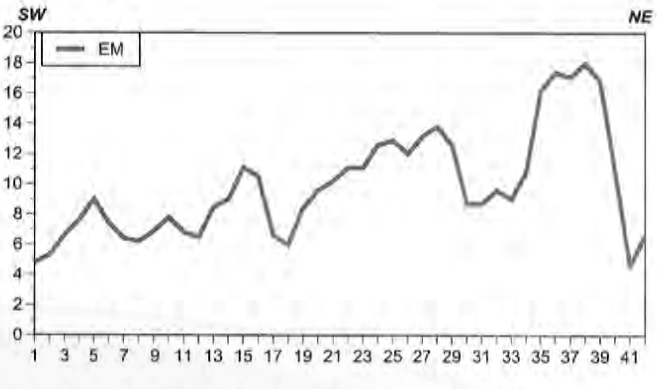

Line 19 was run along strike of the kimberlite dike beginning at the center of line 18. The profile shows the same anomaly that was detected in line 18 plus four additional conductivity anomalies of 11.1, 12.9, 13.8, and 18.0 mmhos/meter, respectively, farther to the northeast.

Lines 18, 19, 20, and 21 (below) tested the kimberlite dike in SE section 3, T19N, R70W. Here, the kimberlite is sporadically exposed on the surface. Where not exposed, the kimberlite is outlined by blue ground and distinct vegetation anomalies. The appearance of the kimberlite is that of a well-defined dike with a very thin soil profile. The thin soil (or blue ground) profile would suggest that the kimberlite here should produce a good magnetic anomaly and a poor EM anomaly. The EM surveys show that the kimberlite produces a distinct, symmetrical, weakly conductive anomaly with a maximum conductivity of 7.5 mmhos/meter compared to a background of about 1 mmho/meter.

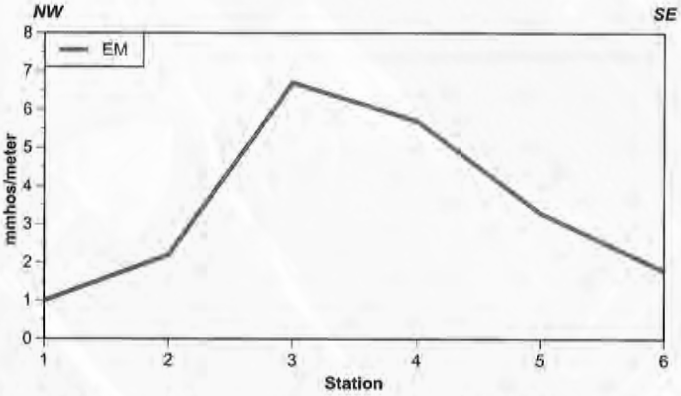

Line 20 was run from northwest to southeast and detected a 6.5-mmho/meter-conductivity anomaly over the dike.

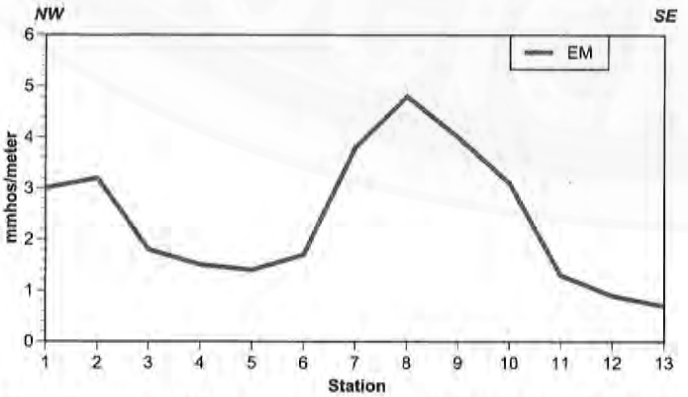

Line 18 was run from northwest to southeast across the kimberlite, detecting a 4.5-mmho/meter-conductivity anomaly over the dike.

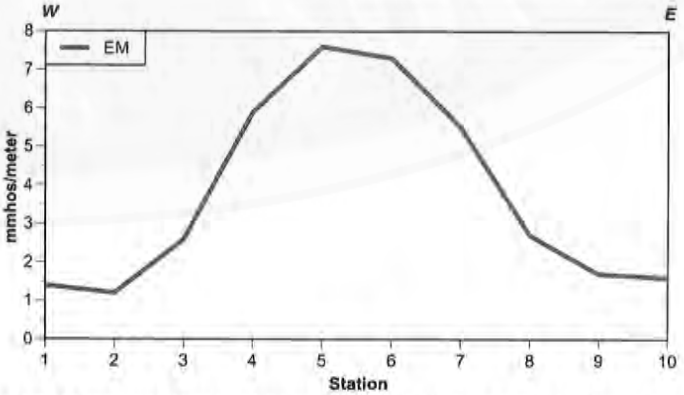

Line 21 was run from west to east and detected a symmetrical conductivity anomaly of about 7.5 mmhos/meter centered over the dike.

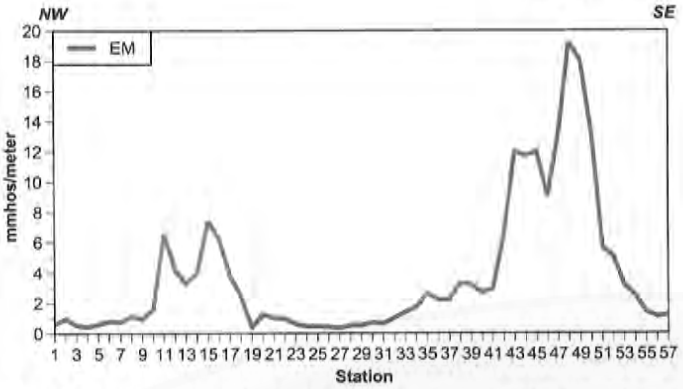

Line 22 crossed the main part of the dike complex and a small spur to the south. The EM survey along the northwest to southeast line detected both the spur (7 mmhos/meter maximum conductivity) and the primary dike (20 mmhos/meter maximum conductivity) compared to a background conductivity of 1 mmho/meter.

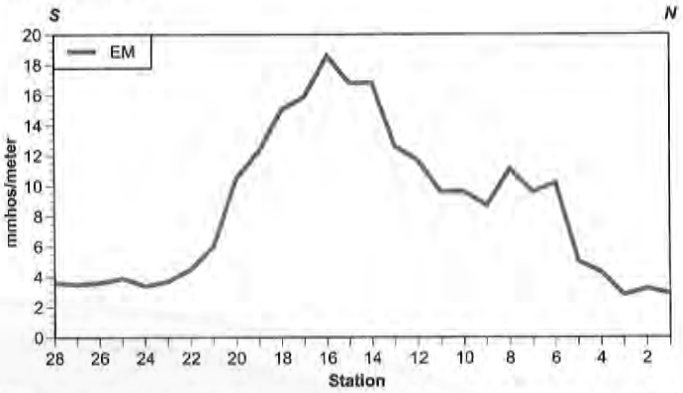

The depression northeast of that tested by lines E and F (below) yielded a 19-mmho/meter-conductivity maximum in north to south **Line C**.

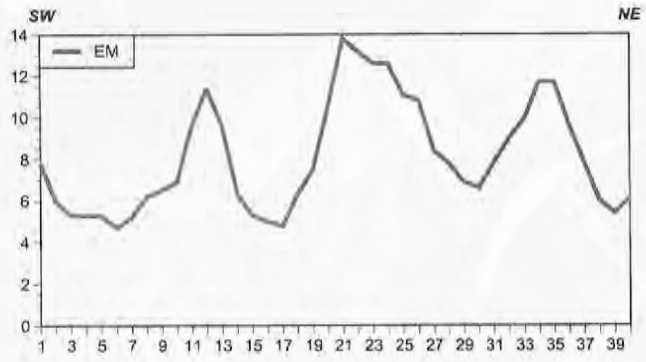

A depression located in NW section 9, T19N, R70W, northeast of that tested by lines C and D (below) contained three distinct conductivity anomalies along southwest to northeast **Line A**. The conductivity anomalies ranged from 12 to 14 mmhos/meter.

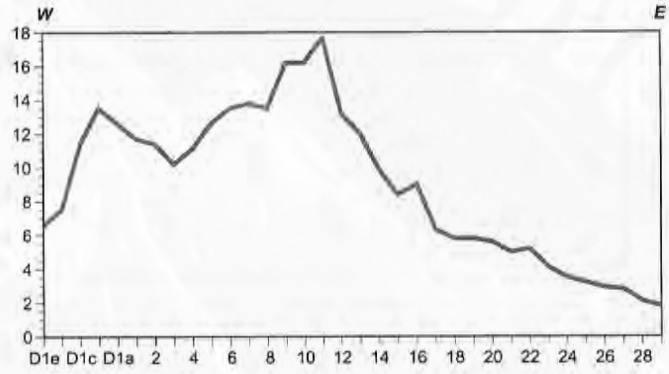

Line D, an east to west line perpendicular to line C, produced a similar anomaly to that detected in line C (above).

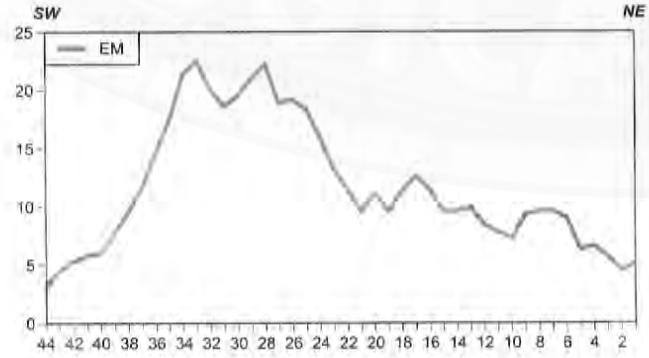

Along **Line B**, which was run at about a 60° angle from line A, maximum conductivity of 23 mmhos/meter was detected.

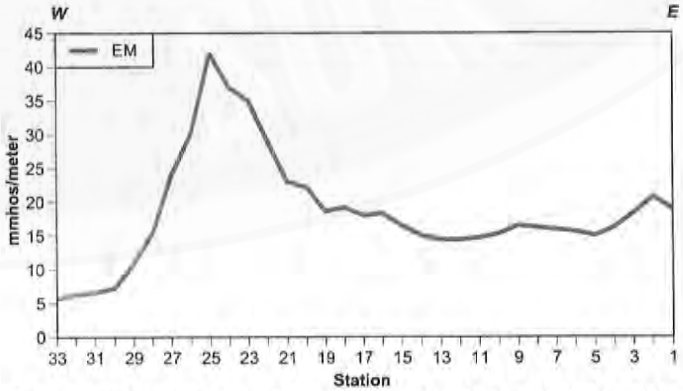

The depression northeast of that tested by lines G and H (below) yielded a strong conductor along east to west **Line E**. The conductor was especially intense at station 25 and reached a maximum conductivity of 43 mmhos/meter, compared to the average conductivity of about 18 mmhos/meter.

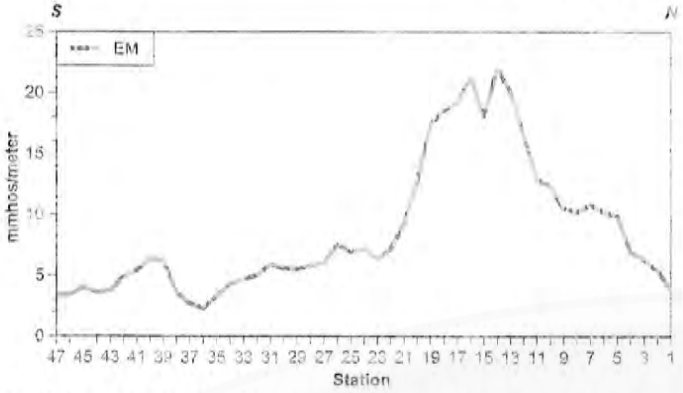

North to south **Line F**, which was run perpendicular to line E, yielded a similar anomaly to E, although the average and maximum conductivity were less.

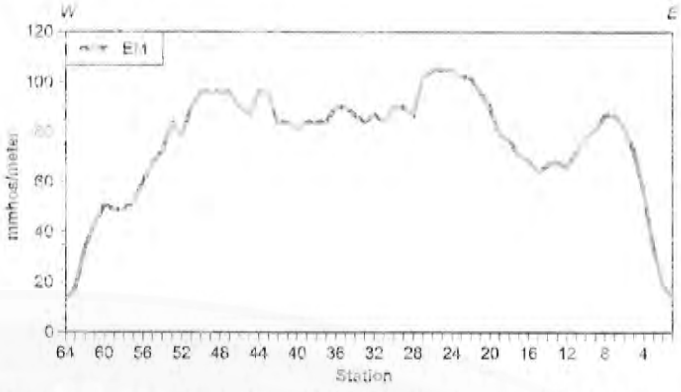

A conductivity peak of about 105 mmhos/meter was detected along much of east-west **Line I**, perpendicular to line 11 (above), over a width of 800 feet.

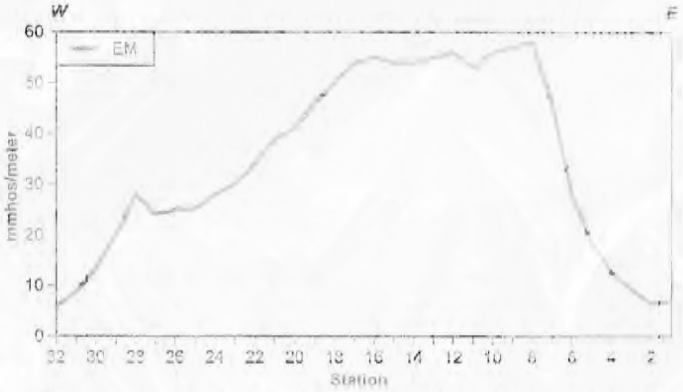

Another depression to the northeast of that tested by lines 11 (above) and I (below) yielded a prominent anomaly along lines G and H. **Line G** was an east to west line perpendicular to line H. A strong conductor was detected.

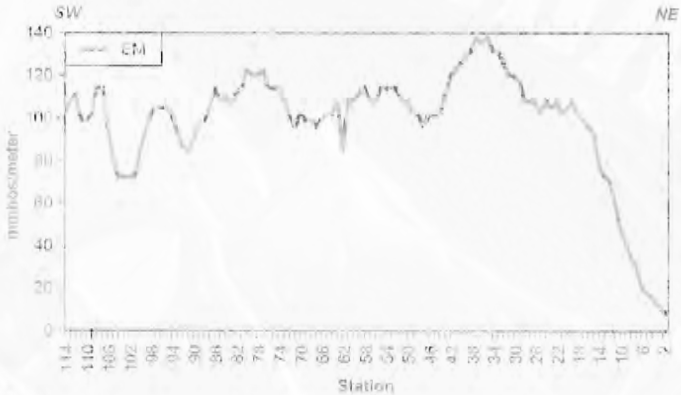

Northeast to southwest **Line J** across the southern edge of the depression showed an intense EM anomaly. The first few feet of this line was in granitic rock, which was poorly conductive. From the granite, the line continued westward into the depression, where a conductivity peak of 140 mmhos/meter was measured. The line terminated in the Tertiary paleoplacer.

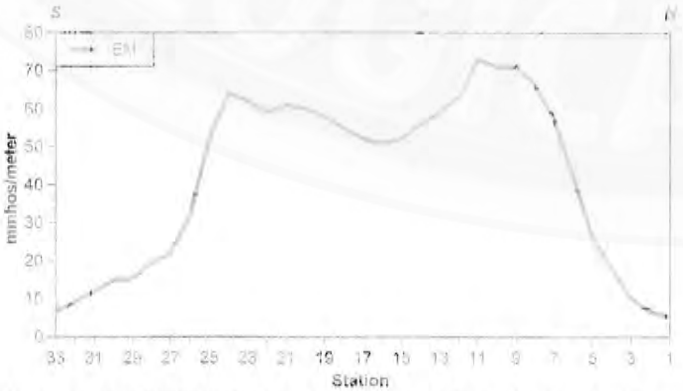

A strong conductor was also detected in **Line H** (perpendicular to line G) over a 315- to 360-foot length, with a peak conductivity of 75 mmhos/meter.

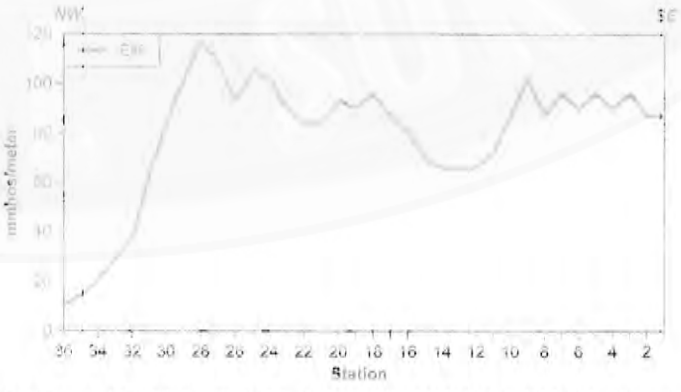

Southeast to northwest **Line K** was run across a kimberlite outcrop surrounded by the Tertiary paleoplacer. The EM profile showed a high conductivity over all but the last five stations to the northwest. The conductivity peaked at almost 120 mmhos/meter.

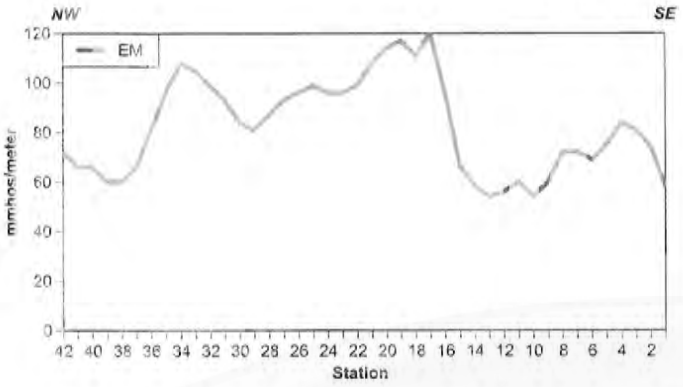

Line L, a southeast to northwest line, was run to the east of line 5 within the Tertiary paleoplacer. The EM profile showed a high background conductivity of 75 mmhos/meter as well as an anomalous region ranging from 100 to 120 mmhos/meter.

Appendix B – Diamond preservation

Much of the following is summarized from McCallum and Waldman (1991), Schulze and others (1995), and Coopersmith and Schulze (1996). It is currently thought that as kimberlitic magmas ascend through the upper mantle, xenocrystic diamonds are collected from eclogite, pyrope harzburgite, chromite harzburgite, and pyrope lherzolite. These diamonds are then subjected to rapidly changing conditions during transportation to Earth's surface that could lead to resorption and/or graphitization. Survival of diamond at elevated temperatures outside the diamond stability field within the kimberlite magma is linked to low oxygen fugacity, rapid emplacement, and rapid temperature drops; thus, elevated oxygen levels and slow emplacement favor diamond resorption.

Ferrimagnetic ilmenite (low MgO) high in Cr_2O_3 may provide an indication of high oxygen fugacity. Such ilmenites are reported from some diamond-poor kimberlites, and these ilmenites characteristically show exsolution textures (typical of those in the Iron Mountain kimberlites). It is speculated that the exsolution textures develop during slow ascent of the kimberlite during which diamonds are resorbed.

In contrast, picroilmenite in diamond-rich kimberlites typically exhibits low ferric iron and relatively high Cr and Mg contents. The picroilmenite, which is not related to diamond crystallization, is interpreted to form during later magmatic processes and metasomatic activity, and thus may provide an indication of diamond preservation. Even though kimberlite may originate within the diamond stability field, the magma may be subjected to later oxidizing environments resulting in high Fe^{3+}/Fe^{2+} ratios (high hematite component) in the ilmenite. In such cases, it has been suggested that the entrained metastable diamonds may be substantially resorbed, producing graphite, CO_2, or CO. In one experiment conducted by the WSGS, a 0.1-carat industrial diamond was placed in an oxidizing flame blown from a Bunsen burner, and the diamond was burned in under 5 minutes.

Homogeneous ilmenites are found in kimberlites that are interpreted to have risen comparatively fast. Within a fractionating magma, early-formed ilmenites may be Cr- and Mg-rich. Subsequent co-precipitation of ilmenite, silicate, and possibly carbonate from the parent magma may result in later-formed ilmenites having lower Cr_2O_3 and MgO contents. High Cr_2O_3 and MgO contents in ilmenite may provide a relative measure of low oxygen fugacity and conversely, lowered or depleted Cr_2O_3 and MgO contents in ilmenite may indicate high oxygen fugacity.

Using the relations noted above, Cr_2O_3-MgO plots for ilmenites have been used to evaluate trends for diamond preservation. When ferrous iron (Fe^{2+}) in the ilmenite crystal is oxidized to ferric iron (Fe^{3+}), MgO depletion along with Cr_2O_3 enrichment is thought to relate to coupled substitution accompanying the addition of Fe^{3+} in Fe^{2+} lattice sites, and provides a measure of increased oxidation state.

Gurney (1984, 1989) and Gurney and others (1993) reported that *"ilmenites with low Fe^{3+}/Fe^{2+} ratios are associated with higher diamond content than those with more Fe^{3+}, whereas diamonds are not associated with ilmenites of high Fe^{3+} content at all."* Griffin and others (1997) reported that ilmenite megacrysts from several significantly diamondiferous kimberlites (Orapa, Koffiefontein, Kimberliey/Wesselton, Liqhobong, and Schuller); several weakly diamondiferous kimberlites (Frank Smith, Monastery, Kao, Klipfontein, and Kamfersdam); and several barren kimberlites supported Gurney's observations. The ilmenites from most of the significantly diamondiferous kimberlites tend to be dominated by high-Mg, high-Cr ilmenites. This is apparently not the case with the ilmenites found in the Iron Mountain and Stateline districts.

McCallum and Waldman (1991) reported that chrome depletion in ilmenites in the Iron Mountain kimberlites suggested oxidation of the ilmenites. They interpreted that the district had no potential for diamonds. Thus, the presence of the oxidized ilmenites (as in other areas) should signal high probability for diamond resorption. In fact, the Iron Mountain kimberlites are a frequently cited example of a diamond-free group of kimberlites with oxidized ilmenite compositions (Gurney, 1989; McCallum and Waldman, 1991). These authors cited the high (39%) hematite component in the Iron Mountain ilmenites as further evidence for their oxidation.

However, Schulze and others (1995) and Coopersmith and Schulze (1996) pointed out that there are a number of diamond-producing kimberlites, all having ilmenites with high hematite contents similar to Iron Mountain. These authors pointed out that "unresorbed diamonds and relatively high ore grades are found in kimberlites mined at Mir (200 carats per 100 tonnes), Frank Smith (known for its sharp-edged octahedrons), DeBeers (90 carats per 100 tonnes), Monastery (50 carats per 100 tonnes), and Kelsey Lake (known for many spectacular gem-quality octahedrons with little evidence of resorption)" (Schulze and others, 1995). Ilmenites in the Kelsey Lake kimberlites contain as much as 38% hematite (Schulze and others, 1995; Coopersmith and Schulze, 1996). Using the high hematite content of ilmenites as an indication of oxidation and resorption of diamond provides some contradictory results.

The ilmenite geochemistry from kimberlite at the Kelsey Lake diamond mine (**Figures 20** and **21**) and Iron Mountain (**Figures 12** and **22**) is nearly identical. At Iron Mountain, ilmenites have rims enriched in MgO relative to the cores at constant Cr_2O_3. The MgO-Cr_2O_3 ratios in Kelsey Lake ilmenites (**Figure 21**) are essentially indistinguishable from the Iron Mountain ilmenites (**Figure 22**), and show a negative correlation between MgO and Cr_2O_3. Thus, the chrome/magnesian ratios and chrome depletion in ilmenites appear to provide inconsistent information on diamond preservation (Coopersmith and Schultz, 1996). MgO depletion in the ilmenites also appears to provide misleading information and, in this case, may not be reliable.

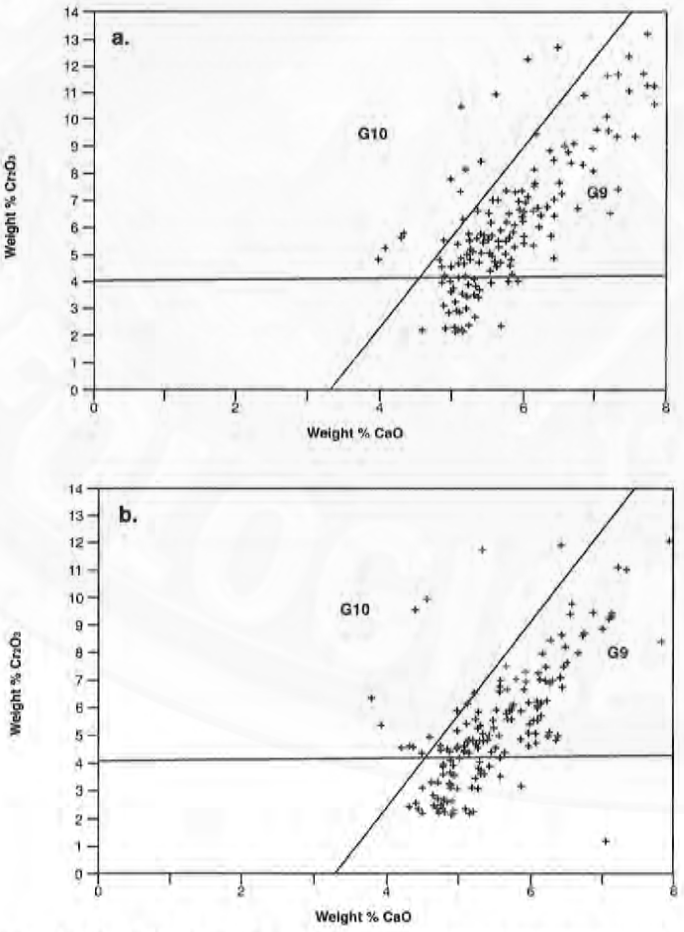

Figure 20. Plots of Cr_2O_3 and CaO contents of pyrope garnets from the (a) Kelsey Lake #1 and (b) Kelsey Lake #2 diamondiferous kimberlites (modified from Coopersmith, 1991). Those garnets that plot in the G10 field to the left of the inclined line have chemistry similar to garnet inclusions in diamond.

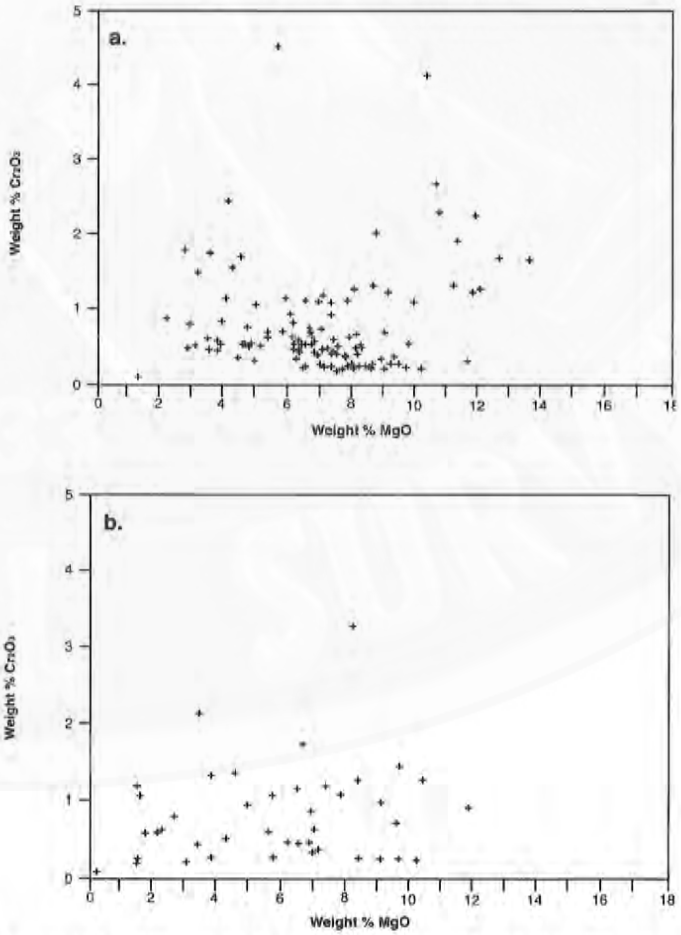

Figure 21. Plots of Cr_2O_3 and MgO contents of picroilmenites from the (a) Kelsey Lake #1 and (b) Kelsey Lake #2 diamondiferous kimberlites (modified from Coopersmith, 1991). Compar with picroilmenites from Iron Mountain (**Figure 22**).

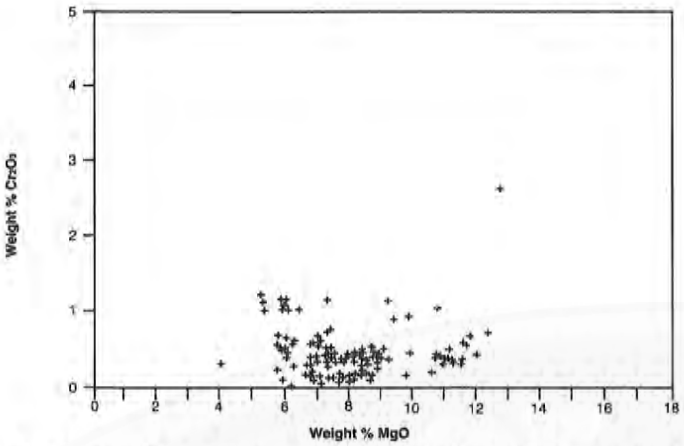

Figure 22. Geochemistry of picroilmenites from the Iron Mountain kimberlites (modified and adapted from McCallum and Waldman, 1991).

The Kelsey Lake kimberlites have yielded many gem-quality, octahedral diamonds with little or no evidence of resorption. In fact, diamond production at the mine includes a large percentage of high-quality gemstones with octahedral habit, suggesting diamond preservation was favorable (Schulze and others, 1995). The geochemistry of ilmenites found in Iron Mountain kimberlites is more similar to ilmenites from the Kelsey Lake kimberlites than it is different, and the possibility of more diamonds being found at Iron Mountain must be considered.

Appendix C – Geophysical lines and electromagnetic profiles, Middle Sybille Creek area

This contains descriptions of geophysical lines and electromagnetic (EM) profiles in the Middle Sybille Creek area, Laramie Mountains, Wyoming. Stations are 30 feet apart. See **Figure 16** for locations of geophysical lines.

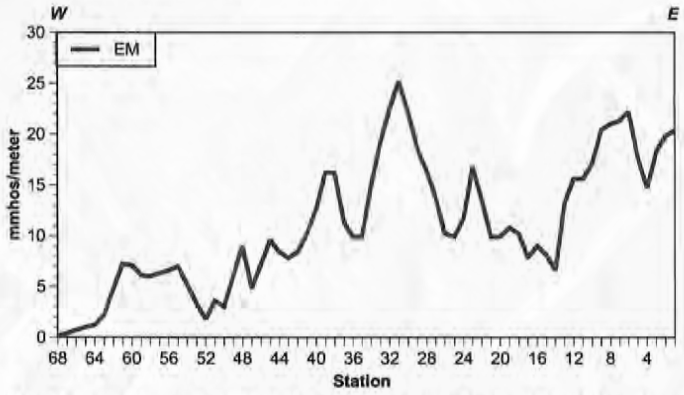

Line 1 began on the east side of Middle Sybille Creek, crossed the creek and continued west across the hay meadow, crossed the intrusive, and ended west of the Radichal kimberlite. No distinct EM response was detected over the kimberlite outcrop, primarily because the Radichal kimberlite occurs as a massive outcrop with no blue ground; the kimberlite was not expected to be conductive. Conductors were identified east of the kimberlite in the hay meadow. The most distinct anomaly was identified west of Middle Sybille Creek, and the conductivity peaked at 25.2 mmhos/meter. The data suggests the presence of a hidden, clay-rich zone at this point.

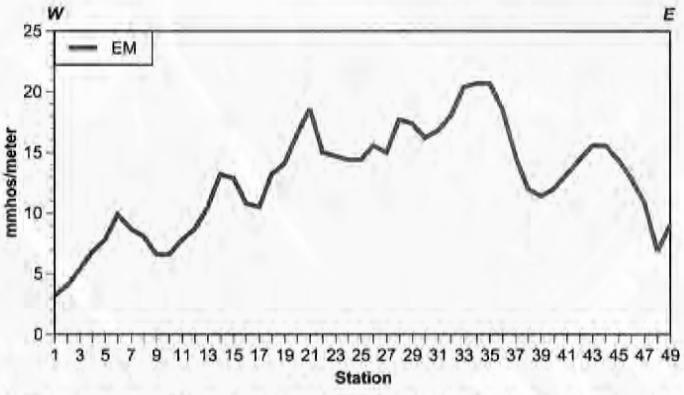

Line 2 was parallel to line 1 and ended at Middle Sybille Creek. Line 7 (see below) continued east of the creek. Line 2 produced an erratic anomaly with a maximum conductivity of about 20 mmhos/meter.

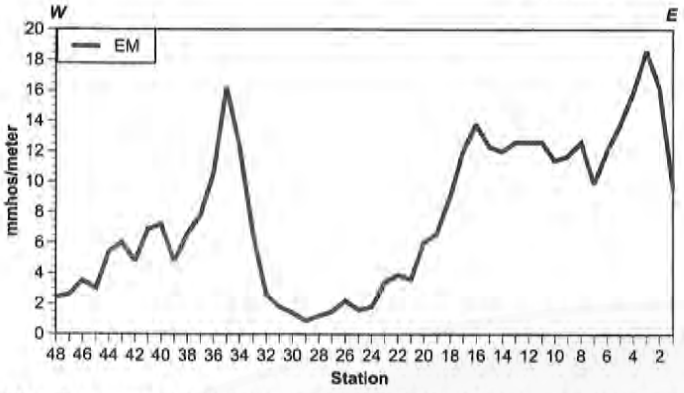

Line 3 was an east to west line located south of line 2 and traversed most of the hay meadow. At a topographic low just east of Middle Sybille Creek, a distinct conductor (maximum conductivity of 18.6 mmhos/meter) was detected over a 90-foot width.

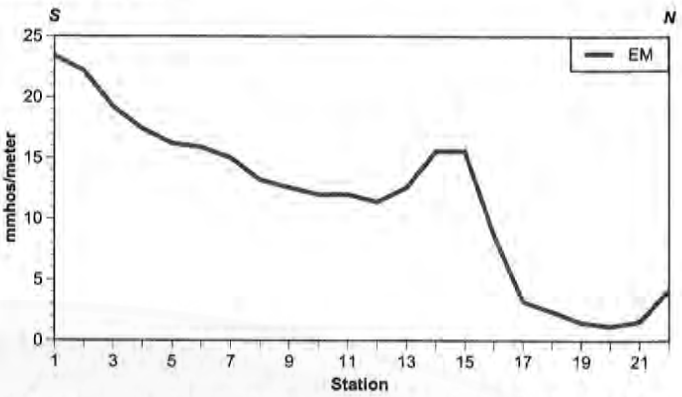

Line 6, a south to north line, extended line 5 to the north. It did not show any distinct anomalies.

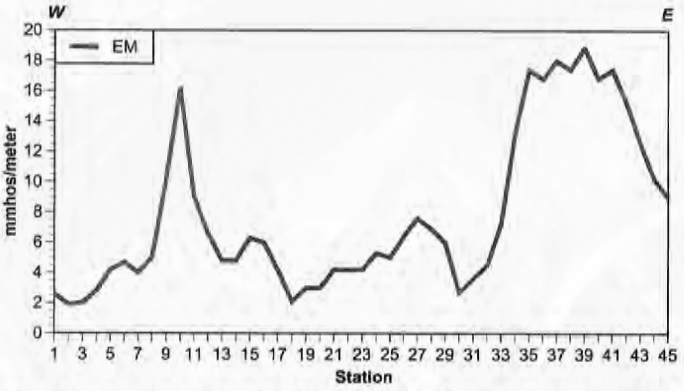

Line 4 was a west to east line located south of Line 3. It was designed to test anomalies in grassy vegetation. The western vegetation anomaly was associated with a spike in the EM (with a maximum conductivity of 16.9 mmhos/meter over a 90-foot width). A second anomaly detected to the east yielded maximum conductivity of 18.9 mmhos/meter over 360 feet.

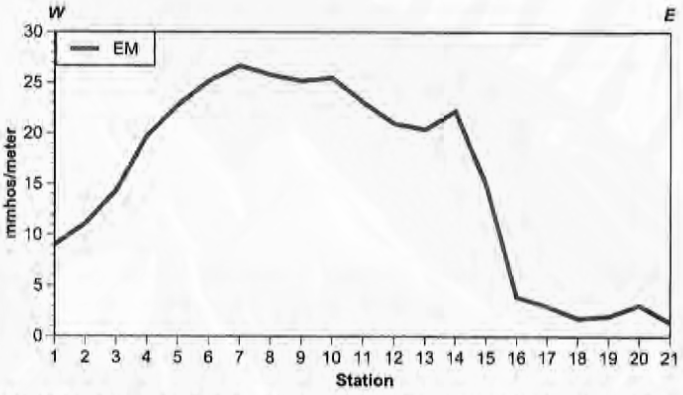

Along **Line 7**, a west to east line which is the eastward extension of line 2, a 26.7-mmho/meter maximum conductivity anomaly was detected over a width of 450 feet. Much of the line was located in wet ground and part of the line extended over dry ground.

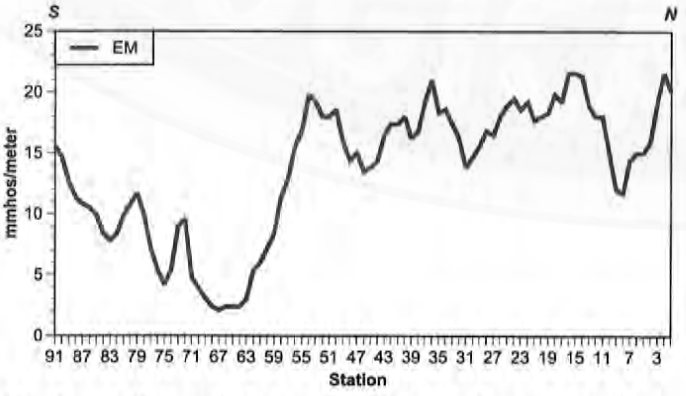

Line 5, a north to south line, crossed lines 1, 2, 3, and 4. Line 6 continued this line farther north. Overall, the line did not show any distinct anomalies.

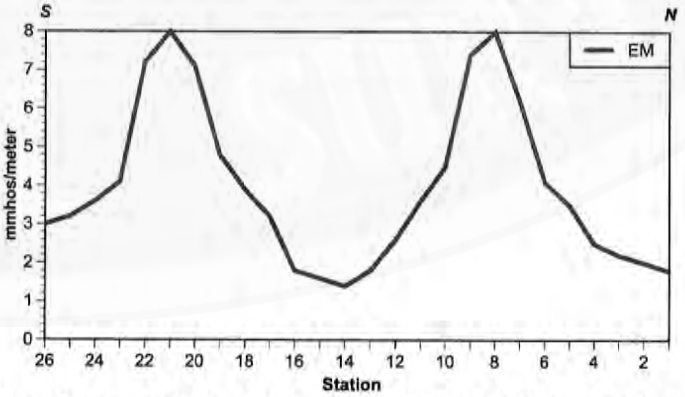

Line 8 was a north to south line that crossed the Radichal kimberlite blow and continued south. The line produced two weak (8 mmhos/meter maximum conductivity) anomalies south of the kimberlite. One was located in a topographic low; the second was covered by sagebrush. Both anomalies were quite distinct compared to low background conductivity. The low background was the result of exposed rock outcrop with thin soil cover.

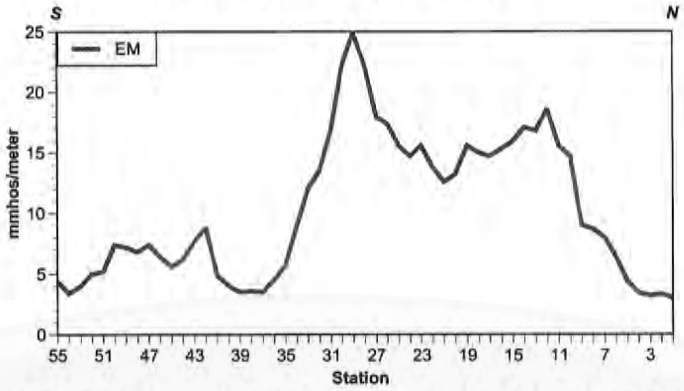

Line 9, a north to south line east of line 5, yielded a distinct EM anomaly with a maximum conductivity of 24.9 mmhos/meter over an 840-foot width.

Appendix D – Geophysical lines and electromagnetic profiles, Indian Guide area

This contains descriptions of geophysical lines and electromagnetic (EM) profiles over structurally-controlled depressions in the Indian Guide area, Laramie Mountains, Wyoming. Stations are 30 feet apart. See **Figure 18** for locations of geophysical lines and a topographic map.

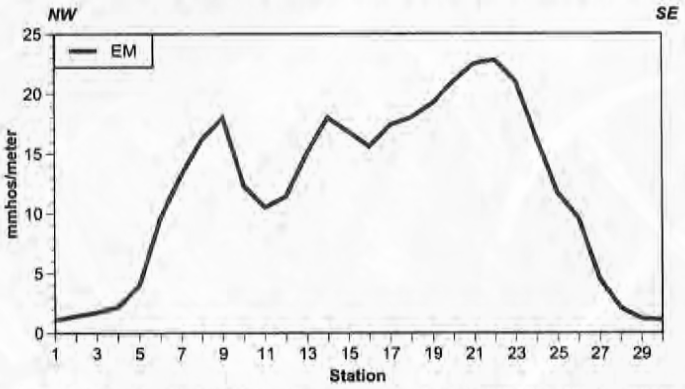

Line 1 and line 2 (below) were run over the northwestern-most depression in section 16 T19N, R71W. **Line 1**, a northwest to southeast line over the center of the depression, detected a conductor 600 feet wide. The conductivity ranged from 9.6 to 22.8 mmhos/meter.

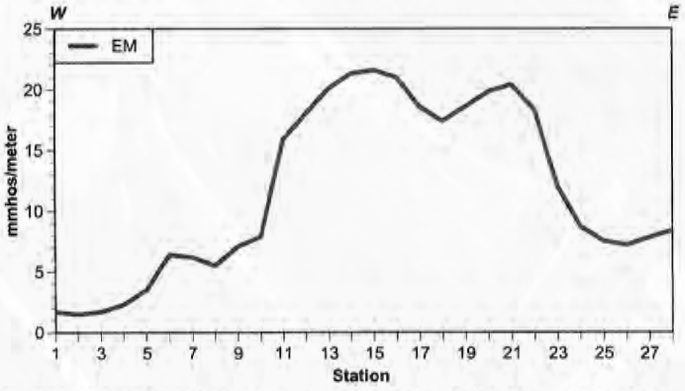

Line 3 was run from east to west perpendicular to Line 4 (below) in a depression in SW section 9, T19N, R71W. A conductor ranging from 7.9 to 21.6 mmhos/meter over 420 feet was identified along this line.

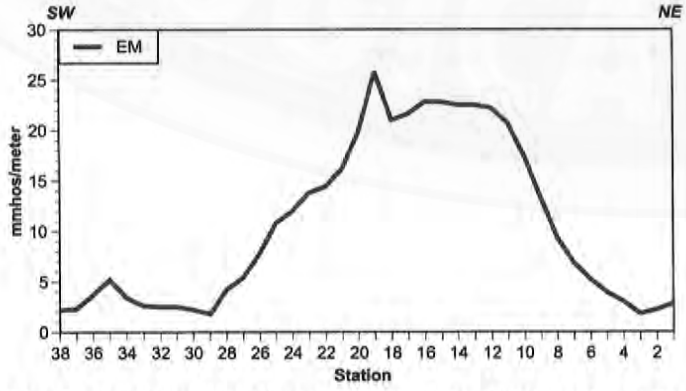

Line 2, a northeast to southwest line which crossed line 1 at the center of the depression, detected a 7.8- to 25.8-mmho/meter conductor over a 510-foot width.

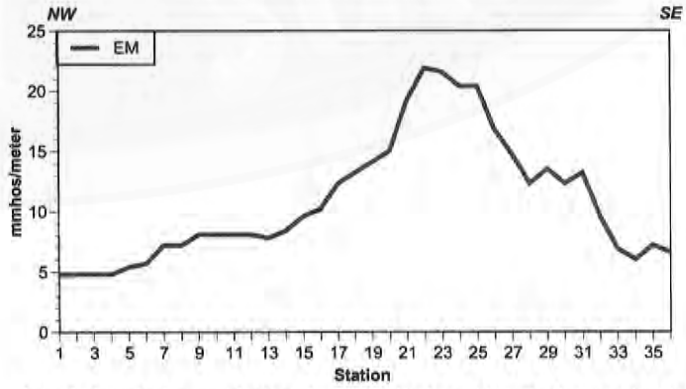

Line 4 detected a conductor similar to that on Line 3; the conductor ranged from 9.6 to 21.9 mmhos/meter over a length of 480 feet.
A short distance southwest of lines 3 and 4 in NE section 17, T19N,

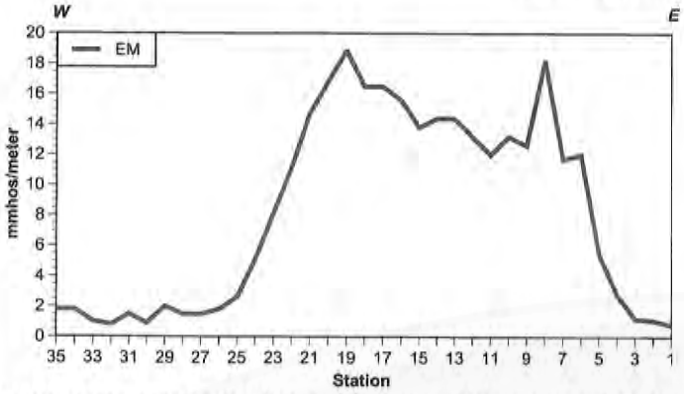

R71W, weak conductivity (8.1 to 18.9 mmhos/meter) was detected along **Line 5** (east to west) over a length of 480 feet.

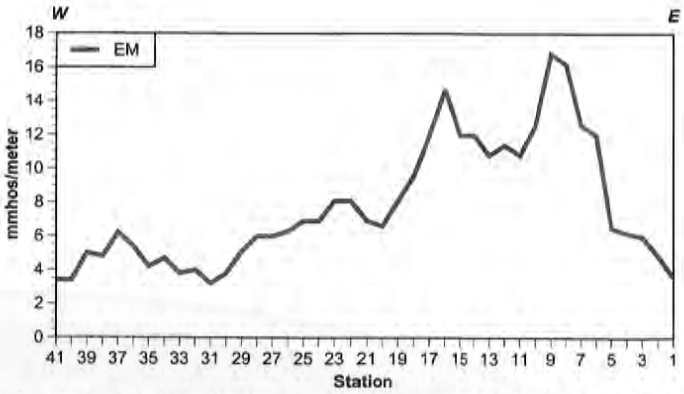

Line 8, an east to west line along the southern edge of the water-filled depression, yielded a weak conductor (8.1 to 16.8 mmhos/meter) over a length of 390 feet.

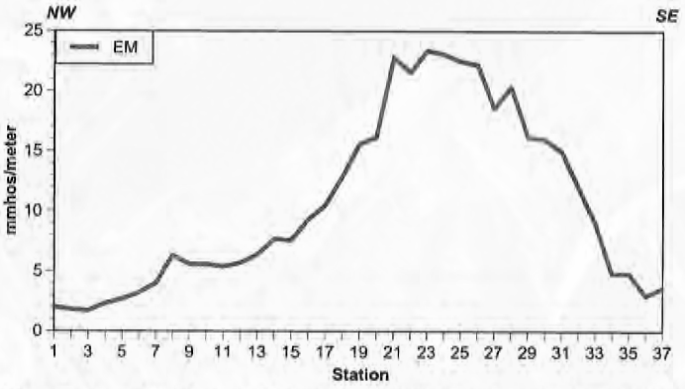

Line 6, a northwest to southeast line, crossed line 5 near the western edge of the depression. This line produced a conductor ranging from 7.6 to 23.4 mmhos/meter over a length of 540 feet.

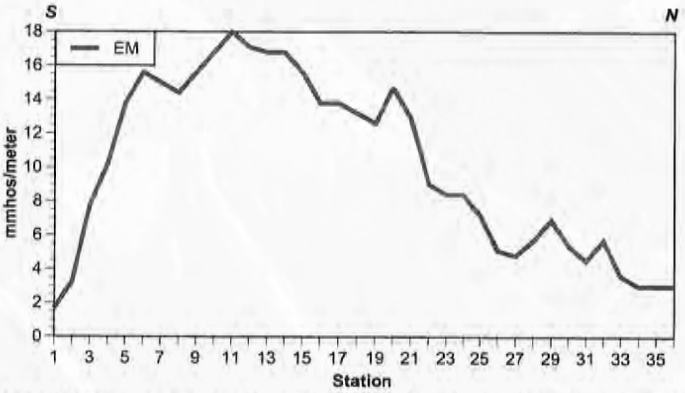

Line 9 was run from south to north over the depression and detected a conductor ranging from 3.2 to 18 mmhos/meter over a distance of 700 feet.

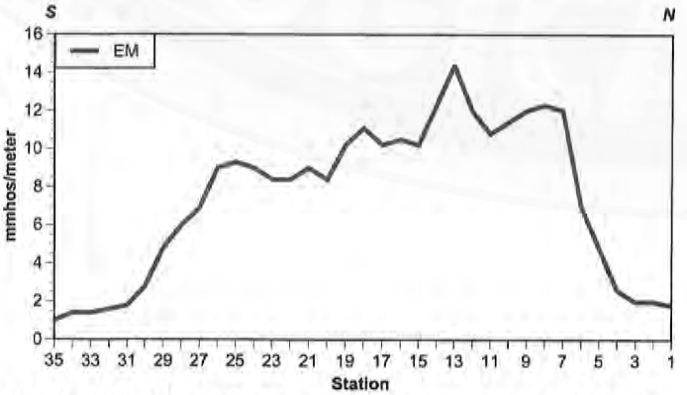

Line 7, a north to south line, yielded a weak conductor (7 to 14.4 mmhos/meter) over a length of 570 feet in SE section 8, T19N, R71W.

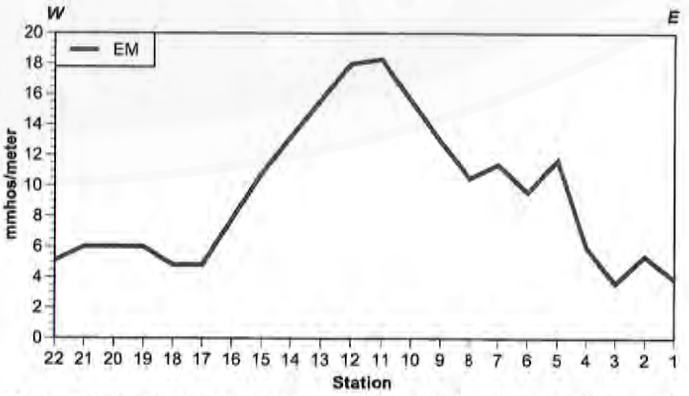

Line 10 was run from east to west and showed a weak conductor (9.6 to 18.3 mmhos/meter) over a length of 300 feet.

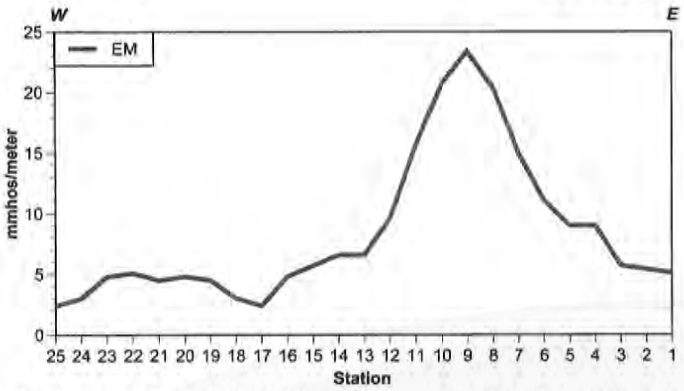

Line 11 and line 12 (below) were routed over the next depression to the west of the depression in lines 9 and 10 (above). A conductor (>15 mmhos/meter maximum) was identified over a length of 240 feet along the east to west **Line 11**.

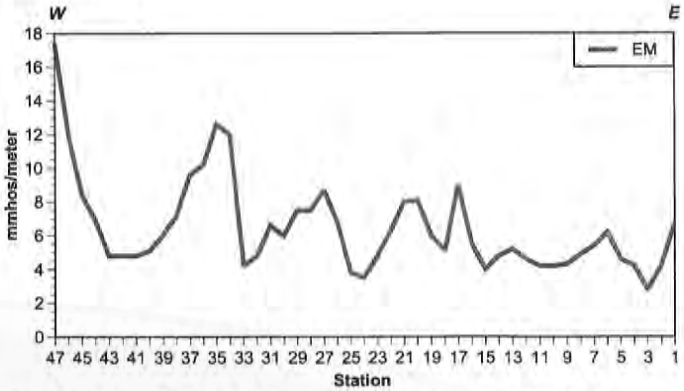

Line 14 was run in an east to west direction over two depressions adjacent to one another. No significant conductors were detected along this line.

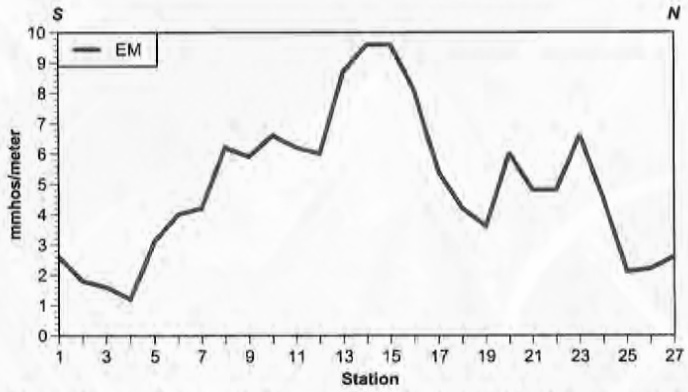

Line 12, a south to north line perpendicular to line 11, showed a weak conductor (6 to 9.6 mmhos/meter) near the low point of the depression.

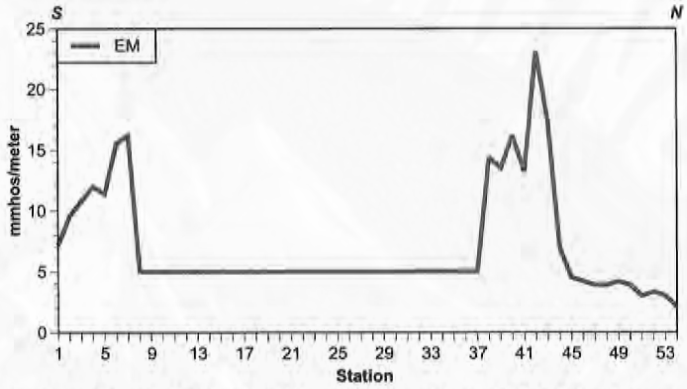

Another 0.5 mile farther west from line 14, a large 1200-foot-diameter, circular water-filled depression in SE section 7, T19N, R71W, was investigated by lines 15, 15A, 16, and 16A. Along the southern shore, a conductor (7.2 to 16.2 mmhos/meter) was identified by the south to north **Line 15** before the signal was lost due to standing water. The northern shore produced a conductor ranging from 13.2 to 23.1 mmhos/meter.

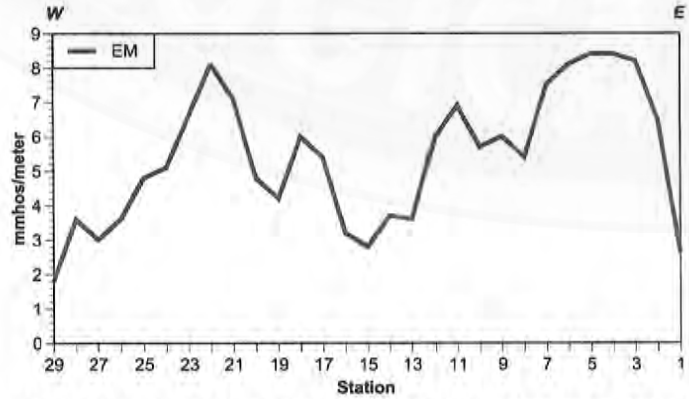

Line 13 was an east to west line located over the depression west of lines 11 and 12 (above). No detectable conductor was identified along the line.

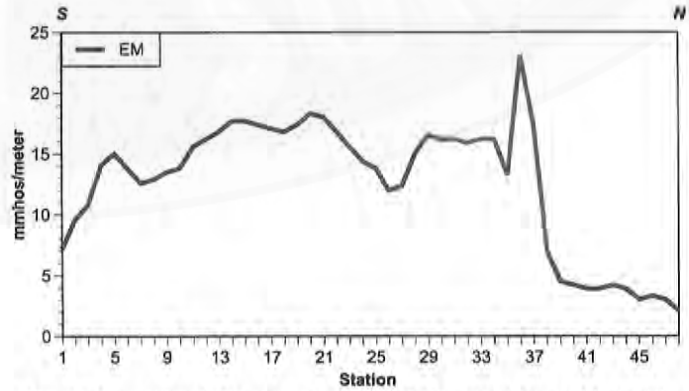

Line 15A traversed the eastern shore of the pond to avoid standing water. A conductor ranging from about 10 to 23.1 mmhos/meter was measured over a distance of 1100 feet.

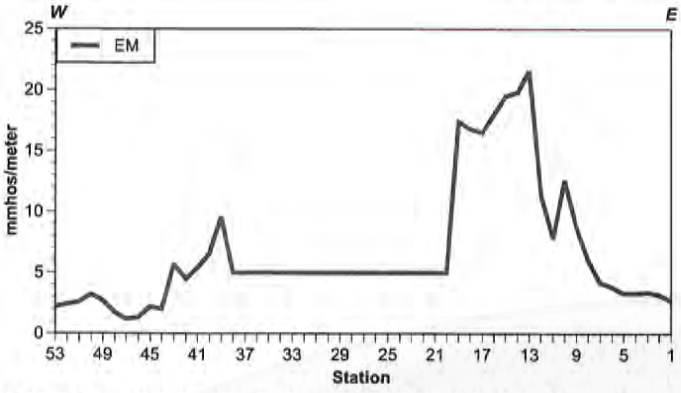

Line 16 was run in an east to west direction perpendicular to line 15. The signal was lost over standing water but measured conductivity up to 7.8 mmhos/meter on the east side and conductivity up to 21.6 mmhos/meter on the west side of the standing water.

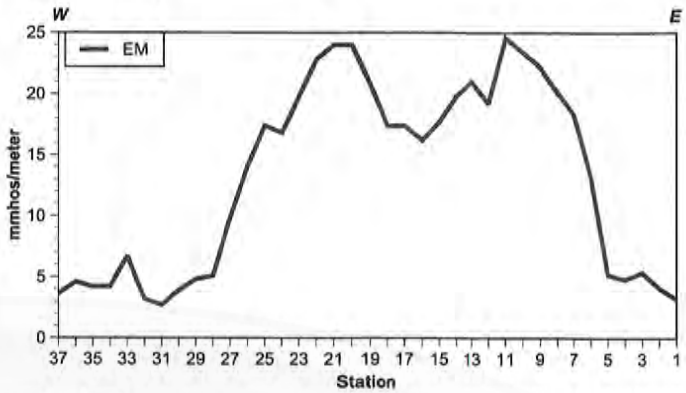

Lines 17 and line 18 (below) were run in another depression identified to the north of the depression investigated by lines 15 and 16 (above). **Line 17** yielded a conductor ranging from 9.9 to 24.6 mmhos/meter over a distance of about 600 feet along an east-west line.

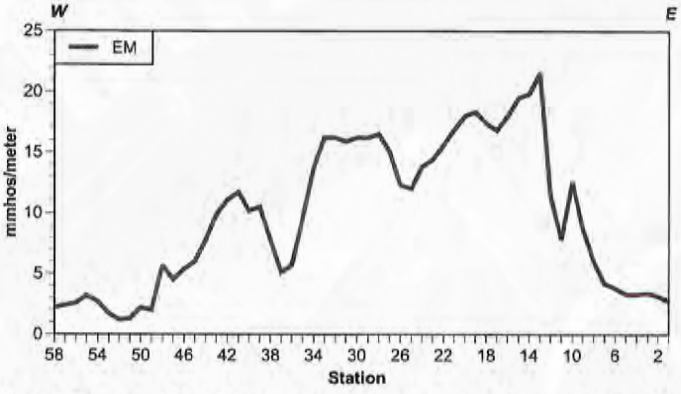

Line 16A was also run from east to west but circled around the north end of the pond to avoid deep water. The line encountered the same conductor as line 16 with a maximum conductivity of 21.6 mmhos/meter.

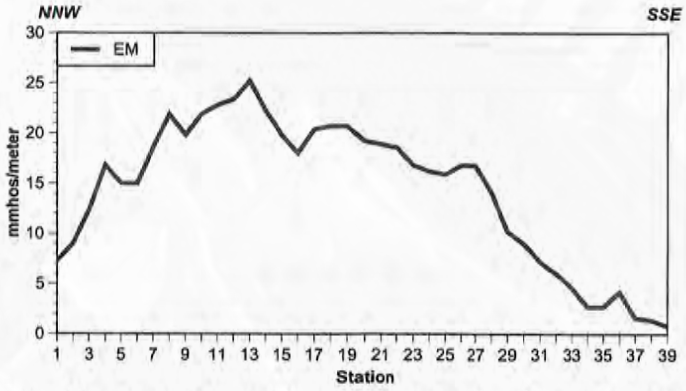

Line 18, a north-northwest to south-southeast line that crossed Line 17, yielded a 7.2- to 25.2-mmho/meter conductor over about 930 feet.


STATE OF WYOMING
1933
GEOLOGICAL SURVEY

STATE OF WYOMING
1933
GEOLOGICAL SURVEY

GEOLOGY OF THE IRON MOUNTAIN KIMBERLITE DISTRICT AND NEARBY KIMBERLITIC INDICATOR MINERAL ANOMALIES IN SOUTHEASTERN WYOMING

RI-54

ISBN 1-884589-33-2

Geology—Interpreting the past to provide for the future

Wyoming State Geological Survey
Lance Cook, State Geologist
Laramie, Wyoming

Report of Investigations 54, Plate 1

Location map of stream sediment samples in part of the Rock River 1:100,000-scale Quadrangle

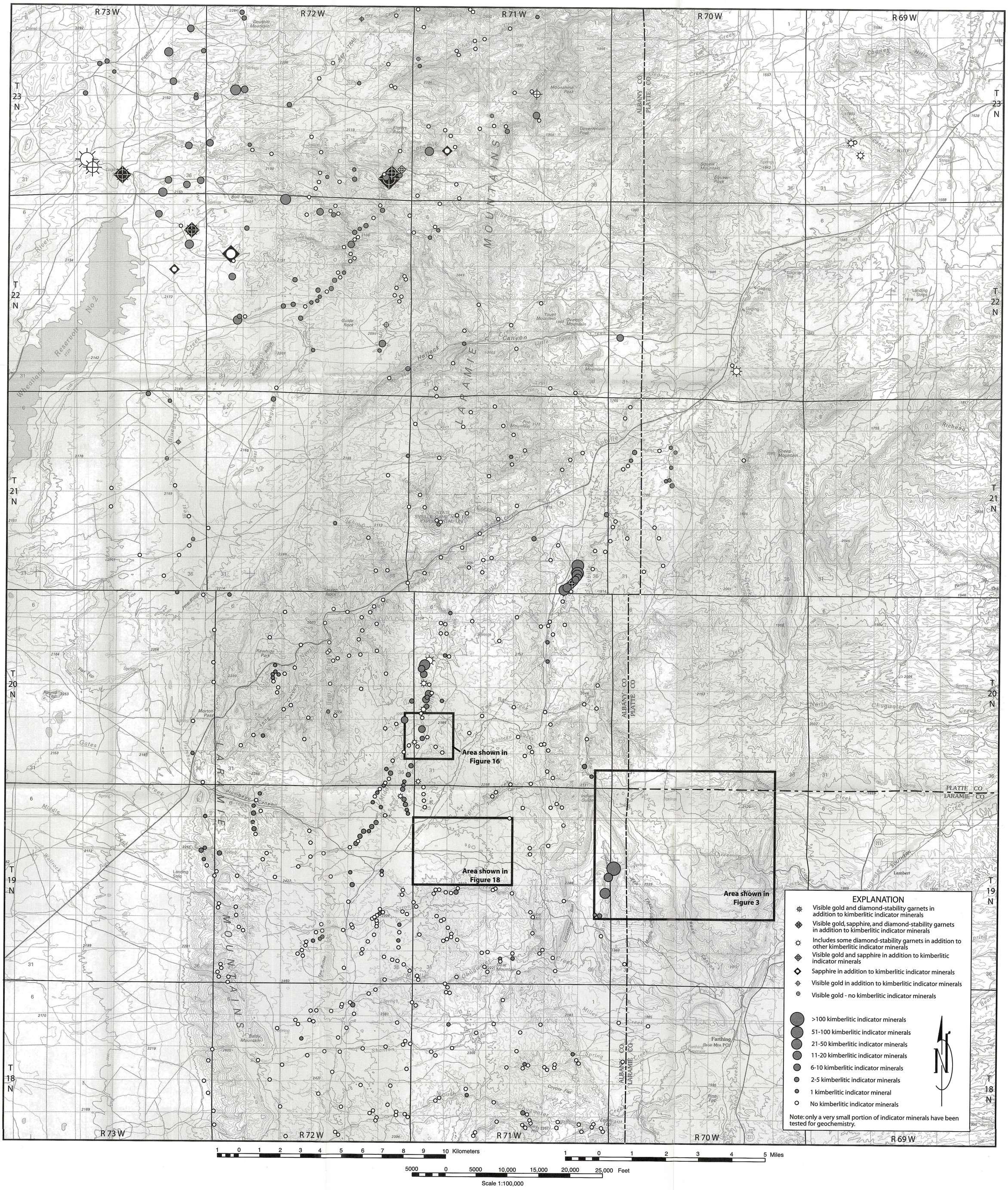

LOCATION MAP OF STREAM SEDIMENT SAMPLES IN PART OF THE ROCK RIVER 1:100,000-SCALE QUADRANGLE, WYOMING, SHOWING KIMBERLITIC INDICATOR MINERAL ANOMALIES

by

W. Dan Hausel, Robert W. Gregory, Roger H. Motten, and Wayne M. Sutherland

2003

Wyoming State Geological Survey
Lance Cook, State Geologist
Laramie, Wyoming

Report of Investigations 54, Plate 2

Location map of stream sediment samples in part of the Laramie 1:100,000-scale Quadrangle

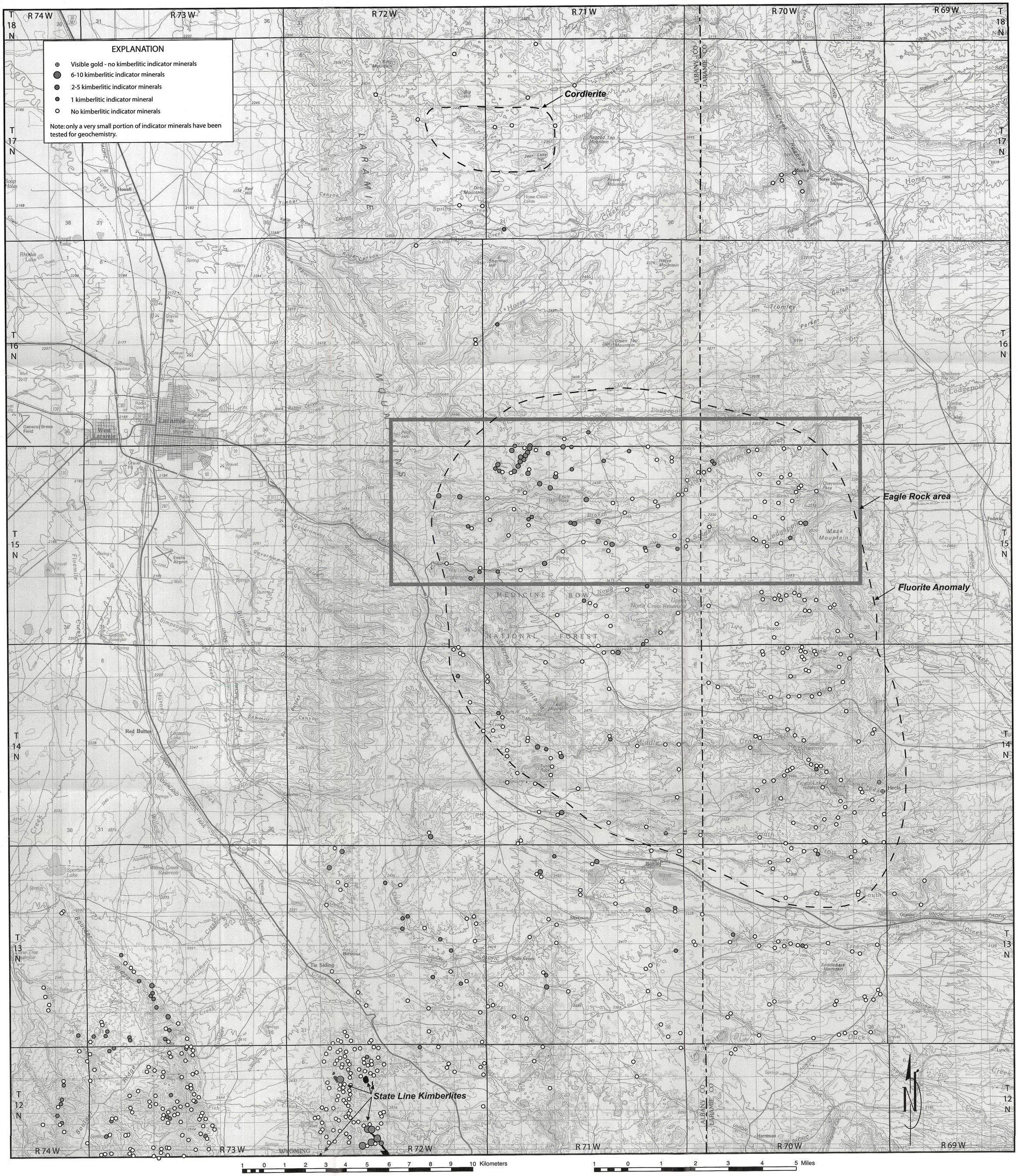

LOCATION MAP OF STREAM SEDIMENT SAMPLES IN PART OF THE LARAMIE 1:100,000-SCALE QUADRANGLE, WYOMING, SHOWING KIMBERLITIC INDICATOR MINERAL ANOMALIES

by
W. Dan Hausel, Robert W. Gregory, Roger H. Motten, and Wayne M. Sutherland

2003

Wyoming State Geological Survey
Lance Cook, State Geologist
Laramie, Wyoming

Report of Investigations 54, Plate 3
Location map of stream sediment samples in part of the Laramie Peak 1:100,000-scale Quadrangle

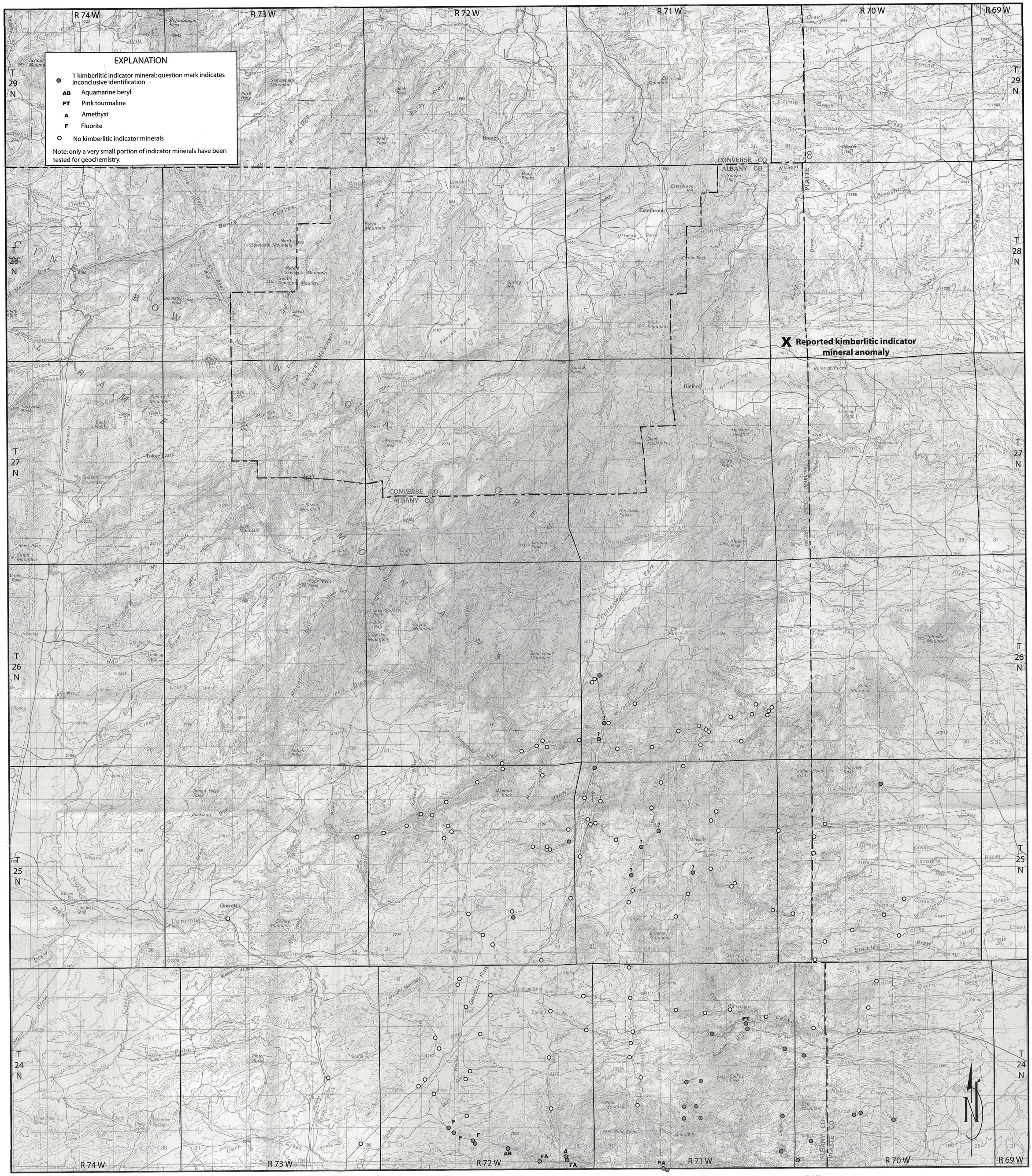

LOCATION MAP OF STREAM SEDIMENT SAMPLES IN PART OF THE LARAMIE PEAK 1:100,000-SCALE QUADRANGLE, WYOMING, SHOWING KIMBERLITIC INDICATOR MINERAL ANOMALIES

by
W. Dan Hausel, Robert W. Gregory, Roger H. Motten, and Wayne M. Sutherland
2003